PALEOSOL EVOLUTION IN A FLUVIAL SEQUENCE STRATIGRAPHIC FRAMEWORK, CRETACEOUS FERRON NOTOM DELTA, SOUTH CENTRAL UTAH, U.S.A.

A Dissertation

Presented to

the Faculty of the Department of Earth and Atmospheric Sciences

University of Houston

In Partial Fulfillment

of the Requirements for the Degree

Doctor of Philosophy

By

Oyebode Ayobami Famubode

May 2014

PALEOSOL EVOLUTION IN A FLUVIAL SEQUENCE STRATIGRAPHIC

FRAMEWORK, CRETACEOUS FERRON NOTOM DELTA,

SOUTH CENTRAL UTAH, U.S.A.

Oyebode Ayobami Famubode

APPROVED:

Dr. Henry S. Chafetz, Co-Chair

Dr. Janok P. Bhattacharya, Co-Chair

Dr. Ian Evans

Dr. Julia S. Wellner

Dr. Timothy M. Demko

Dr. Steven G. Driese

Dean, College of Natural Sciences and Mathematics

ACKNOWLEGEMENTS

I would like to express my special appreciation and thanks to my advisor, Dr. Janok P. Bhattacharya for his steadfast support and guidance during the course of this research. I have been influenced by his independence, his emphasis on critical thinking, and his unwavering passion for the geosciences. I thank Dr. Henry Chafetz, Dr. Williams Dupré, Dr. Ian Evans, Dr. Julia Wellner, Dr. Timothy Demko, and Dr. Steven Driese for serving on my committee and for their valuable inputs and suggestions during the course of this research. I also thank Benjamin Browning, Danfix D'Souza, Omar Montes, and Yang-yang Li for their outstanding assistance on the field in Utah. My deepest gratitude goes to my loving wife, Olufunmi, for her steadfast support and patience. I thank my dearest parents for their sacrifice and unwavering supporting for my education through the years. I thank them for raising me to become the person I am today. I also thank my sisters, my entire family, and friends, for their support. This work was made possible by funding to J. P. Bhattacharya's Quantitative Sedimentology Laboratory Consortium sponsored by Anadarko, BP, Chevron, Nexen, Shell, ExxonMobil, Pioneer, Ecopetrol, Inpex, and BHP Billiton, and was also partially supported by a separate grant from ExxonMobil Upstream Research Company. I also acknowledge the support of Chemostrat Inc. in geochemical sample analysis.

PALEOSOL EVOLUTION IN A FLUVIAL SEQUENCE STRATIGRAPHIC FRAMEWORK, CRETACEOUS FERRON NOTOM DELTA, SOUTH CENTRAL UTAH, U.S.A.

An Abstract of a Dissertation

Presented to

the Faculty of the Department of Earth and Atmospheric Sciences

University of Houston

In Partial Fulfillment

of the Requirements for the Degree

Doctor of Philosophy

By

Oyebode Ayobami Famubode

May 2014

ABSTRACT

Hydromorphic paleosols have been previously thought as ever wet and poorly developed, and lacking useful paleoenviromental and paleoclimatic indicators. However, a suite of pedogenic features and geochemical attributes of hydromorphic floodplain paleosols of the youngest non-marine (100ka) sequence in the Cretaceous Ferron Notom Delta indicate the prevalence of shrink-swell processes, suggesting fluctuating soil moisture conditions. Alternating soil moisture conditions suggest seasonality in rainfall, linked to a paleoclimate with more wet periods than dry. Vertical organization of paleosols in the sequence reveals simple and compound vertical paleosol profiles that were integrated with channel-fill deposits to produce a high-resolution interpretation of the sequence. Detailed facies analysis reveal 11 depositional facies that build 33 fluvial aggradational cycles, 9 fluvial aggradation cycles sets, and 3 sequences, within what was previously classified as a single sequence. Fluvial aggradation cycles in the succession are either simple floodplain bedsets or single channel stories that are bounded by paleosols. They represent rapid depositional events that probably span less than 500 years when compared to modern analogs of the Ferron Notom Delta, and were followed by short hiati (10 to < 500 years), possibly reflecting short-term avulsions. Fluvial aggradational cycle sets in the succession are aggregates of fluvial aggradational cycles, bounded by relatively mature paleosols or erosionally top-truncated. They represent multiple small-scale depositional events that span not more than 10Ka, followed by relatively long (1 to < 5Ka) hiati, which suggest relatively long-term river avulsions. Fluvial aggradational cycle sets are often capped by coals and carbonaceous strata. Associated marine trace fossils above coal

beds suggest marine transgression due to compactional subsidence or eustatic sea-level rise. The similarity in the scale of cyclicity in fluvial aggradation cycle sets (10Ka) and marine parasequences of the Ferron Notom Delta (10 to 15Ka) may suggest a link between non-marine and marine cyclicity. Fluvial sequences are aggregates of fluvial aggradational cycle sets that are bounded by unconformities or their correlative conformities that represent relatively longer periods (5 to < 15Ka) of subaerial exposure and pedogenic development. Cyclicity on the sequence-scale in this succession is attributed to high-frequency Milankovitch-scale (~20Ka; 40Ka) fluctuations in sea level.

TABLE OF CONTENTS

CHAPTER 1

INTRODUCTION

1.1 OVERVIEW

This dissertation provides documentation of hydromorphic floodplain paleosols, and constituent facies of the youngest non-marine (100Ka) sequence in the Cretaceous Ferron Notom Deltaic Complex. It integrates floodplain deposits with channel-fill sandstones to provide a high-resolution sequence-stratigraphic interpretation of the sequence, and compares cyclicity observed in the non-marine strata to previously documented cyclicity in associated marine strata.

1.2 DISSERTATION ORGANIZATION

This dissertation is composed of four chapters. Chapters 2 and 3 make up the main body of the dissertation. Each of these two chapters is a manuscript that will be submitted to a peer-viewed journal.

Chapter 2 documents the characteristics of hydromorphic floodplain paleosols in the youngest non-marine sequence of the Cretaceous Ferron Notom Deltaic Complex. It provides a detailed description of macroscopic and microscopic features in the paleosols, as well as their geochemical attributes. It discusses the paleoenvironment in which these features developed, and the paleohyrodology of that environment. It discusses the likely paleoclimate under which they developed. It also discusses the factors that control vertical and lateral variations in maturity observed in the paleosols, and the factors influencing cyclicity. The manuscript of this chapter will be submitted to Sedimentology. The paper is co-authored with Janok P. Bhattacharya. I took the main responsibility of preparing the text and figures, with editorial contribution from Janok P. Bhattacharya, Timothy M. Demko, Henry Chafetz, Ian Evans, and William R. Dupré.

Chapter 3 focuses on integrating observations from hydromorphic floodplain paleosols with other floodplain deposits and channel-fill sandstones, to produce a high-resolution sequence stratigraphic interpretation of the youngest non-marine sequence in the Cretaceous Ferron Notom Delta. It provides a detailed description of the facies that build cyclic fluvial aggradation cycles, fluvial aggradation cycle sets, and sequences. It also discusses the factors controlling cyclicity and compares the cyclicity in non-marine strata to those observed in associated marine strata. The manuscript of this chapter will be submitted to the Journal of Sedimentary Research. The paper is co-authored with Janok P. Bhattacharya. I took the main responsibility of preparing the text and figures, with editorial contribution from Janok P. Bhattacharya, Steven G. Driese, Ian Evans, and Henry Chafetz.

Chapter 4 summarizes conclusions from the previous two chapters (i.e. chapter 2 and chapter 3).

CHAPTER 2

HYDROMORPHIC PALEOSOL INTERPRETATIONS OF AN ANCIENT COASTAL FLOODPLAIN, FERRON NOTOM DELTA, UTAH, USA

2.1 INTRODUCTION

Despite extensive investigation of the Ferron Sandstone over the years (e.g., Chidsey et al. 2004; Fielding 2010; Li et al. 2010 etc.), no detailed study of paleosols has been conducted. Recent work by Zhu et al. (2012) on the Ferron Notom Deltaic Complex makes passing reference to paleosol features but did not include a systematic analysis of the non-marine facies. Floodplain deposits are important in analyzing the intrinsic versus extrinsic factors that control fluvial sedimentation and architecture (Wright and Marriot 1993; Plint et al. 2001; McCarthy and Plint 2003, 2013). Floodplains serve the dual purpose of preserving both the sedimentary (i.e. erosion and deposition) and pedogenic (i.e., non-depositional) record of ancient fluvial systems (Arndorff 1993; McCarthy and Plint 1999).

The Ferron Notom Delta serves as an example of an ancient fluvio-deltaic system in which sandy channel belts and incised valleys are associated or overlain by extensive floodplain deposits (Li et al. 2010; Zhu et al., 2012). The exposed or partially exposed surface of floodplains favored the development of hydromorphic paleosols. Hydromorphic paleosols (“Gleysols” Taxonomic classification of Mack et al. 1993) form under conditions of soil saturation, and waterlogging with prevailing anaerobic conditions and consequent Fe reduction, often accompanied by formation of H_2S and pyrite precipitation (Hurt et al. 1998; Hurt and Carlisle 2002). It is expected that soils that develop under such conditions would lack soil structures and pedogenic features that are characteristic of well-developed or well-drained paleosols. It has also been proposed that hydromorphic paleosols lack good paleoenvironmental (Mack 1992) or paleoclimatic indicators. To address this, floodplain paleosols in the youngest fluvial sequence (sequence 1) in the Cretaceous Ferron Notom Delta were examined to determine whether hydromorphic paleosols provide a decipherable record of floodplain pedogenesis and associated climate and drainage records.

The purpose of this study therefore is to: (1) provide detailed description and interpretation of microscopic and macroscopic features of hydromorphic floodplain paleosols of the youngest fluvial sequence of the Ferron Notom Delta; (2) examine vertical and lateral variability in the paleosol development and understand the factors (intrinsic and extrinsic) that influence such variations; (3) reconstruct the pedogenic (including soil-saturation) history of the vertical succession of paleosols in this sequence; and (4) explore the broader implications of the pedogenic history for the depositional and climatic history of an ancient Cretaceous fluvio-deltaic system.

2.2 GEOLOGIC SETTING AND STUDY AREA

The Ferron Notom Delta was one of a series of clastic wedges that prograded into the epeiric Western Interior Seaway, which extended from the Boreal Sea in Arctic Canada to the Gulf of Mexico in the Cordilleran foreland basin (Fig. 1) during the Late Cretaceous (Cotter 1974; Uresk 1978; Hill 1982; DeCelles and Giles 1996; Bhattacharya and Tye, 2004).

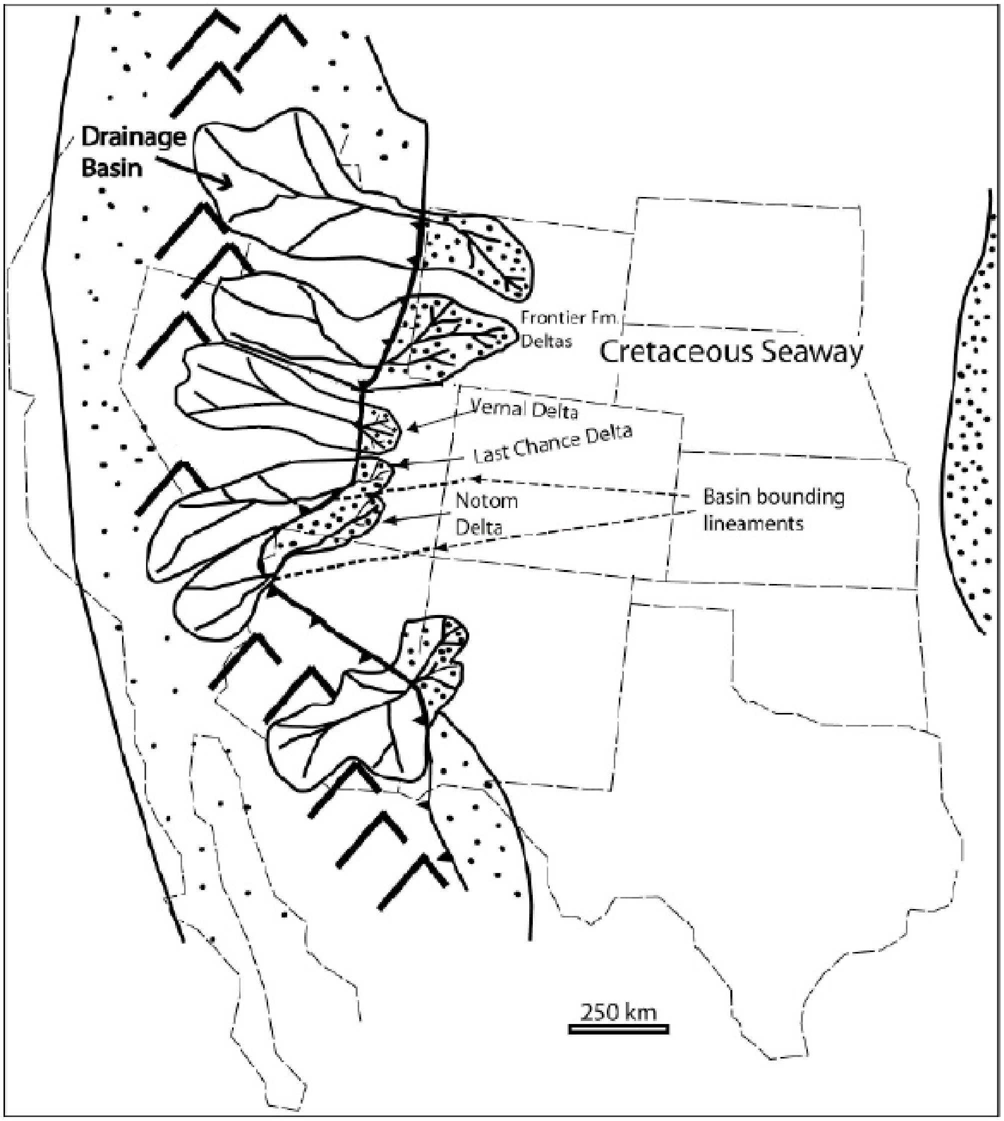

Figure 1.− Paleogeographic reconstruction of the Western Interior Seaway that shows the drainage basin and deltas of rivers that flowed into the seaway. Notom Delta flowed towards northeast. Modified after Bhattacharya and Tye (2004), based on reconstructions by Gardner (1995) and Williams and Stelck (1975).

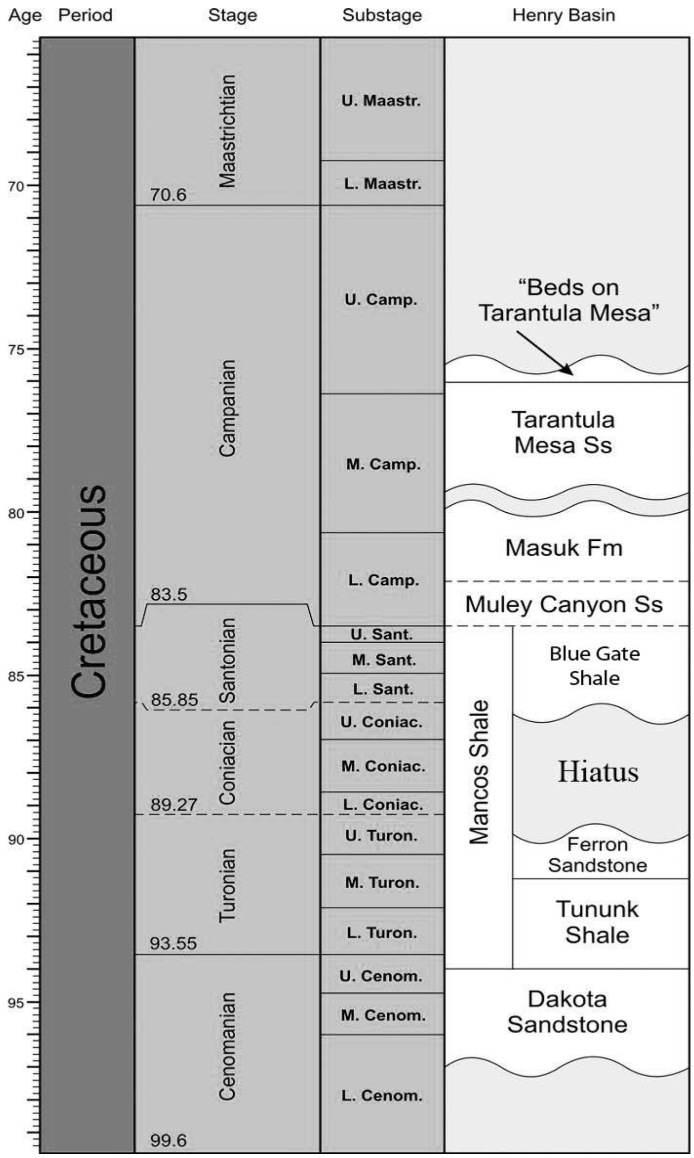

Figure 2.─ Upper Cretaceous stratigraphic column showing successions in the Henry Mountains area. Ferron Sandstone is bound conformably below by the Tununk Shale and unconformably above by the Blue Gate Shale (Fielding 2010).

The Cordilleran foreland basin formed as a flexural response to thrust sheet loading in the Sevier fold-and-thrust belt during the Late Cretaceous (DeCelles et al. 1995; DeCelles and Giles, 1996). The Ferron Sandstone is bounded conformably below by the Turonian Tununk Shale, and unconformably above by the Santonian Blue Gate Shale. The contact between the Ferron and the Blue Gate Shale also consist of a transgressive surface of erosion. All three are members of the Mancos Shale Formation (Fig. 2; Peterson and Ryder, 1975). A regional sequence stratigraphic study of the Ferron Notom Deltaic Complex revealed 6 sequences (including 1 sequence set) that span approximately 600,000 years, as determined by isotopic dating of sanidine in bentonite layers (Zhu et al. 2012). Each sequence is interpreted to be deposited in about 100,000 years (Fig. 4).

The compound incised-valley fills at the base of the upper two sequences (sequences 1 and 2) shows evidence for two to three episodes of erosion and transgressive filling (Li et al. 2010; Li and Bhattacharya 2013). The compound incised-valley fill at the base of the youngest fluvial sequence 1 is overlain by a succession of channel belt and floodplain deposits, including paleosols, which are the focus of this study. The study area is in the Sweetwater Creek drainage, between the Henry Mountains and Utah Highway 24 (Fig. 3). This location was chosen for its continuous, lightly weathered cliff exposures of floodplain deposits and paleosols, which stretches for a distance of about 2300 meters.

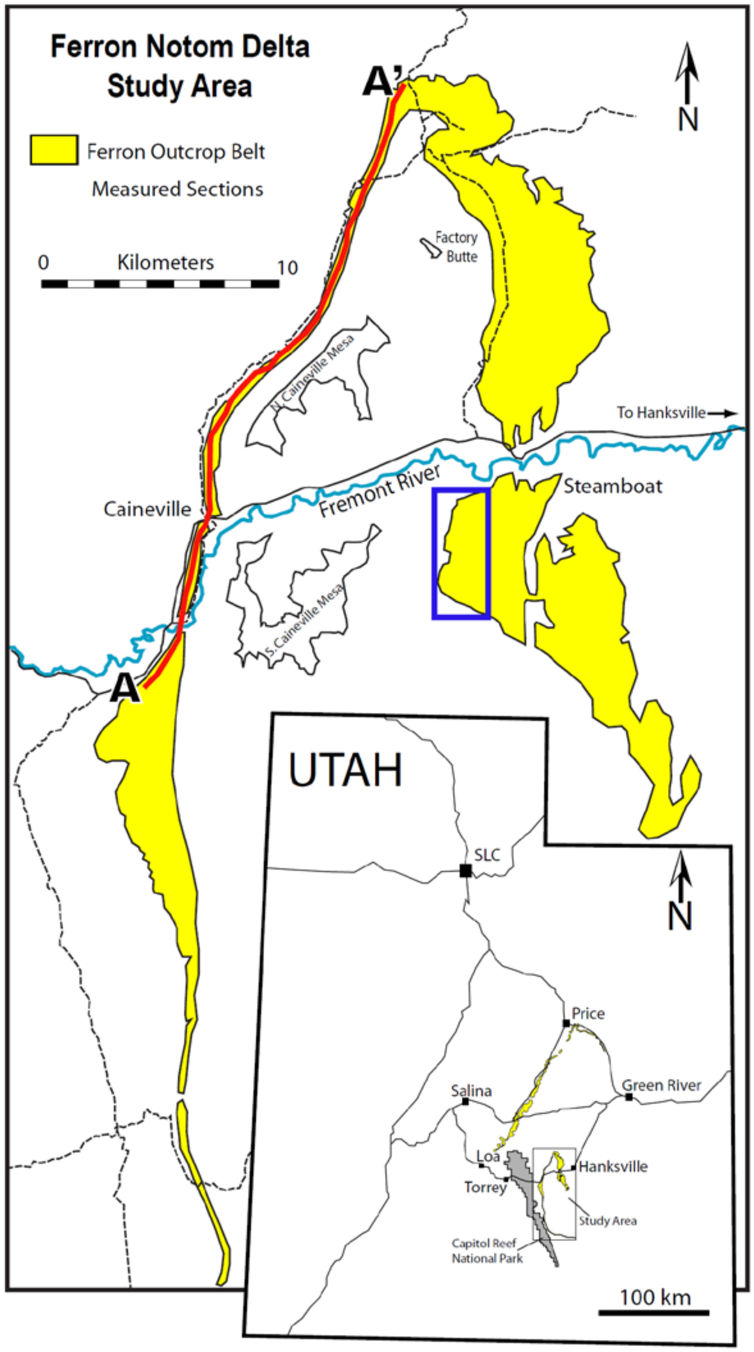

Figure 3.—Inset map shows the general location of the study area in south central Utah. Larger map shows the outline of the Ferron Notom Sandstone outcrop. Area in blue box is Sweetwater Creek drainage. The red line represents the outline of the cross section in Figure 4.

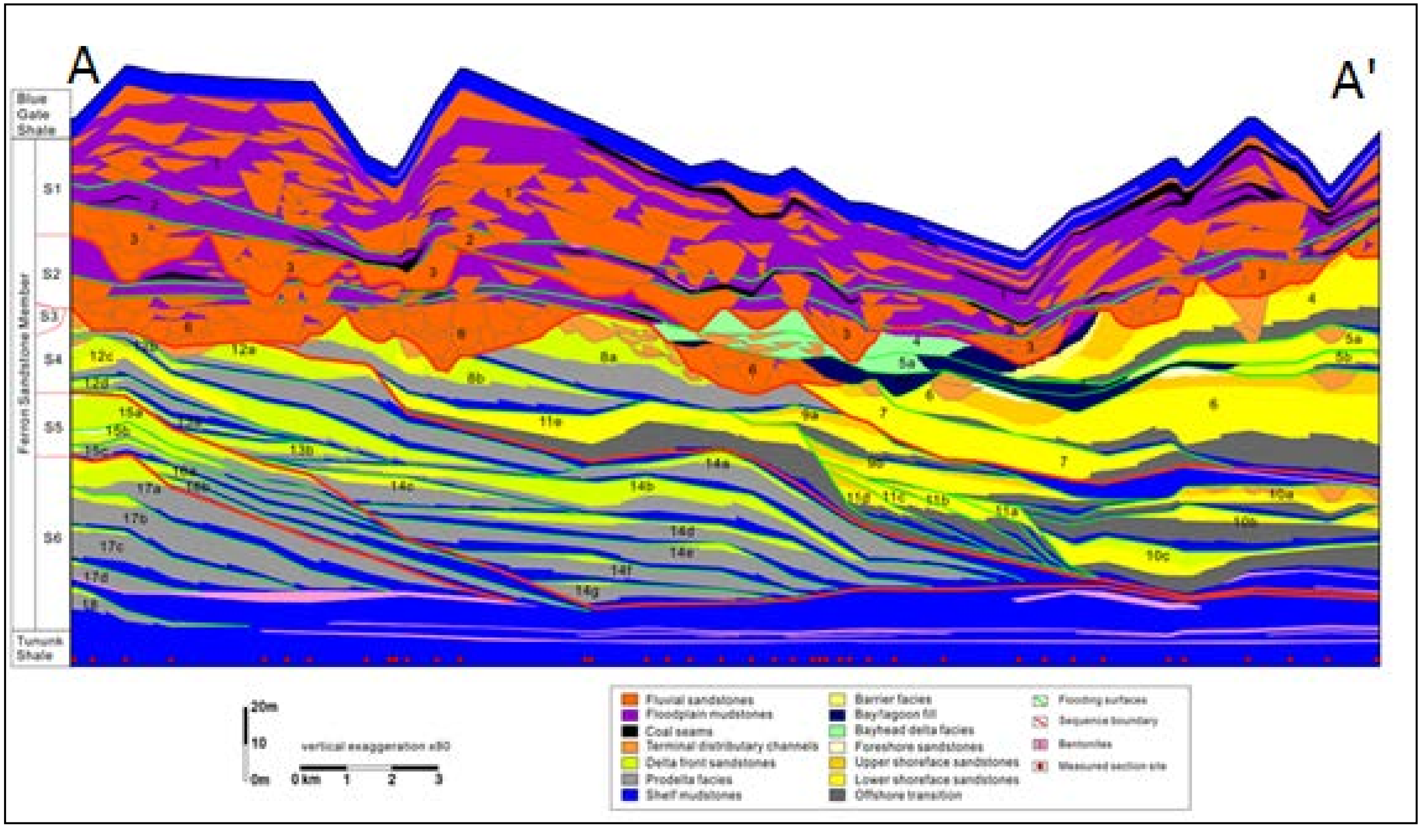

Figure 4.─Regional dip sequence stratigraphy of the Ferron Notom Deltaic Complex shows six high-frequency Milankovitch-scale depositional sequences (S6 to S1). Cross section outline is shown in Figure 3. The focus of this study is on floodplain deposits and paleosols (in purple) of sequence 1 (S1).

2.3 METHODOLOGY

Floodplain paleosols were examined in outcrop and trenched where covered or highly weathered. Stratigraphic sections were logged with an emphasis on paleosol descriptions (Retallack, 1988). The intensity of rooting or rooting index (R.I.) of paleosols was also tracked and recorded. Determination of rooting index (R.I.) of a paleosol in the succession was based on visual comparison of strata without any root trace (R.I. = 0) and well-rooted paleosols (R.I. = 5). Moderately rooted paleosols have a rooting index of 2 to 3.

Paleosol colors, aggregate sizes, and mottle proportions were described using a Munsell soil-color chart. Paleosol samples were collected at 30 cm intervals; they were dried and later impregnated with epoxy resin and cut into oriented thin-sections (51 x 76 mm, Spectrum Petrographics, Inc.). Whole thin sections were scanned using a regular paper scanner in order to see important paleosol features.

Thin-sections were examined under both plane- and cross-polarized light using an Olympus BX51 research petrographic microscope equipped with a 12.5 Mpx digital camera at Baylor University and a Zeiss AX10 petrographic microscope equipped with a 5 Mpx camera at Exxon Upstream Research Center. Identified features were observed under several magnifications (from 12.5 – 200 magnification). Microscopic organic matter was examined using ultraviolet fluorescence (UVf) to detect any preserved plant cellular structures.

Paleosol samples were also collected in paleosol profile at 10cm intervals for geochemical analysis. Prior to geochemical analysis, any surface contamination was removed from samples by washing. Samples were later dried, and pulverized using agate mortar and pestle. Inductively-coupled plasma mass spectroscopy and optical emission spectroscopy (ICP/MS & OES) techniques via a Li-metaborate fusion procedure were used to detect major and minor elements and their respective proportions. Data were reported for 10 major elements (Al, Si, Ti, Fe, Mn, Mg, Ca, Na, K, and P), 26 trace elements and 14 rare earth elements.

2.4 FACIES AND FACIES ASSOCIATIONS

Facies identified in sequence 1 include: channel-fill sandstone; tide-influenced heterolithic channel-fill; crevasse-splay sandstone, siltstone, and mudstone; levee sandstone and mudstone; abandoned-channel mudstone, siltstone, and very fine-grained sandstone; overbank mudstone and siltstone; floodplain-lake mudstone and siltstone; carbonaceous mudstone and siltstone; and coal (Fig. 6). Except for channel-fill deposits, most of the facies represent floodplain deposits. Floodplains are broadly divided into two sub-environments (Fisk 1944; Allen 1965), they are: (1) areas proximal to main channels, and (2) areas farther away from main channels (i.e., backswamps or flood basins). Levees and crevasse-splays constitute areas proximal to main channels, whereas other facies constitute the backswamp or floodbasin environments.

However, there are transition zones between these sub-environments. For example crevasse-splay channels may extend to a backswamp, whereas abandoned channels are transitional from the time of initial to full abandonment and may be overlain by floodplain backswamp deposits. Paleosols are developed in both sub-environments, adjacent and distal to channels. Mudstone paleosols develop mostly on floodplain-lake fills, and backswamp mudstones and siltstones. Siltstone and fine-grained sandstone paleosols developed on levees, crevasse-splays, abandoned channel-fills, and on the uppermost parts of trunk channel deposits. The proportion of mudstone paleosols to siltstone and very fine-grained sandstone paleosols in the studied interval is roughly 60: 40.

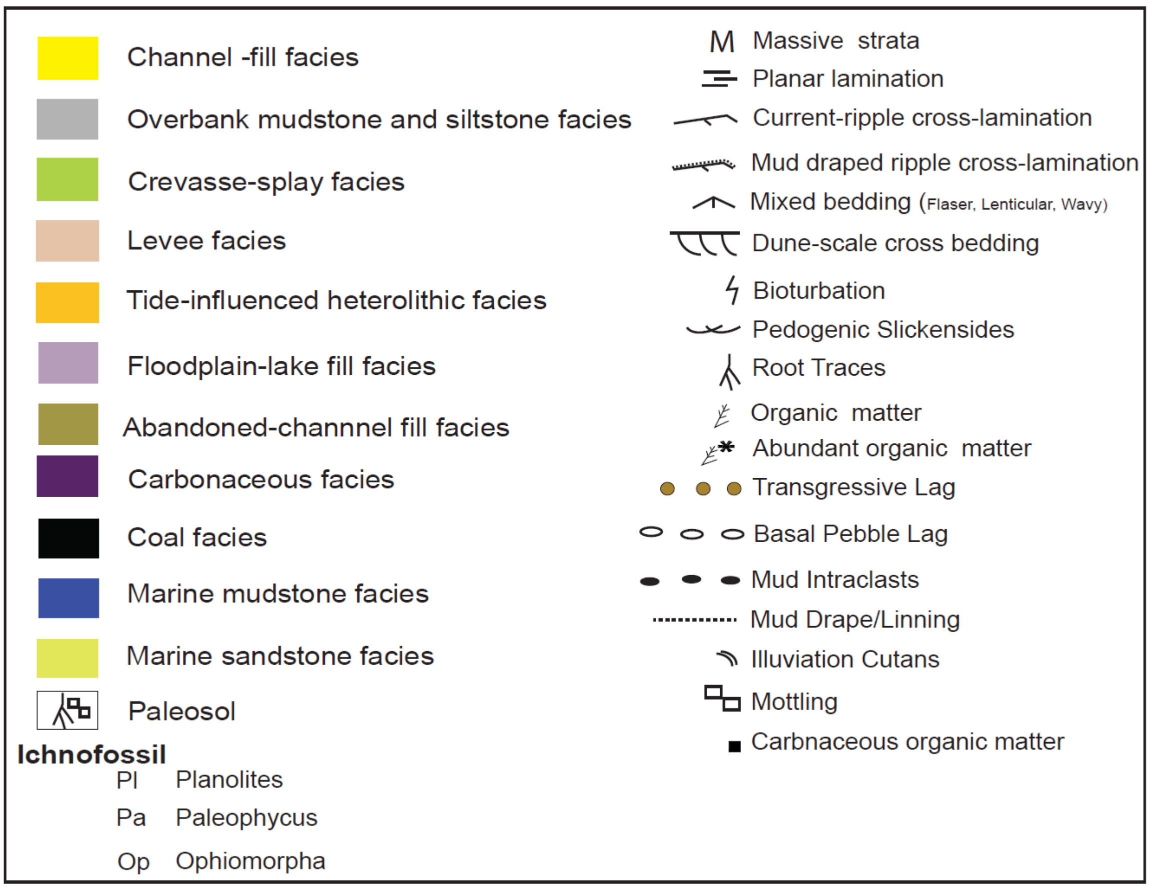

Figure 5.— Legend for Figure 6, 12, 13 and 14

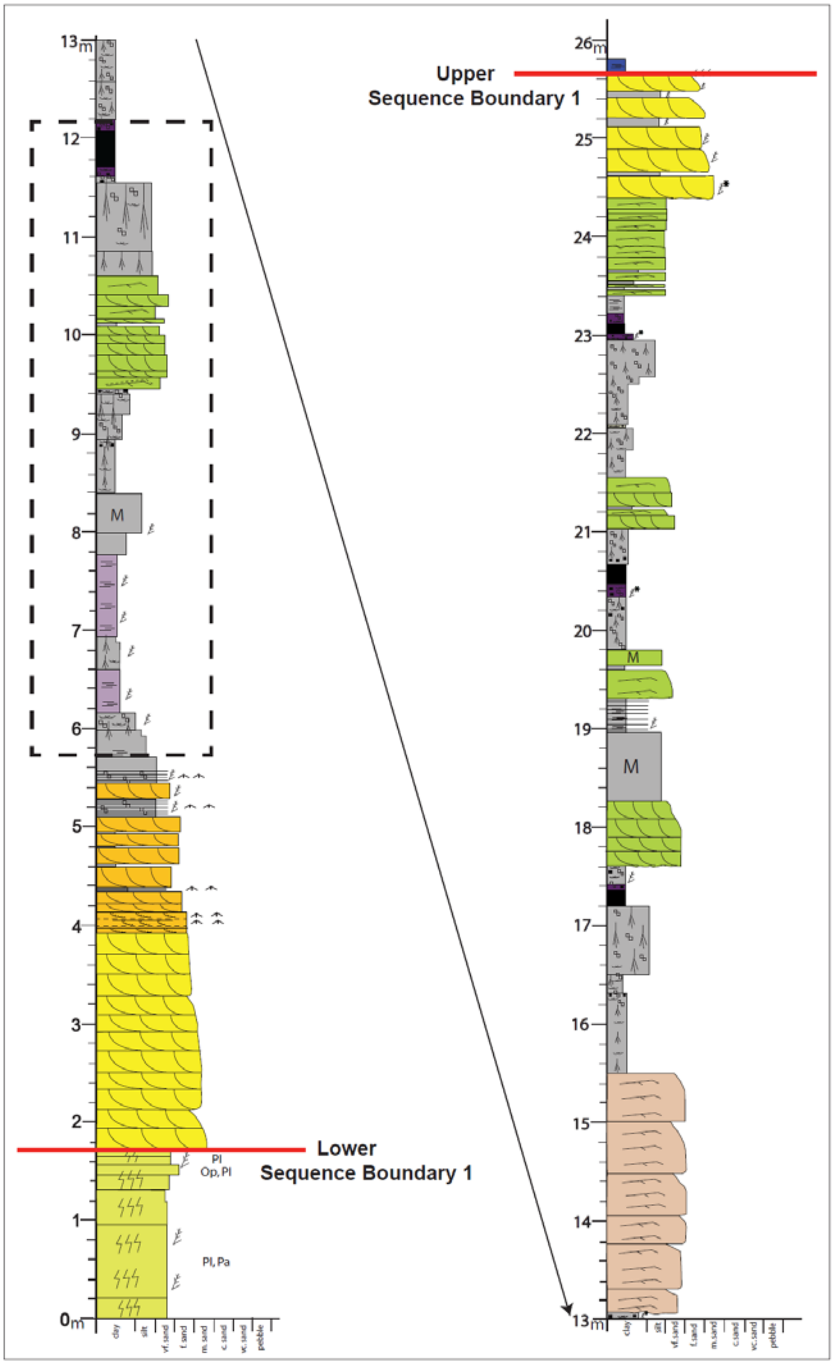

Figure 6.— Type measured section showing representative facies in sequence 1. The red lines mark the upper and lower boundaries of the sequence. The section in the dashed box is the same section in Figure 12 and 13, and in the cross-section in Figure 14. See legend in Figure 5.

2.5 PALEOSOL PROFILES

Paleosols in sequence 1 consist of weakly to well-developed multiple horizons that do not conform to original lithological contacts, and are distinguished in the field by their distinctive color and associated features. Horizon contacts can be gradational, diffuse, or sharp. Descriptions of the different types of horizons identified in this study, their thickness and their associated pedogenic features are summarized in Table 2. Master paleosol horizons are denoted by capital letters A, B, C, or O (Soil Survey Staff 1999; Retallack 2001). Subordinate letters (e.g., Bg, Bssg, or Btg) are used to distinguish the characteristics of similar master paleosol horizons based on specific distinguishing features (e.g., Bg = strong gleying or Btg = accumulation of clay and strong gleying) (Soil Survey Staff 1999; Retallack 2001; Table 2). The characteristics and significance of these distinguishing features will be discussed in detail in the next section.

A typical paleosol profile (Fig. 7) in this study consists of a lower undisturbed C or Cg horizon, typically with preserved sedimentary structures (e.g. parallel lamination or current ripple-cross lamination). This is succeeded by a gray, thick, rooted, and bioturbated B horizon (Bg, Bssg, or Btg) with weak to well-developed soil aggregates, vertic features, incipient clay richness and preserved organic matter. The B horizon is commonly overlain by a dark gray, A horizon containing more preserved organic matter. The A horizon may form the uppermost part of the paleosol profile, or may transition into more organic-rich O horizon that is characterized by carbonaceous mudstones and coal. Nonetheless, this is a simple description of the paleosol profiles observed in this study.

The description of paleosol profiles in Table 2 indicate overlap in characteristics between successive paleosol horizons, and these are denoted accordingly (e.g., AB, BC).

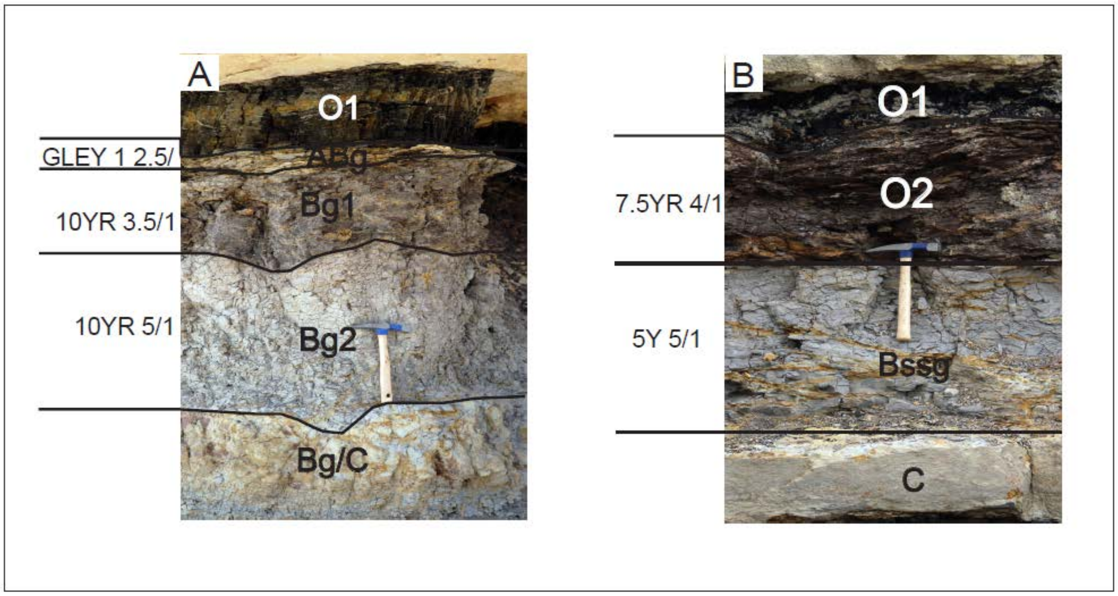

Figure 7.─ Paleosol profiles in sequence 1. **A**) Strongly gleyed, silty paleosol with multiple horizons. Bg horizons consist of fine to medium, weakly to moderately developed angular to subangular blocky ped structures and constituent redoximorphic features including Fe oxide pore linings. The paleosol is capped by a coaly organic-rich paleosol which consist of an O horizon. **B**) Strongly gleyed, muddy paleosol that consist of multiple horizons. The Bssg horizon contains abundant slickensides. It shows very weak to moderate ped development with constituent redoximorphic features, including iron pore linings. It is capped by a coaly organic-rich paleosol that has multiple O horizons.

Table 1.— Pedogenic features described from hydromorphic paleosols of the Ferron Notom Delta

Feature	Dimensions	Description	Interpretation
Biological Features			
Root traces	0.1 - 25 cm width < 5 - 60 cm depth of penetration	Vertically or sub-vertically oriented traces that taper and branch downward Preserved as carbonized films of organic matter, open branching voids or partially or completely clay-filled branching voids	Indicates subaerial exposure and vegetative growth (Retallack 1988, Leckie et al. 1989)
Faunal burrows	0.5 – 7 mm length 100 - 1500µm width	Vertical or sub-vertical tube- or worm-shaped features with curved bottoms Iron (Fe) oxide coatings burrow margins or impregnation of filled burrows	Burrowing activity of insects and worms that suggests subaerial exposure and surface stability (Retallack 2001; McCarthy and Plint 2000) Fe oxide coatings and impregnation indicate zones of aeration and oxidation in poorly drained paleosols
Organic matter	0.01 – 5 cm diameter	Dispersed or layered, opaque, dark carbonized fragment in soil matrix that lack discernible cellular structure	Preserved plant fragments, and likely fecal material. Abundance suggest widespread vegetative growth and preservation under poorly drained and reducing conditions (Wright 1992; Arndorff 1993; Leckie et al. 1989)

Table 1.─ Continued.

Feature	Dimensions	Description	Interpretation
Physical Features			
Peds	5 – 500 mm diameter	Stable aggregates of paleosols separated by surfaces of weakness (voids, planes) or by clay coatings (ped cutans) Very fine to coarse angular blocky to subangular blocky aggregates or coarse, wedge-shaped aggregates in clay-rich horizons	Result from a combination of biological processes (e.g., root activity, fauna burrowing), and physical processes (e.g., shrinking and swelling) due to repeated wetting and drying (Retallack 1988; 2001; Wright 1992; McCarthy and Plint 1999)
Pedogenic slickensides	Variable (0.5 - 50 cm) length	Striations and grooves on the surface of clay-smeared peds Form medium to large-scale arcuate slip surfaces bounded by wedge-shaped peds Associated with coatings on the surface of angular blocky to subangular blocky peds (stress cutans)	Form as consequence of differential movement of peds under stress due to shrink-swell processes in clay-rich caused by repeated episodes of wetting and drying during pedogenesis (Gray and Nickelsen 1989; Gustavson 1991)
Sepic-plasmic (birefringence or b- fabric)	Variable (40 – 2000µm) length	Alignment and reorientation of clays into distinct elongate zones that exhibit uniform to sweeping extinction patterns May align in one direction (masepic), two directions (bimasepic), around voids (vosepic), or around skeleton grains (skelsepic)	Microfabric developed as a result of pressure and tensile stresses exerted by shrink-swell processes that indicate repeated wetting and drying (Wright 1992; McCarthy and Plint 2003; Driese and Ober 2005; Kovda and Mermut 2010)

Table 1.— Continued.

Feature	Dimensions	Description	Interpretation
Voids	Variable (up to 500 µm) width	Planes, packing voids, channels and chambers	Planes and packing voids suggest shrink-swell processes due to repeated wetting and drying in paleosols (Brewer 1964) Channels form as a result of root activity, and chambers from as a result of faunal burrowing (Brewer 1964)
Redoximorphic Features			
Color		Dominance of low-chroma (N,1, and 2) colors with variations in hues (GLEY 1, 5Y, 2.5Y, 10YR, 7.5YR, 5YR) and values (1 to ≤ 7.5)	Result of strong gleying, which is loss of primary coloration as a result of Fe reduction in poorly drained soils (Wright 1992)
Mottling		Irregular colored patches on gleyed or gray paleosols; colors vary from light- to pale- to orange- to brownish yellow Percentage increases upward in profile from 1 to 30%	Result of local redox changes due to fluctuating drainage conditions (Duchaufour 1982; Wright 1992; Wright et al. 2000; Autin and Aslan 2001)
Ferruginous Coatings	10 – 1000 µm width	Dark red or dark brown simple coatings (actual surface coatings) to hypo-coatings (adjacent to, rather than on surface) around root traces, burrows, and voids	Formed in zones of aeration around openings under otherwise reducing conditions as paleosols became less saturated and better drained (McSweeney and Fastovsky 1987)

Table 1.— Continued.

Feature	Dimensions	Description	Interpretation
Ferruginous Nodules	10 – 250 µm diameter	Opaque or dark brown cubic, subrounded or irregular –shaped nodules with brownish orange diffuse outer boundaries; occur as concentrated or dispersed aggregates	Result of segregation of Fe oxides in paleosol matrix due to repeated wetting and drying conditions during pedogenic development (McCarthy and Plint 1999, 2003).
Textural Features			
Illuviated pedogenic clay	200 – 4000 µm width 600 – 6000 µm thickness	Bright yellow to orange clays that show diffuse to clear multiple bands (microlaminations) with and sharp contacts with surrounding matrix Occur as void margin coatings or dense complete or incomplete infillings of voids	Formed as a result of physical translocation of clay from lower to upper parts of the paleosol profile due to repeated wetting and drying (Wright 1992; 2003; Ufnar 2007) Laminations suggest successive addition of translocated clay
Pedorelicts	Variable (up to 3 mm) diameter	Small subrounded clayey aggregates often impregnated with Fe oxides, and may appear as floating in showing no link to paleosol matrix	Eroded, reworked and transported remnants of previously formed paleosols incorporated into parent material of younger paleosols (Ellis and Mellor 1995; McCarthy and Plint 1998) Suggests truncation of upper portion of older paleosols.
Papules	1000 – 2000 µm width	Disintegrated illuviated clays that are partially dispersed or incorporated into the paleosol matrix.	Movement and displacement within the soil profile due to shrink-swell processes or rooting activity (Kemp 1985; McCarthy and Plint 1998)

Table 2.— Summary description of hydromorphic paleosol horizons in the Ferron Notom Delta

Horizon	Thickness	Description	Features
O	20 – 70 cm	Dark coaly and carbonaceous mudstone or siltstone horizon. Uppermost horizon in paleosol profiles	High organic matter content; horizon top consist of *Teredolites* and *Thalassinoides*
Ag or ABg	5 – 50cm	Muddy to silty organic-rich horizon below O horizon; could also be the uppermost horizon in paleosol profile when there is no O horizon Transitional between Ag and Bg due to commonly thin Ag horizon	High organic matter content but relatively less than O horizon content; strong gleying; low chroma colors significant mottling (15 – 30% surface area); few to common root traces; weakly developed, very fine to fine, angular blocky to subangular blocky peds
Bg	20 – 150 cm	Silty to sandy horizon below Ag or ABg horizons	Relatively low organic matter content compared to O, Ag or ABg horizons; strong gleying; low chroma colors; significant mottling (10 – 20% surface area); few to common root traces; few illuviated clays; weakly developed, fine to medium, angular blocky to subangular blocky peds; rare to few slickensides.
Bssg	40 – 200 cm	Mudstone horizon that develop below Ag or ABg horizons	Relatively low organic matter content compared to O, A or ABg horizons; strong gleying; low chroma colors; significant mottling (10 – 20%); common to abundant root traces; few to substantial illuviated clay accumulation; well developed, coarse wedge-shaped peds and abundant slickensides

Table 2.─ Continued

Horizon	Thickness	Description	Features
Btg	40 – 70 cm	Silty to sandy horizon below Ag or ABg horizons	Relatively low organic matter content compared to O, Ag or ABg horizons; strong gleying; low chroma colors; significant mottling (10 to 20% surface area); common to abundant root traces; significant illuviated clay accumulation; moderately to well-developed medium to coarse angular blocky to subangular blocky peds; rare to few slickensides
BCg	10 – 50 cm	Muddy to sandy horizon below Ag, ABg, Bg, Bssg or Btg horizons. Transitional between these horizons and the underlying Cg horizon	Relatively low organic matter content compared to O, Ag or ABg horizons; few to common preserved sedimentary structures strong gleying; low chroma colors; some mottling (1 -5% surface area); few to very few root traces; rare illuviated clay accumulation; none to very weakly developed ped structures; rare to few slickensides
C or Cg	10 – 20 cm	Parent material or strata with no pedogenic alteration Bottom horizon in paleosol profiles	Preserved sedimentary structures; minimal to substantial gleying; some mottling (1- 5% surface area); no pedogenic features

2.6 PALEOSOL FEATURES

A series of macroscopic and microscopic biological, physical, redoximorphic, and textural features were observed that helped to identify paleosols in the studied area. Some specific features can be observed both in outcrop and under the microscope. The characteristics and interpretation of these features are discussed below and are summarized in Table 1.

2.6.1 Biological Features

2.6.1.1 Root traces

Description─ Paleosols in this study are characterized by an abundance of preserved vertical and sub-vertically oriented root traces ranging from 0.1 to 25 cm wide (Fig. 8A, 8B, 8C). The root traces taper and branch downward from the top of the paleosol profile into smaller rootlets and root hairs with increasing depth. Patterns vary from shallow (< 5cm) to relatively deep penetrating roots (up to 60cm). Modes of preservation of roots in these paleosols vary. Most are preserved as partly or fully carbonized (lignitic) impressions of the original plant material. In some cases, the original plant material has completely decayed or its carbonized impression has been removed, leaving a void that is either filled with illuviated clay or left unfilled as an open void. Some elongated root traces have been compressed due to compaction (Fig. 8C). There is no evidence of calcification of roots, such as is common in more arid settings. Outer margins of preserved root traces consist of Fe oxide coatings. Carbonized root traces observed under UVf revealed no preserved original plant tissue or cellular structure, except total carbonization. In this study, root traces often penetrate AB, B and BC horizons (Table 1, Table 2).

Interpretations─ Fossil root traces are diagnostic features of post-Silurian paleosols (McSweeney and Fastovsky 1987; Fastovsky and McSweeney 1987; Retallack 1988, 1997; Leckie et al. 1989; Wright 1992). Rooting in Ferron paleosols indicates subaerial exposure and plant colonization that led to soil development (Retallack 1988). Extensive rooting suggests abundant vegetative growth during the development of these paleosols (Leckie et al. 1989). The carbonization of original organic fossil-root matter suggests a predominance of reducing (anaerobic) conditions that prevented oxidation or decay (Wright et al. 2000). The depth of penetration of preserved root traces suggests a shallow water table that fluctuated from a shallow depth of less than 5 cm from the surface up to a depth of 60 cm or at most 100 cm (if post-burial compaction is considered). This also indicates an alternation of very poor drainage conditions to relatively better drainage conditions (Soil Survey Staff 1993).

2.6.1.2 Burrows

Description─ Vertical or sub-vertical preserved burrows in this study are differentiated from root traces by their non-branching curved and closed bottoms, and their tube- or worm-shaped appearance that may appear as segmented (Fig. 8D). Apart from *Thalassinoides* and *Teredolites* associated with coaly O horizons (Table 2) that were observed in outcrop, burrows observed in this study were identified under the microscope.

The lengths of these vary from 0.5 to 7 mm. The margins of these microscopic burrows are coated with iron (Fe) oxides or are lined by thin organic coatings. In some cases preserved and completely filled burrows are totally impregnated by iron (Fe) oxides.

Interpretation─ Preserved burrows in these paleosols are attributed to the activity of insects and worms (Retallack 2001; McCarthy and Plint 2003) and suggest subaerial exposure and surface stability. Iron (Fe) oxide coating and impregnation of burrows and burrow margins suggest they were likely zones of aeration or oxidation in poorly drained paleosols under otherwise reducing conditions.

2.6.1.3 Organic matter

Description─ Paleosols contain little to abundantly preserved organic matter (OM: Fig. 8E). OM is not peculiar to any paleosol horizon in this study, but paleosol profiles show an upward increase in amount of preserved OM, which contributes to the upward darkening in color observed in paleosol profiles (Fig. 7; Table 2). Microscopic evidence also shows dispersed OM in the soil matrix. Organic materials are dark and opaque and they reveal no cellular structure under UVf. Coals contain the highest proportion of organic matter in the studied interval, followed by carbonaceous mudstones and siltstones. OM is typically layered in carbonaceous mudstones (Fig. 8F). There are no thick coal seams in the studied interval, and the thickness of coal beds, excluding those of associated carbonaceous strata, varies from 20 cm to 30 cm. The combined thickness of coals and associated carbonaceous strata varies from 20 cm to 70 cm.

Interpretation─ Organic matter observed in the paleosols represents mostly carbonized plant fragments and some soil animal waste. Abundance and proportion of OM in these paleosols suggests widespread vegetative growth (Leckie et al. 1989). Some OM was transported as macerated detritus and re-deposited during seasonal flood events (Wright et al. 2000). Preservation of high amounts of OM suggests maintenance of reducing and poorly drained conditions (Arndorff, 1993), which caused reduction in the rate of decomposition of OM (Wright 1992). OM layering in carbonaceous mudstones suggests ponding and accumulation of plant material due to water-table rise.

2.6.2 Physical Features

2.6.2.1 Peds

Description─ Stable aggregates of soils and paleosols are often referred to as peds (Retallack 1988). This study shows weakly- to well-developed angular to subangular blocky peds (Fig. 9A) that increase in diameter from fine (5 - 10 mm: Munsell soil-color chart) to coarse (20 – 50 mm) with depth. Coarse, wedge-shaped ped structures often characterize clayey 'Bssg' horizons. Peds are separated from each other on all sides by voids, and ped surfaces consist of clay coatings often called ped cutans (Brewer 1964).

Interpretation─ Peds formed by destruction of original sedimentary structures caused by pedoturbation, which is a combination of biological processes, such as plant root activity, fauna burrowing, and physical processes such as shrink-swell, caused by repeated wetting and drying in soils (Wright 1992; McCarthy and Plint 1999).

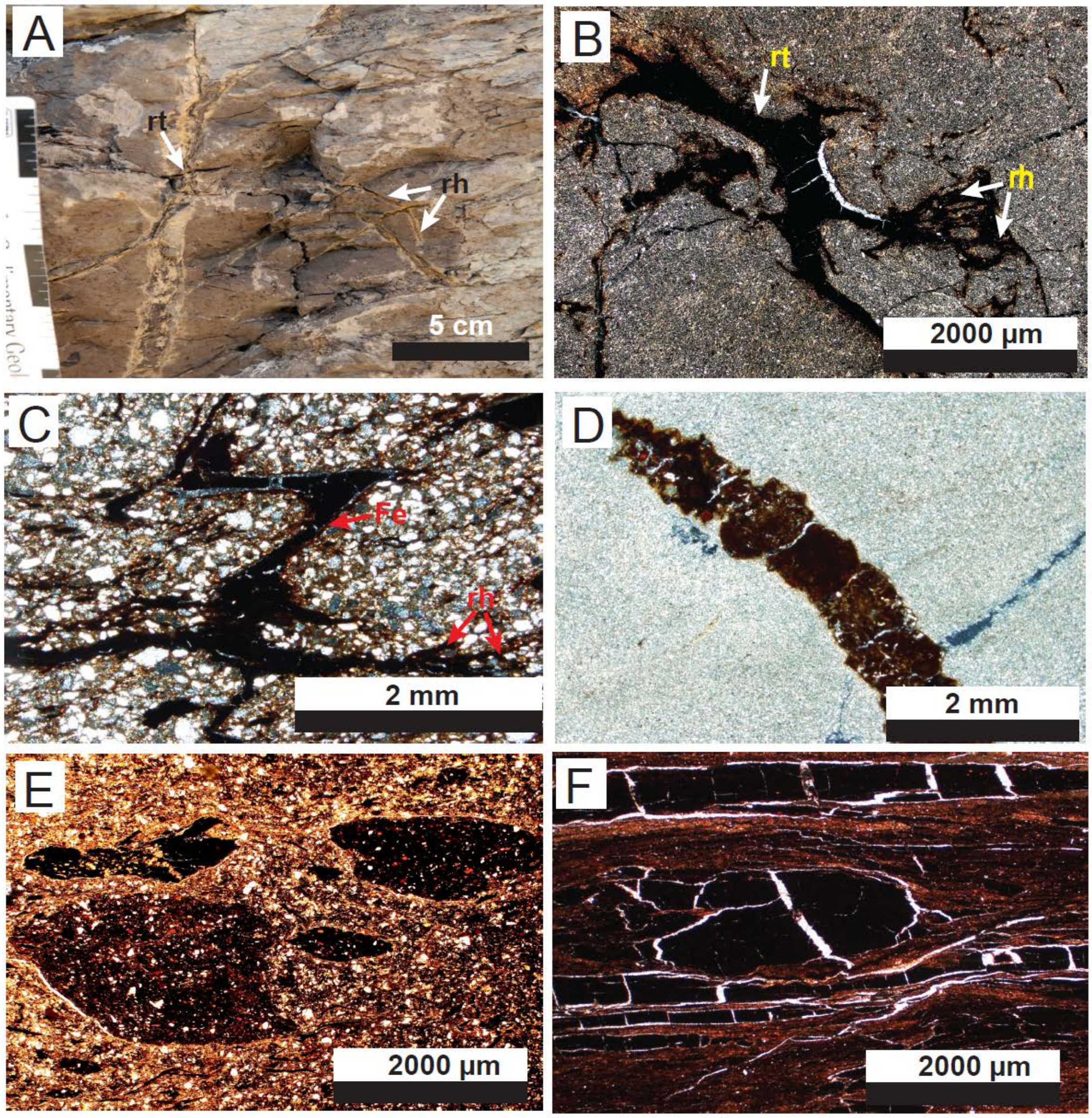

Figure 8.─ Biological macroscopic and microscopic features identified in Ferron Notom paleosols. **A**) Downward-branching carbonized root traces (rt) with attached root hairs (rh). **B**) Branching carbonized root trace (rt) with root hairs (rh) in a drab paleosol matrix. **C**) Compressed carbonized root trace with Iron (Fe) oxide coating on it margins. Compression is likely due to compaction. **D**) Thin section of a segmented fossil faunal burrow that is impregnated with Fe oxide. **E**) Dispersed organic matter in soil matrix. **F**) Layered organic matter in carbonaceous strata.

2.6.2.2 Pedogenic slickensides

Description─ Larger-scale arcuate (concave-convex), polished slip surfaces bounded by wedge-shaped coarse peds are termed pedogenic slickensides (Fig. 9B; Gray and Nickelsen 1989; Southard et al., 2011). They constitute ‘Bssg’ horizons, which are clay-rich horizons (Table 2). Pedogenic slickensides were also observed in other horizons that were not strictly clay-rich, where they constitute striations or grooves on clay-smeared surfaces of peds (Gray and Nickelsen 1989). These are called stress cutans (or pressure face) (Buol et al. 1973; Leckie et al. 1989). In general, this study shows that pedogenic slickensides are more pronounced in mudstone paleosols than in siltstone paleosols.

Interpretation─ Pedogenic slickensides form as a consequence of differential movement of peds under stress due to shrink-swell processes during pedogenesis in clay-rich paleosols (Brewer 1964; Gary and Nickelsen 1989; Leckie et al. 1989; Gustavson 1991; Retallack 2001; Driese and Ober 2005). Slickensides also indicate subaerial exposure (Gary and Nickelsen 1989). Slickensides associated with stress cutans (pressure face) in clay–rich or relatively less clay-rich paleosols form by the pressing of peds against one another (Retallack 2001) due to shrink-swell processes (Brewer 1964; Buol et al. 1973; Leckie et al. 1989).

2.6.2.3 Sepic-plasmic (birefringence, b-) fabric

Description─ This microfabric is visible under cross-polarized light, whereby domains of clays are reoriented and aligned into distinct elongate (or birefringent) zones, and exhibit uniform to sweeping extinction patterns within the soil matrix (Brewer 1964; McCarthy and Plint 1999). Figure (9C, 9D) show two examples of sepic-plasmic fabric: masepic fabric (= one preferred orientation) and vosepic fabric (= oriented clays around voids) observed in clay-rich 'Bssg' horizons where they are most common. Birefringent fabrics are best developed in mudstone paleosols, or siltstone paleosols that have a high proportion of clay.

Interpretation─ Sepic-plasmic fabrics are the product of pressure and tensile stresses within soils caused by shrink-swell processes, which resulted in individual clay reorientation and alignment into planar or elongated zones (Wright 1992; Kovda and Mermut 2010). Shrink-swell processes indicate repeated wetting and drying of the soil matrix under different water tensions (Kemp 1985; McCarthy and Plint 1999, 2003).

2.6.2.4 Voids

Description─ Clearly identified voids in the matrix of these paleosols (Fig. 9E, 9F) include; planes, packing voids, channels, and chambers (Brewer 1964; Bullock et al. 1985). However, a constraint on clear identification and interpretation of voids is the thin-section preparation process (i.e., epoxy impregnation and drying), which may enhance actual voids or create artifacts in paleosol samples.

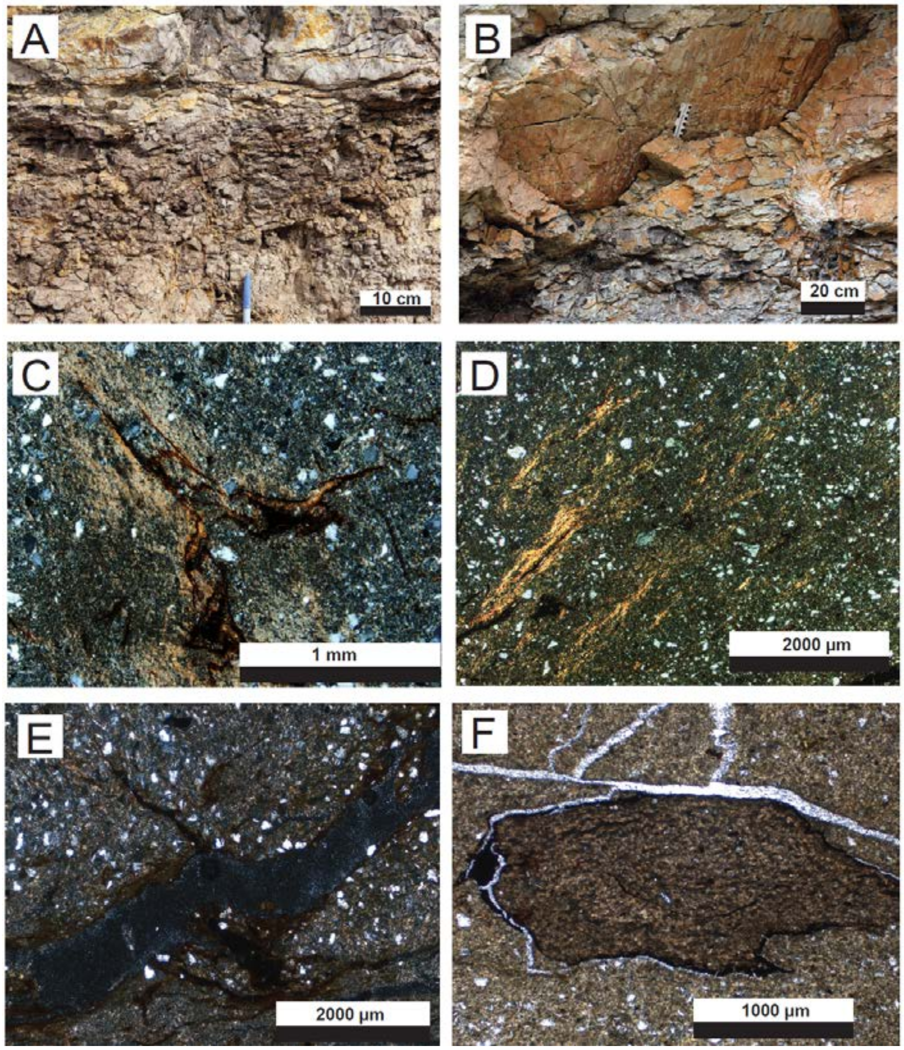

Figure 9.─ Physical macroscopic and microscopic features identified in Ferron Notom paleosols. **A**) Medium to coarse, angular to subangular blocky peds in a well rooted, and well developed Btg horizon of a siltstone paleosol (paleo-Alfisol). **B**) Medium to coarse, wedge-shaped peds showing abundant slickensides in a Bssg horizon of a mudstone paleosol (paleo-Vertisol). **C**) Clay reorientation and alignment around a root channel indicating a vosepic b-fabric. **D**) Clay re-orientation in a single direction indicating a masepic b-fabric. **E**) A root channel represents a void in a paleosol matrix. **F**) A plane, seen around an organic fragment in the picture, represents a type of void in the paleosol matrix.

Interpretation─ Nonetheless, planes and packing voids are attributed to shrink-swell processes as a result of repeated wetting and drying (Brewer 1964; McCarthy and Plint 1999). Channels (Fig. 9E) are attributed to the activity of plant roots, whereas chambers (Fig. 9F) are a result of faunal burrowing in paleosols (Brewer, 1964).

2.6.3 Redoximorphic Features

2.6.3.1 Color

Description─ Ferron hydromorphic paleosols show a dominance of low chroma (i.e., N, 1, and 2) gray color with variations in values (1 to ≤ 7.5), and hues (GLEY 1, 5Y, 2.5Y, 10YR, 7.5YR, and 5YR: Munsell soil-color chart) (Fig. 7, 8A, 9A, 9B).

Interpretation─ The dominance of gray, low-chroma colors of paleosols is attributed to gleying, which represents the loss of primary color as a result of iron (Fe) reduction in paleosols (Wright 1992). This is a well-documented phenomenon in hydromorphic paleosols that are subjected to long periods of soil saturation due to a high water table (Bown and Kraus 1987; Retallack 1997; Wright 1992; Arndorff 1993; Driese and Ober 2005).

2.6.3.2 Mottling

Description─ Ferron paleosols show pervasive mottling, manifested as irregularly colored patches or spots on predominantly gray-colored paleosols and as coatings around preserved root traces (Fig. 10A). Mottle colors vary from light-gray to pale-orange, or pale-brownish-yellow. The surface area covered by mottles increases upward in observed paleosol profiles from less than 1% to about 30%.

Interpretation— Mottling is interpreted as a reflection of localized redox changes due to fluctuating drainage conditions in the paleosols (Duchaufour 1982; Wright et al. 2000; Autin and Aslan 2001). Gray mottles may represent Fe-depletion zones, whereas light-, pale-, or brownish-yellow mottles indicate localized zones of Fe oxidation and perhaps the formation of jarosite, goethite, limonite, or lepidocrocite after the oxidation of pyrite, which may be associated with organic matter in paleosols.

2.6.3.3 Ferruginous coatings

Description— Observations from both outcrop and thin sections consistently show dark-red or dark-brown coatings of Fe oxides and hydroxides on the inner and outer edges of preserved root traces (Fig. 8C, Fig. 10B). Coatings vary from simple (actual surface coatings) to hypo-coatings (adjacent to, rather than on the surface).

Interpretation— Simple and hypo-coatings of iron oxide along root traces suggest local oxidation zones or zones of aeration around root traces under otherwise reducing conditions, indicating that paleosols became less saturated and better drained with time (McSweeney and Fastovsky 1987).

2.6.3.4 Ferruginous nodules

Description─ Ferruginous nodules identified in these paleosols are opaque or dark brown (under cross polars), with orange-colored and diffuse outer boundaries. They have cubic, subrounded or irregular shapes, and occur as concentrated or dispersed aggregates. They may occur in isolated portions of the paleosol matrix or around root channels (Fig. 10C, Fig. 10D).

Interpretation─ Opaque, dark brown nodules shown in Figure 10C and 10D suggest that they are pyrite nodules probably associated with decomposition of organic matter in the soil under better drainage conditions, and were later oxidized to goethite or limonite. Ferruginous nodules suggest segregation of iron (Fe) oxides in the paleosol matrix due to repeated wetting and drying conditions during pedogenic development (McCarthy and Plint 1999, 2003).

2.6.4 Textural Features

2.6.4.1 Illuviated pedogenic clay

Description─ In the studied interval Bg, Bssg, and Btg horizons are characterized by bright yellow to orange, sometimes iron (Fe) oxide-stained clays that show diffuse to clear multiple bands (Fig. 11A, 11B).They appear as dense complete or incomplete infil-lings in voids within the soil matrix, and may also coat the margins of voids or pores. Most of the voids they fill or coat are those left by disintegrated carbonized root traces. When observed in outcrop, they are relatively darker than the adjacent peds. Under the microscope, illuviated clays appear as discrete units with clear or sharp boundaries and exhibit high birefringence, typically in conjunction with sweeping extinction patterns. It was also common to find more illuviated clays in B horizons of siltstone and fine-grained sandstone paleosols than in mudstone paleosols.

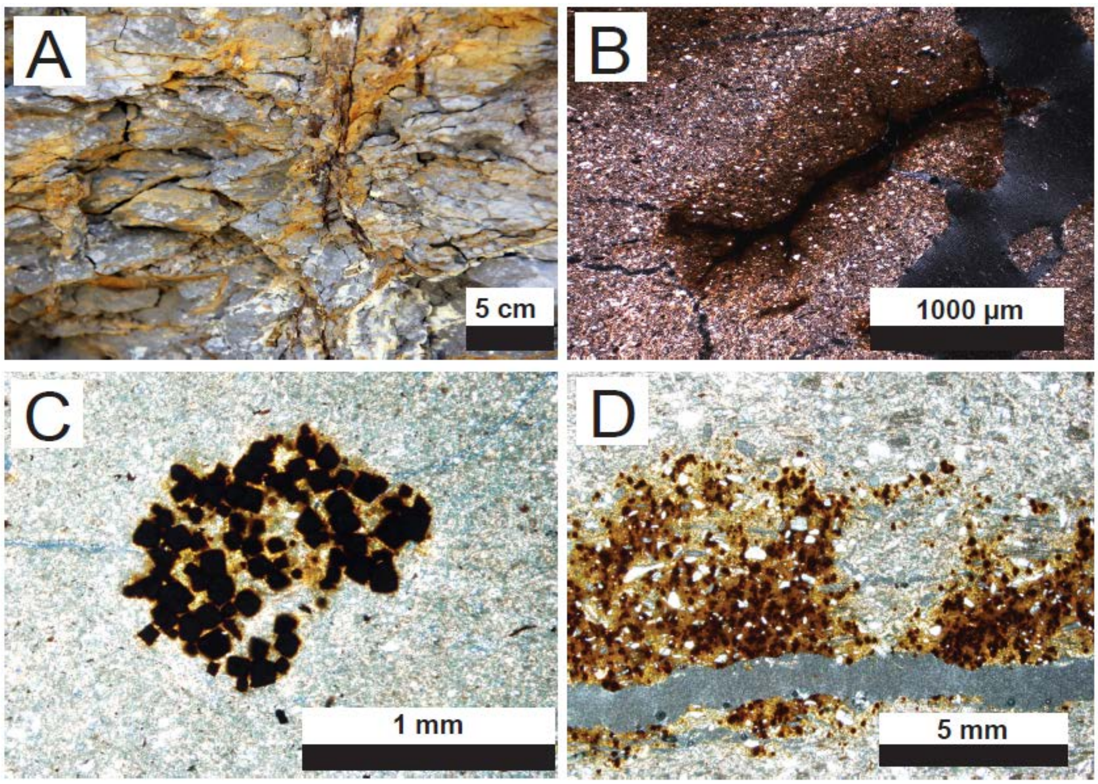

Figure 10.─ Color and redoximorphic features identified in Ferron Notom paleosols. **A**) Gray, light yellow, and orange mottles on a strongly gleyed, rooted paleosol (not the carbonaceous penetrating root trace and Fe oxide coatings along its margins). **B**) Simple and hypo-coatings of Fe oxide around a carbonaceous root trace. **C**) Concentrated aggregates of cubic or subrounded ferruginous nodules in paleosol matrix. Theses nodules are likely pyrite nodules that have oxidized to jarosite. **D**) Dispersed irregularly shaped nodules around a void in a paleosol matrix.

Interpretation— The occurrence of illuviated clays in paleosol horizons is attributed to lessivage, which is the repetitive process of removing clay materials in suspension from an upper horizon (eluviation) to a lower horizon where they accumulate (illuviation) (Wright 1992; Driese and Ober, 2005, McCarthy and Plint 1999, 2003; Ufnar et al. 2005). This process is favored by water-table fluctuations in soils, which allows for eluviation when the soil is saturated (poorly drained) due to high water table and illuviation when it is relatively dry (well drained) due to a low water table. Therefore, illuviation is not favored when the soil is continuously saturated (McSweeney and Fastovsky 1987; Retallack 1988).

This periodic or successive accumulation of clay is reflected by the microscopic bands and layers (micro-stratification or micro-lamination) observed in illuviated clays (Kemp 1985; McSweeney and Fastovsky, 1987; McCarthy and Plint 1999, 2003). The time required for repeated fluctuation of the water table and substantial accumulation of these clays in paleosols suggests that illuviation is a rather slow process (Wright 1992; Retallack 2001; Ufnar, 2006, 2007). Bg and Bssg horizons are not true argillic (illuviated clay-rich) horizons but may be characterized by incipient or substantial clay accumulation (Retallack 2001). However, 'Btg' horizons represent true argillic horizons that contain significant illuviated clay accumulations (Retallack 2001, Ufnar et al. 2005; Ufnar 2006, 2007).

In addition, the observed high occurrence of illuviated clay in siltstone and fine-grained sandstone paleosols is likely a function of porosity. Translocation of clay would have been easier in relatively porous and permeable siltstone and fine-grained sandstone paleosols than in cohesive mudstone paleosols. Illuviated clays in clay-rich mudstone paleosols can also be degraded due to repeated shrinking and swelling, which are more pronounced in them. The relatively dark color of illuviated clays observed in outcrop may be a result of incorporation of finely disseminated Fe-Mn oxides or possibly their organic-matter content.

2.6.4.2 Pedorelicts and papules

Description— Remnants of previously formed paleosols incorporated into successively younger paleosols are called pedorelicts (Fig. 11D). They are identified as small subrounded clayey aggregates often impregnated with iron (Fe) oxides and may appear to be floating in the soil matrix or have no link to the pedogenic features of the surrounding paleosol matrix. Pedorelicts are not peculiar to any paleosol horizon and are common in the Ferron. When illuviated clays appear to have disintegrated and are partially dispersed or incorporated into the soil matrix after their accumulation, they are called papules (Fig. 11C). Papules are common in Bg, Bssg, and Btg horizons of the studied paleosols.

Interpretation— Pedorelicts suggest erosion, reworking and transportation of mostly upper portions of previously formed paleosols during floods, and successive incorporation into younger sediments (potential parent material) that then undergo subsequent pedogenic modification (Fastovsky and McSweeney 1987; Ellis and Mellor 1995; McCarthy and Plint 1998, 1999, 2003; Flaig et al. 2013).

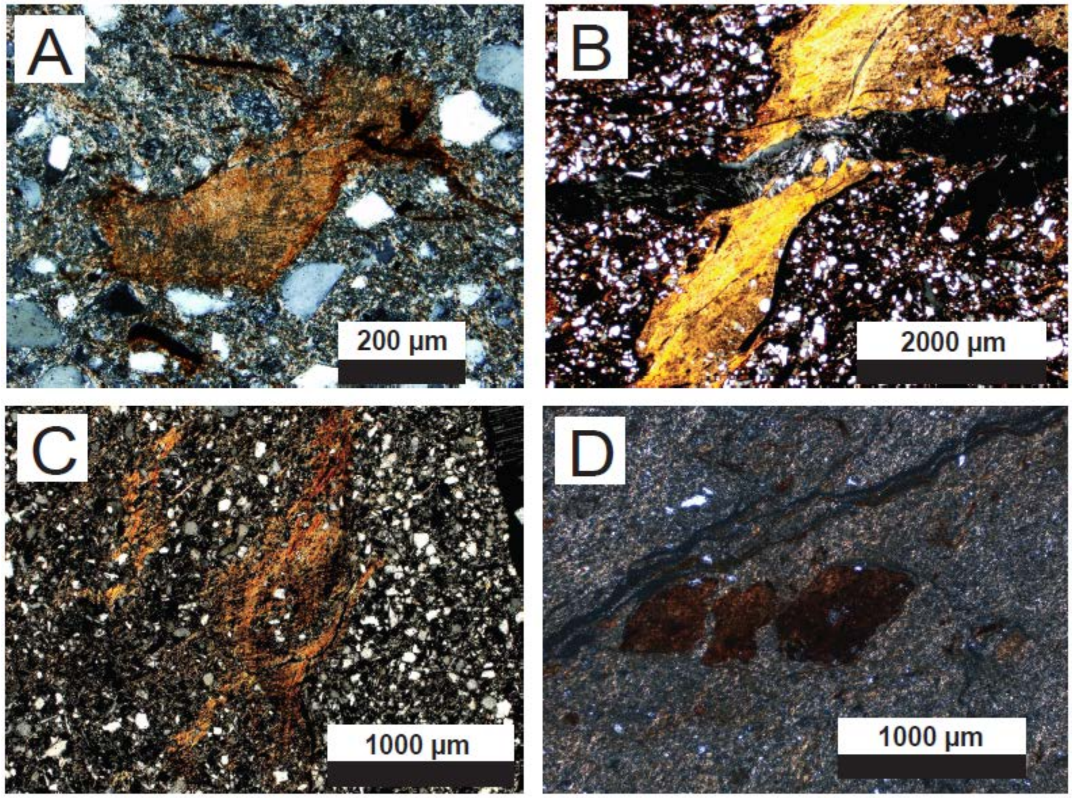

Figure 11.─ Textural features identified in Ferron Notom paleosols. **A**) Microlaminated, void-filling illuviated clay from Bg horizon. The void appears to be a root channel. Notice the Fe oxide coatings on the margins of the void. **B**) Void-filling, bright yellow illuviated clay with clear and sharp boundaries in a Btg horizon. **C**) Degraded illuviated clay from a Btg horizon that has partially dispersed into the soil matrix. This is often referred to as a papule. **D**) Iron oxide-impregnated, subrounded pedorelict in paleosol matrix.

They are good indicators of erosion of A or AB horizons prior to soil burial and preservation. Papules, which are disintegrated and dispersed illuviated clays within the soil matrix, are likely products of movement and displacement within the soil profile that is caused by successive shrink-swell processes related to variability in soil saturation state during development (Kemp 1985, McCarthy and Plint 1998). Movement and displacement of papules may also be due to rooting activity.

2.7 PALEOSOL MATURITY AND DEVELOPMENT

The complexity and thickness of horizonation in paleosols can be used as an index for the length of time for pedogenic development and paleosol maturity (Wright 1992). Therefore, paleosols with weak horizon development (e.g., Ag-Cg) are relatively poorly developed and immature, requiring shorter time-periods for development, compared to those with well-defined horizons (e.g., Ag-Bg-Cg, Ag-Bssg-Bg-Cg, or Ag-Btg-Bg-Cg), which are better developed and relatively mature.

Poorly developed paleosols with weak horizon development (e.g., Ag-Cg), as are observed in this study, are similar to modern-day Entisols, whereas those with relatively better-developed horizons (e.g., Ag-Bg-Cg, Ag-Bssg-Bg-Cg, and Ag-Btg-Bg-Cg) are similar to modern-day Inceptisols, Vertisols, and Alfisols (Soil Survey Staff 1999). If the decompacted thickness of coals and associated carbonaceous strata are considered, they meet the requirement (≥ 40 cm) for classifications as paleo-Histosols, similar to modern-day Histosols with characteristic O horizons (Soil Survey Staff 1999).

Entisols may develop in tens to a few hundred years (Retallack 2001). Inceptisols and Vertisols may also develop in a similar time interval, but incipient illuviated clay accumulation in some horizons observed in this study suggests that they developed in more than a few thousand years (Birkeland, 1999). Alfisols, on the other hand, may develop in a few thousands to tens of thousands of years (Birkeland 1999; Retallack 2001). The modern analogs to these paleosol types are currently developing in humid tropical fluvio-deltaic wetlands of southeast Asia (e.g., Mekong, Rajang, and Mahakam Delta Complexes) (Arndorff 1993; Nummedal et al. 2003; Staub and Gastaldo 2003).

2.8 PALEOENVIRONMENTAL INTERPRETATION OF PALEOSOLS

The pattern of pedogenic development of paleosols in the Ferron Notom Delta is distinct and consistent based upon the observations presented previously. The dull gray, low-chroma colors of paleosols, the preservation of high amounts of organic matter and carbonized root traces, and the association of paleosols with carbonaceous mudstones and coals, suggest poorly-drained and reducing conditions, attributable to a persistent and shallow water-table across the floodplain (Leckie et al. 1989; Besly and Fielding 1989; McCarthy and Plint 1999).

However, the presence of illuviated clay, development of weak to well-developed ped structures, redoximorphic features, and the presence of vertic (i.e., vertisol-like: Southard et al., 2011) features that indicate shrink-and-swell processes (e.g., slickensides, birefringent fabrics, and voids) suggest periodic soil drainage and drying because of episodic lowering of the shallow water-table (McCarthy and Plint 1999; Wright et al. 2000; Autin and Aslan 2001; Driese and Ober 2005).

These observations indicate that periods of pedogenic development, which followed sedimentation and subaerial exposure, were characterized by episodic wet and dry conditions, as a direct result of a fluctuating shallow water-table (Leckie et al. 1989; Autin and Aslan 2001). Nonetheless, the effect of wet and poorly drained conditions appears to be dominant (Wright 1989; Besly and Fielding 1989). This suggests that in most of the paleosols, wet periods, with poor drainage conditions were longer than dry periods characterized by relatively better (or moderate) soil drainage conditions (Wright et al. 2000).

The absence of sphaerosiderite, a common microscopic feature in poorly drained soils may be related to pH conditions of the depositional environment because sphaerosiderite formation requires a pH close to neutral or just below neutral (Ashley et al. 2013). The absence of sphaerosiderite, a common feature in poorly drained hydromorphic soils (McCarthy and Plint 1999, 2003; Driese and Ober 2005, Ludvigson et al. 2013), may also suggest the existence of poorly-drained conditions, but perhaps without sufficient organic biomass to drive microbial mediation (Driese et al., 2010; Ludvigson et al., 2013.

In the studied interval, the maximum organic-layer (coal plus carbonaceous strata) thickness is less than 5 m, and about 10 m for the entire Ferron Notom Delta. This thickness is negligible compared to the coal seam thickness in the Ferron Last Chance (Ryer and Langer 1980; Ryer 1981), and Ferron Vernal Deltaic complexes, which contains a coal-bed methane gas (CBM) field (Edwards et al. 2005). This relatively low abundance of organic matter may suggest high rates of sediment deposition and/or erosion in the studied interval and the Ferron Notom in general. This could have prevented substantial organic accumulation, which drives microbial mediation.

In addition, the persistence of fluctuating wet and dry periods during pedogenic development depends on the length of exposure of the soil within the zone of pedogenic modification (Wright 1992), which on the floodplain, is dependent on the frequency of floodplain sedimentation and/or erosional events (Kraus 1999). Therefore, the maturity of paleosols is directly tied to sedimentation rates in floodplain environments.

2.9 PALEOSOL GEOCHEMISTRY

The bulk geochemical analysis of paleosols reveals major, trace, and rare-earth elements that were used to track the intensity of weathering in selected paleosol profiles. The chemical index of alteration (CIA), which was proposed by Nesbitt and Young (1982), represents an index for measuring the intensity of weathering of feldspar minerals and their hydration to form clay minerals. It is based on the premise that as clay content increases, aluminum (Al) content in paleosols should also increase, and Ca, Na, and K should decrease leading to an increase in the CIA (Sheldon and Tabor 2009). Using molecular ratios of these elements, CIA is estimated using the equation:

$$CIA = \left(\frac{Al}{Al + Ca + Na + K}\right) x\ 1000$$

A modification to the CIA is the CIA-K, which can be useful for estimating paleoprecipitation (Sheldon et al 2000; Driese and Ober 2005). The CIA-K is calculated using the equation:

$$CIA - K = \left(\frac{Al}{Al + Ca + Na}\right) x\ 100$$

Using the method derived by Sheldon et al. (2002) from Bw and Bt horizons in modern soils, paleo-mean annual precipitation (paleo-MAP) was calculated using the equation:

$$\text{Paleo- MAP (in mm/yr)} = 14.265\,(\text{CIA} - \text{K}) - 37.632, \quad \text{where } r^2 = 0.73$$

The concentration of titanium (Ti) and zirconium (Zr), which are resistate and relatively immobile elements in paleosols, can also be used to indicate weathering and subaerial exposure during pedogenic development (McCarthy and Plint 1998; Sheldon and Tabor 2009; Flaig et al. 2013). This is based on the assumption that there were no dust or aerosol additions of these elements to the floodplain surface. The ratio of barium (Ba) and strontium (Sr) also indicates leaching during weathering in paleosols (Sheldon and Tabor 2009). Sr has a higher solubility relative to Ba; therefore it will leach faster than Ba during weathering.

2.10 VARIABILITY IN PALEOSOL DEVELOPMENT

2.10.1 Vertical variability

A single (or simple) paleosol profile in the studied interval consists of a single or more pedogenically modified horizon (s) and a basal unaltered stratum (Fig. 12). Vertical successions of paleosol profiles consist of multiple (or simple) paleosol profiles with a lesser degree of pedogenesis and an uppermost profile that is relatively more developed (Fig. 12). These compound successions show upward increases in the intensity of rooting, ped-structure development, and illuviated-clay accumulation. The uppermost profile is often capped by carbonaceous mudstone/siltstone and coal, or in some cases may be erosionally truncated. Geochemical profiles (Fig. 13) of these compound vertical successions of paleosols profiles show an upward increase in intensity of weathering (increased CIA), increased leaching (increased Ba/Sr ratio), and increased accumulation of resistate elements (Ti and Zr).

2.10.2 Lateral variability

Individual paleosol profiles in the studied interval that developed on siltstone substrates are generally relatively better-drained and better-developed compared to mudstone paleosols. Most of the siltstone paleosols were distal crevasse-splay and levee deposits, abandoned-channel fills and the uppermost parts of fining–upward channel fills before they were pedogenically modified. Most mudstone paleosols, on the other hand, were backswamp mudstones and floodplain-lake fills. Lateral variations in rooting intensity were also observed in correlated simple and compound paleosol profiles (Fig. 14).

2.11 INTERPRETATION OF PALEOSOL VARIABILITY

A simple paleosol profile represents a phase of initial and rapid floodplain deposition followed by a subsequent phase of pedogenesis (Leckie et al. 1989; Autin and Aslan 2001). Figure 15 illustrates this inferred cycle of deposition and subsequent pause in sedimentation and exposure characterized by incipient pedogenesis that lasted for a few tens to a few hundreds of years (Willis and Behrensmeyer 1994; Bridge 1995; Atchley et al 2004; Cleveland et al 2007).

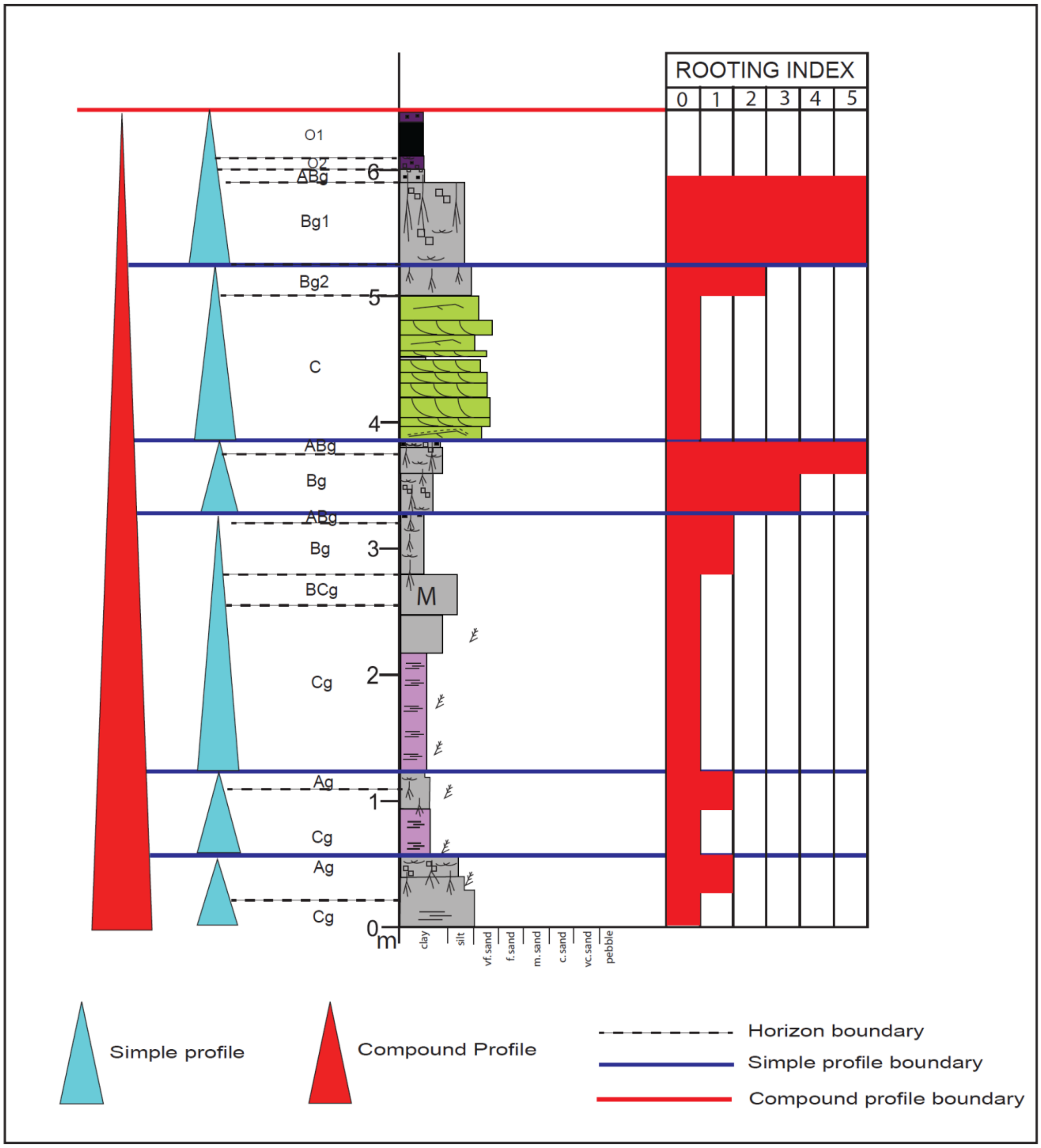

Figure 12.— Six simple paleosol profiles characterized by incipient pedogenesis, stack to form a compound vertical succession characterized by upward increase in intensity of rooting. The uppermost paleosol profile represents the most developed paleosol in the succession. It is capped by carbonaceous mudstone and coal. See legend for facies and features in Figure 5.

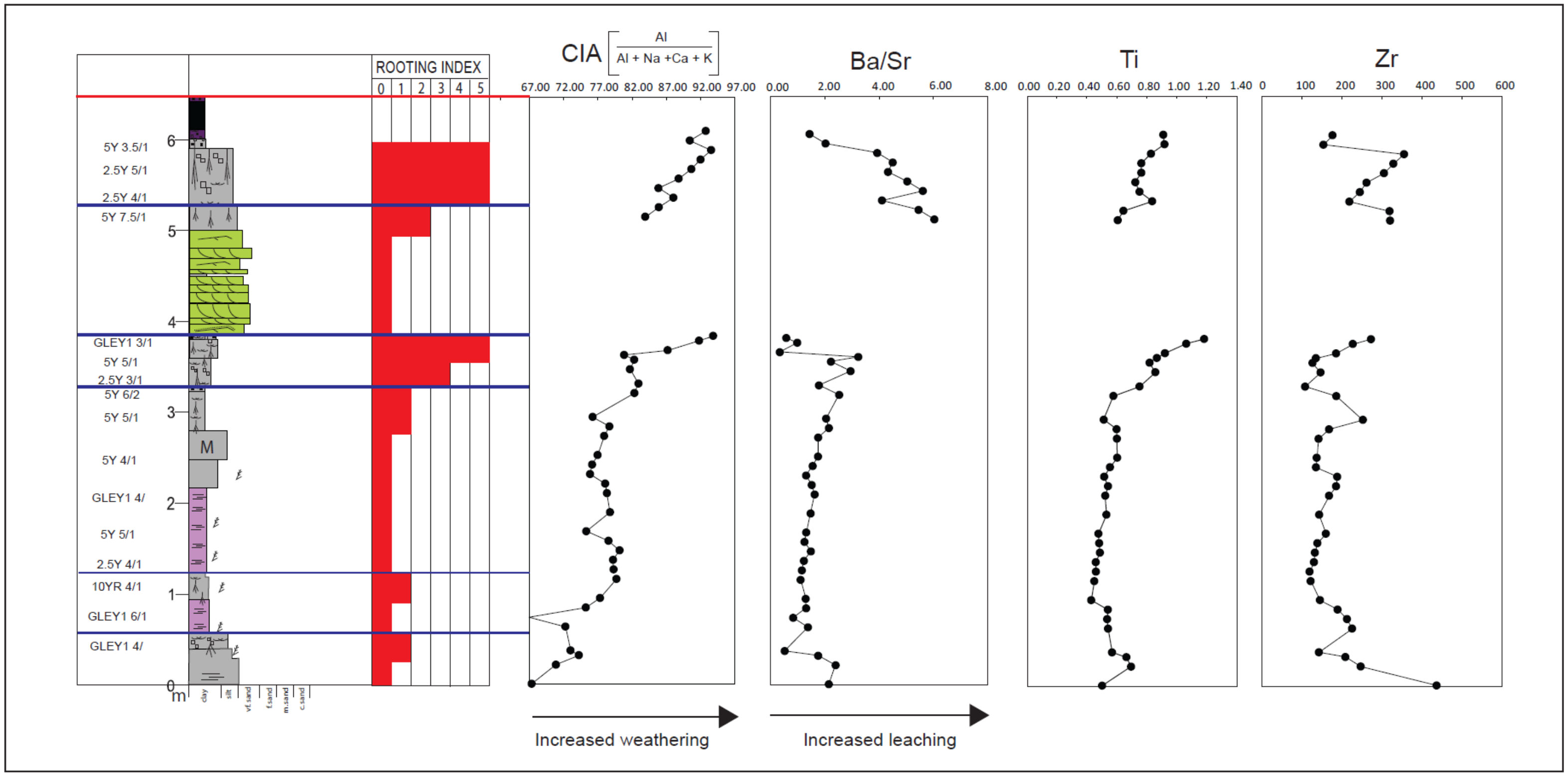

Figure 13.— Geochemical profile of a compound vertical paleosol succession in the Ferron Notom showing upward increase in the degree of weathering and leaching as indicated by the chemical index of alteration (CIA) and Ba/Sr ratio, respectively. Upward increase in the proportion of Ti and Zr, which are immobile resistate elements that concentrate in paleosols after weathering, also suggest that the uppermost profile in the compound succession was exposed for a significant period of time. See legend for facies and features in Figure 5 and boundary legend in Figure 12.

A compound vertical succession of paleosol profiles represents successive rapid and episodic depositional events (Fig. 16) with intermittent pedogenesis, that culminated in a relatively long period of stability and exposure characterized by increased pedogenic development (a few thousand years in Inceptisols and Vertisols, and a few to more than ten thousand years for Alfisols) (Willis and Behrensmeyer 1994). These are similar to compound paleosol successions produced by the non-steady depositional model of Kraus (1999), except that they may be complicated by erosion (i.e., compound-truncated: Kraus 1999). The uppermost paleosol profile in this compound succession is similar to the leached coal-underlying paleosol described by Wright (1989).

The carbonaceous strata and coals that cap compound vertical successions have no pedogenic relationship with the underlying leached paleosols (Wright 1989). Rather, they represent a later phase of increased water-table levels (likely shallower than 5cm from the surface), and mark the transition from a period characterized by alternating poorly-drained and relatively moderately well-drained conditions, to a period of permanent very poor drainage (everwet) conditions (Fastovsky and McSweeney 1987; Gardner et al. 1988; Wright 1989, 1992; Driese and Ober 2005).

They also represent a transition from coastal floodplain backswamps to coastal peat-swamps characterized by prolonged soil saturation, hydromorphism, and peat accumulation (Wright 1989; Driese and Ober 2005). Marine trace fossils (*Teredolites* and *Thalassinoides*) associated with these coal beds suggests marine transgression either due to compactional subsidence or eustatic sea-level rise (Bromley et al. 1984; Savrda 1991; MacEachern and Pemberton 1992; Benton and Harper 1997; Gingras et al. 2004).

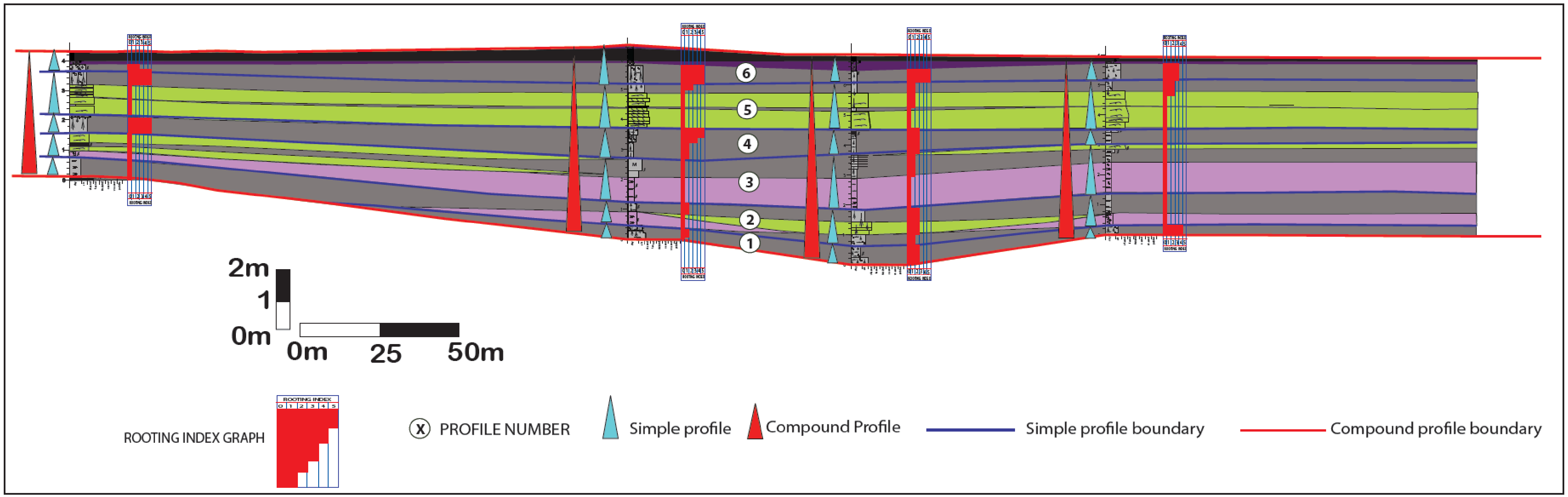

Figure 14.— Lateral variation in rooting intensity and parent material texture in correlated floodplain paleosols. Observe from left to right, that the simple paleosol profile 4 shows a gradual decrease in rooting intensity as well as a change in texture from siltstone to mudstone, which may suggest transition from an area relatively proximal to the main channel to a relatively distal part of the floodplain. See legend for facies and features in Figure 5.

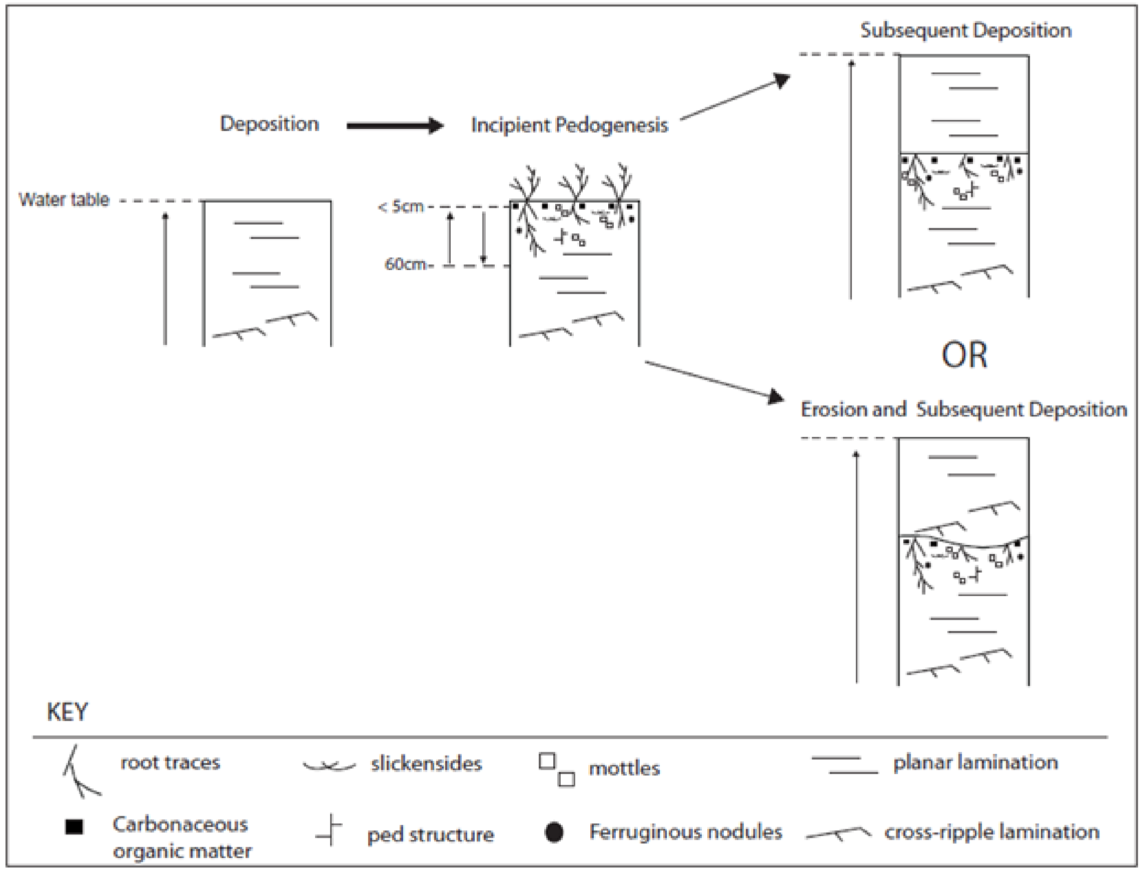

Figure 15.— An illustration of development of simple paleosol profiles on floodplains. They represent stages of rapid floodplain deposition followed by incipient pedogenesis due to low sedimentation rates or due to processes related to avulsion.

In terms of lateral variations in paleosol development, drainage conditions in paleosols were most likely influenced by inherent depositional texture of their respective substrate (Fastovsky and McSweeney 1987; Wright 1989; Arndorff 1993). Therefore, water-level fluctuations in silty and sandy paleosols would have been more effective during pedogenic development than in relatively more cohesive and low-permeability mudstones.

The implication is that paleosols that developed in higher floodplain sub-environments, proximal to the main channel (e.g., levee and crevasse-splay), were generally better-drained, whereas those that developed in the lower backswamp sub-environment were usually saturated and poorly-drained for longer periods due to a shallow water table (Leckie et al. 1989; Arndorff 1993; Wright et al 2000). In addition, lateral variation in rooting intensity observed in paleosols may have been a reflection of more vegetative growth in well drained and relatively higher areas in the floodplain and less growth in seasonally water logged areas.

Therefore, lateral variations in drainage and overall pedogenic development were influenced by topography or elevation differences between floodplain sub-environments (Fastovsky and McSweeney 1987; Wright 1989, Besly and Fielding 1989; Autin and Aslan 2001; Driese et al., 2008). This type of catenary relationship in the floodplain environments is illustrated in Figure 17.

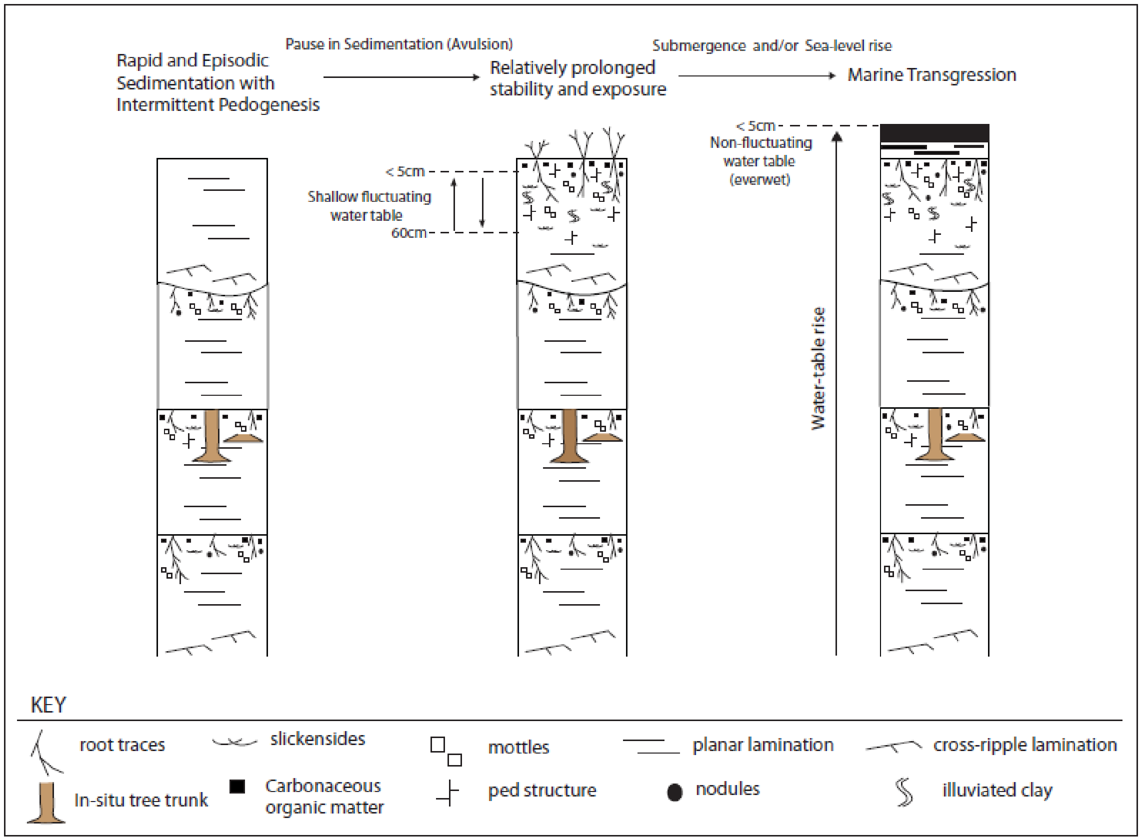

Figure 16.— Compound vertical succession represents successive rapid depositional events that end in a relatively long period of stability and exposure, characterized by significant pedogenic development.

2.12 CONTROLS ON CYCLICITY

Alternations in soil moisture state (i.e., hydromorphism) caused by episodic shallow water-table fluctuations in these paleosols may be linked to the seasonality of rainfall (Fastovsky and McSweeney 1987, Wright et al 2000). Seasonality of rainfall is measured by the number of wet months in a year compared to the number of dry months (Cecil 2003; Cecil and Dulong 2003). However, the predominance of wet and reducing conditions, manifested by low-chroma paleosol colors and high organic C preservation, and a shallow, fluctuating water table, manifested by redoximorphic features, suggest there were more wet months than dry (Cecil 2003; Cecil and Dulong 2003; Driese and Ober 2005); hence, the interpretation of low seasonality of rainfall.

In addition, the bulk geochemical data set obtained from paleosols in this study suggests that mean annual precipitation (MAP) vary from 1100 to 1400 mm/yr. This suggests humid or perhumid (everwet) conditions with low seasonality (minimal to aseasonal) of rainfall, where the number of wet months varies from 10 to 12, and is similar to the mean annual precipitation in modern sub-tropical to tropical climates (Cecil 2003; Driese and Ober 2005). However, such estimates based on geochemical data from saturated coastal floodplain paleosols should still be viewed with caution, since wetness due to rising water table levels can be caused by other factors (e.g., sea-level rise, and river floods).

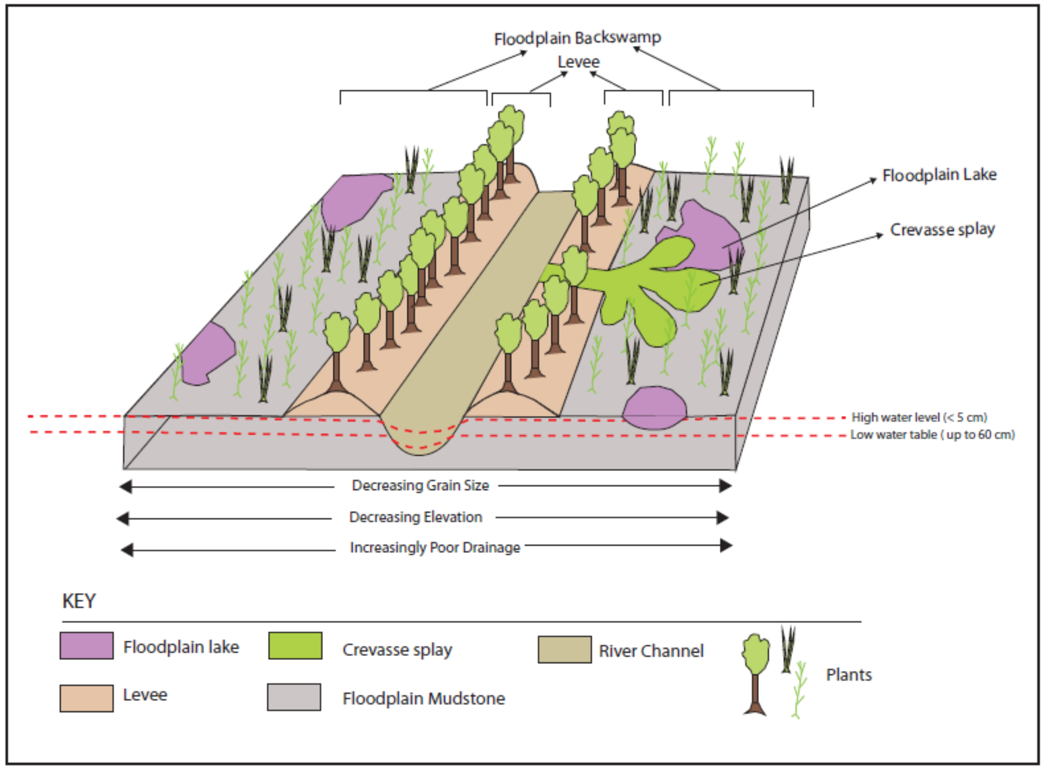

FIG 17.— An illustration of the floodplain environment highlighting the influence of textural characteristics of parent material and topography on lateral variations in pedogenic development. Higher areas of the floodplain are relatively better drained and consist of relatively coarser, porous, and permeable sediments. Relative mature, better drained paleosols may develop in these areas. Lower areas are often poorly drained and consist of finer sediments and cohesive mudstones. Relatively immature, poorly drained paleosols may develop in these areas.

Rapid and episodic floodplain depositional events that often terminate pedogenesis in simple paleosol profiles are attributed to rapid overbank flooding events, which may be linked to crevassing and levee progradation. The time of exposure and pedogenesis that follow these events are attributed to low rates of deposition or abandonment due to avulsion (Bridge 1984; Willis and Behrensmeyer 1994; Atchley et al. 2004). The relatively prolonged periods of stability and pedogenic development that concludes this successive phases of rapid depositional events in compound vertical successions represents a longer pause in sedimentation that may be related to major river avulsions (Bridge 1984; Kraus 1987; Willis and Behrensmeyer 1993; Atchley et al. 2004).

However, the development of mature paleosols that have horizons with substantial illuvial-clay accumulations (i.e., Btg horizons) in an otherwise wet depositional environment suggest significant and relatively prolonged periods (5000 to 15000 years) of subaerial exposure and pedogenesis that may be related to periods of sea-level fall, and the formation of a stratigraphic discontinuity (McCarthy and Plint 1998; Birkeland 1999; Ufnar 2006, 2007). Coals and carbonaceous strata (Histosols) above compound vertical successions of paleosol profiles suggest marine transgression, characterized by high water table level and accumulation of peat, either due to sea-level rise or due to compactional subsidence.

These observations highlight the combined influence and complex linkage of allocyclic and autocyclic controls in the construction of fluvial systems and linked deltaic systems. Further work on the Ferron Notom paleosols focuses on the correlation of simple and compound vertical successions of paleosol profiles, their lateral extent, and correlation of bounding surfaces and other significant stratigraphic surfaces within a sequence-stratigraphic framework.

2.13 CONCLUSIONS

Floodplain paleosols in the youngest sequence in the Ferron Notom Deltaic Complex formed in a humid, sub-tropical to tropical climate characterized by low to very low seasonality of rainfall in an environment characterized by shallow fluctuating water-table levels. Paleosols were subjected to alternating very poorly drained to moderately well-drained conditions. Simple paleosol profiles represent phases of rapid overbank flooding and subsequent pedogenesis, which may be linked to reduced sedimentation, pause in sedimentation, or periods of abandonment due to avulsion. Compound vertical successions of paleosol profiles represent successive phases of rapid and episodic overbank deposition that ended in periods of relative stability and prolonged exposure caused by a relatively long pause in sedimentation that may be linked to major river avulsions or sea-level fall. They are characterized by upward increases in relative maturity and are capped by carbonaceous mudstone or siltstones, and coals. The coals and carbonaceous strata that cap these successions form either as a result of soil saturation associated with water-table rise due to marine transgression caused by eustatic sea-level rise, or compactional subsidence of abandoned and exposed areas. This study serves as the basis for more extensive sequence stratigraphic analysis of Ferron non-marine strata and highlights the significance of floodplain paleosols in paleoenviromental interpretations of ancient river landscapes.

CHAPTER 3

SEQUENCE STRATIGRAPHIC ANALYSIS OF THE YOUNGEST NON-MARINE SEQUENCE IN THE CRETACEOUS FERRON NOTOM DELTA, SOUTH CENTRAL UTAH, U.S.A.

3.1 INTRODUCTION

There have been several attempts to identify cyclic hierarchies in fluvial strata (e.g., Allen, 1974; Bridge 1984; Kraus 1987; Willis and Behrensmeyer 1994) that broadly match the hierarchical division of marine strata into parasequences, parasequence sets, and sequences (Van Wagoner et al. 1990; Shanley and McCabe, 1994; Wright and Marriott, 1993). For example, Atchley et al. (2004) identified three hierarchies of alluvial cyclicity, integrating both channel and floodplain deposits, in their study of Upper Cretaceous to Lower Tertiary non-marine strata in west Texas.

These hierarchical subdivisions included (1) paleosol-capped, meter-thick fluvial aggradational cycles (FACs), which record periodic local channel avulsions, (2) paleosol-capped decameter-thick fluvial aggradational cycle sets (FAC-sets), which record major channel avulsions, and (3) hectometer-thick fluvial sequences, which are aggregates of fluvial aggradation sets. Prochnow et al. (2006) and Cleveland et al. (2007) have respectively applied this method in characterizing the Upper Triassic Chinle Formation in Utah and New Mexico, but there have been few other attempts. These previous studies did not have associated or equivalent marine strata or and thus it was not possible to compare the alluvial cyclicity with associated or equivalent marine sequences and systems tracts. Also, these previous studies did not have adequate chronometric controls in the respective studied intervals.

This study examines the youngest sequence in the chronometrically age-dated Ferron Notom Delta complex; a non-marine sequence that has been previously sub-divided into three non-marine "parasequences" based on broad channel-stacking patterns and identification of possible brackish facies linked to coastal plain flooding events (Zhu et al. 2012). The Zhu et al. (2012) study was regional in nature and did not undertake detailed analysis of the cyclicity within the associated floodplain deposits.

The purpose of this study is to conduct a more detailed facies and stratigraphic analysis of this non-marine sequence by: (1) incorporating detailed descriptions of channel and floodplain facies, (2) identification and analysis of fluvial aggradational cycles and associated paleosols, (3) correlation of cyclic depositional events across a several kilometer-long stretch of outcrop, (4) comparison of this cyclicity to the hierarchy of marine cycles within the Ferron Notom Delta complex, and (5) evaluation of possible controls on development of high-frequency (sub-Milankovitch) non-marine cycles, particularly autogenic versus allogenic controls. The study will evaluate: (1) the frequency and scale of cyclic depositional events in a non-marine sequence, (2) lateral extent of fluvial aggradational cycles and associated paleosols, (3) the relationship of these non-marine cycles to associated or linked marine strata, and (4) the major allogenic or autogenic controls on cyclicity.

3.2 GEOLOGICAL SETTING AND PREVIOUS WORK

The Western Interior Foreland Basin developed between the North American Craton to the east and the Cordilleran volcanic arc to the west as a flexural response to east-oriented thrust sheet loading of the Sevier orogenic belt (Decelles et al. 1995; Decelles and Giles 1996; Ryer and Anderson 2004; Edwards et al. 2005). Rapid subsidence of this foredeep on the eastern side of the Sevier orogenic belt spanned most of the Cretaceous period (Decelles and Giles 1996; Ryer and Anderson 2004). The Western Interior Seaway filled the foredeep as a result of continued subsidence and eustatic sea-level rise during the Cretaceous.

This epeiric seaway extended from the Boreal Sea in the north, to the Gulf of Mexico (Uresk 1978). A series of clastic wedges, along the margin of the seaway, sourced from the adjacent Sevier orogenic belt, prograded eastward into the seaway (Bhattacharya and MacEachern 2009; Fielding 2010, 2011) (Fig. 1). The Turonian Ferron Sandstone Member of the Mancos Shale Formation is comprised of three of these clastic wedges (i.e., the Ferron-Last Chance, Ferron-Vernal and the Ferron-Notom) (Cotter 1974; Uresk 1978; Hill 1982; Bhattacharya and Tye 2004; Ryer and Anderson 2004; Zhu et al. 2012). Paleogeographic reconstruction shows a 40°-50°N paleolatitude for the Ferron clastic wedges during the Cretaceous (Bhattacharya and MacEachern 2009), suggesting a sub-tropical climate due to expansion of tropical climate conditions into higher latitudes during the Cretaceous greenhouse climate.

The Ferron Notom clastic wedge crops out in the Henry Mountains and Caineville areas of south- central Utah. It is bounded below by the Tununk Shale and unconformably above by the Santonian Blue Gate Shale, both members of the Mancos Shale Formation (Fig. 2; Peterson and Ryder 1975). The Ferron-Notom wedge was informally divided into an upper fluvial and lower marine unit (Peterson and Ryder 1975; Uresk 1978; Hill 1982). The lower unit consists of shoreface and delta-front sandstones and marine shales, whereas the upper unit consists of channel-fill sandstones, floodplain deposits, and coals (Peterson and Ryder 1975; Hill 1982; Fielding, 2010, 2011; Li et al. 2010). However, Zhu et al. (2012) showed that the upper fluvial unit contains an interfingering transgressive marine tongue (Fig. 19A), and recently Richards (2014, in prep.) showed that it contains two. This study focuses on the uppermost fluvial unit above these transgressive marine units.

Li et al. (2010) and Zhu et al. (2012) conducted a regional sequence stratigraphic study of the Ferron-Notom Deltaic Complex (Fig. 19A, 19B). Their regional cross-sections reveal 1 sequence set, 5 sequences, 18 parasequence sets, and 43 parasequences. Based on $^{40}Ar/^{39}Ar$ isotopic dating of sanidine crystals in bentonite horizons within the sedimentary package, Zhu et al. (2012) determined the duration of deposition of the entire Ferron-Notom delta to be approximately 600,000 years. On the average, deposition of each sequence is assumed to have taken about 100,000 years, indicating that they represent high-frequency (4^{th} or 5^{th} order) Milankovitch-scale sequences. The upper two sequences (sequence 1 and sequence 2) are marked by compound valley systems (Fig. 19A, 19B).

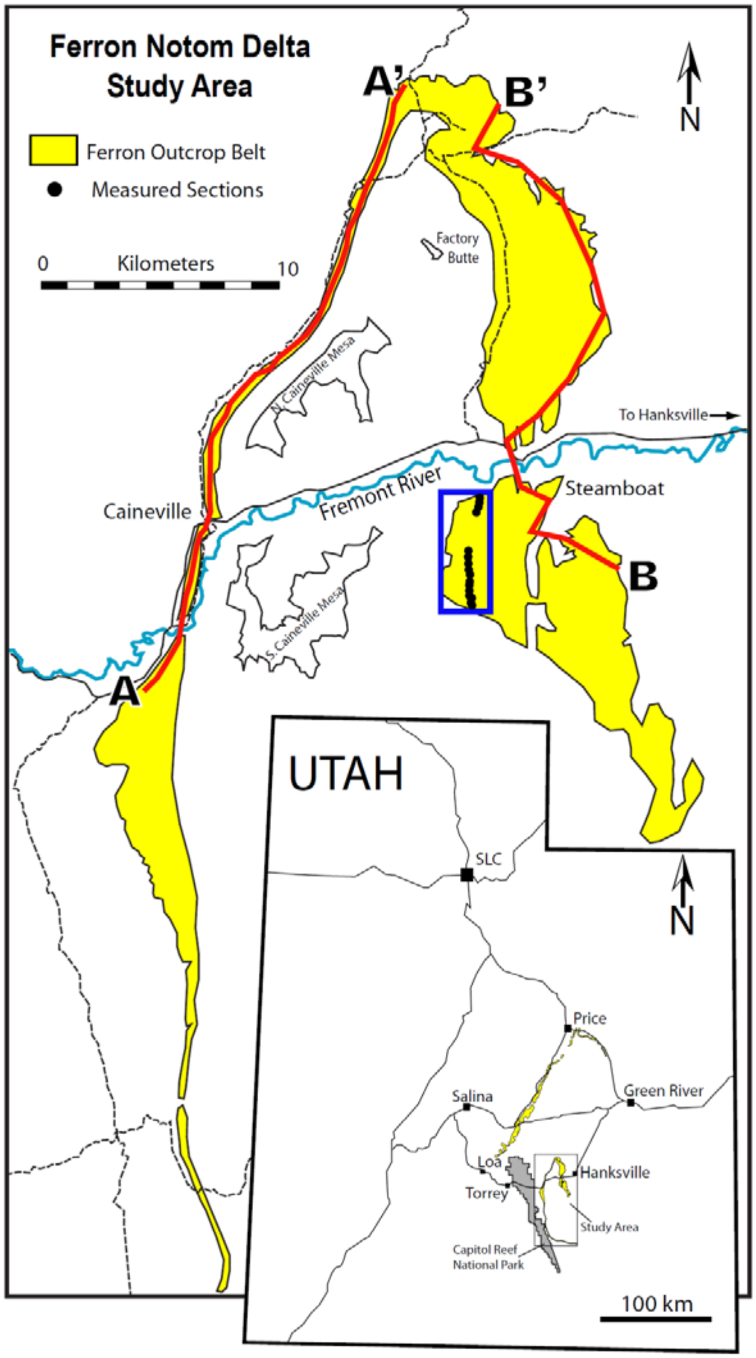

Figure 18.− Maps showing the Ferron Notom outcrop in south-central Utah. Red lines represent regional dip (A - A') and strike (B – B') cross-section in Figure 18. Blue box is the study area and black dots represent the cross-section outline, which are expanded in Figure 20 (modified after Zhu et al. 2012).

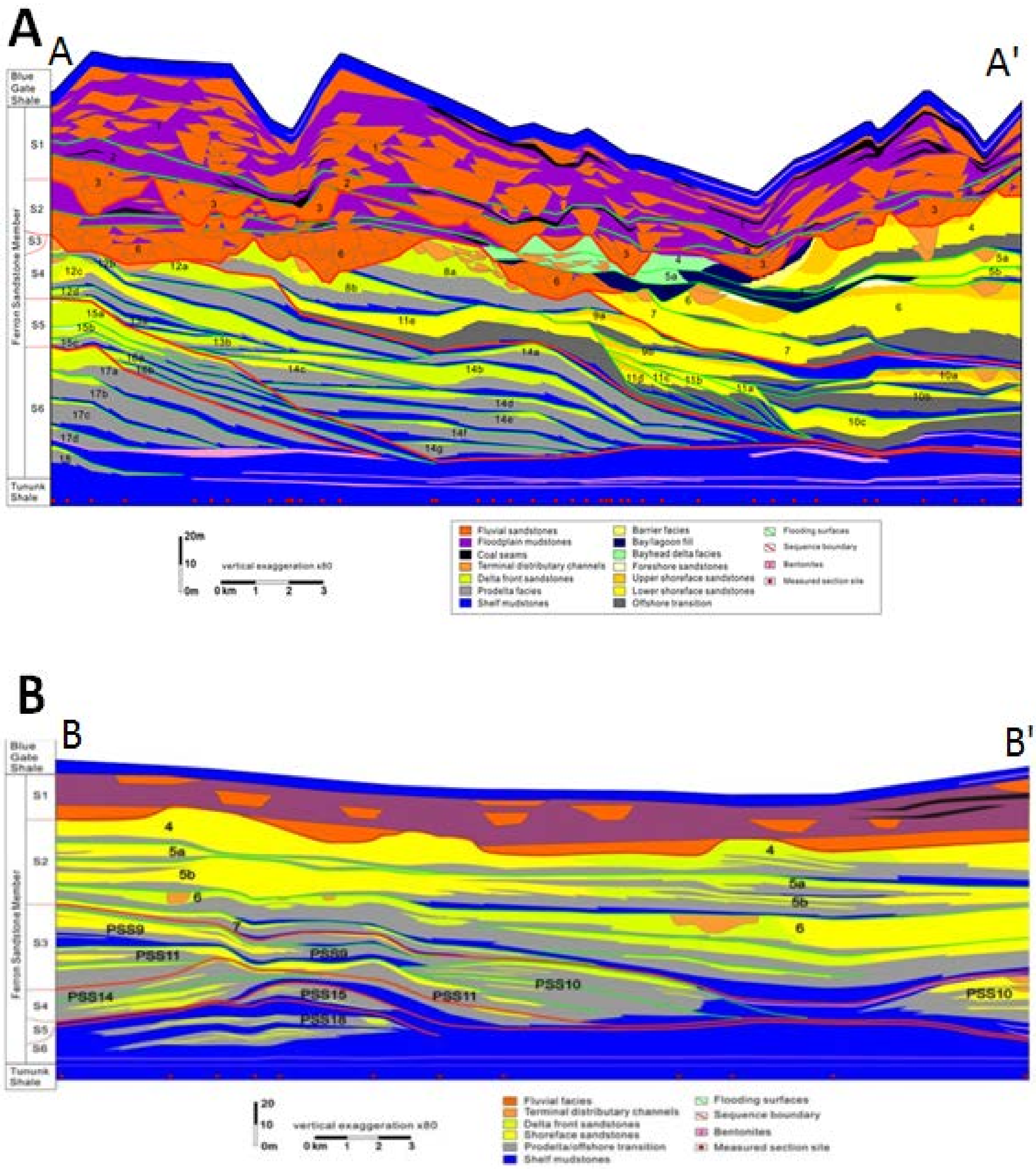

Figure 19.− Regional sequence stratigraphy of the Ferron Notom Delta in cross section. **A)** Depositional-dip cross section (Zhu et al. 2012). **B)** Depositional-strike section (Li et al. 2010). See Figure 18 for both cross section outlines. This study focused primarily on Sequence 1, which is the uppermost and youngest sequence.

The uppermost incised valley constitutes the lower part of the youngest sequence 1. It truncates marine strata and erodes most of the fluvial deposits of the underlying sequence 2 (Zhu et al. 2012). The uppermost valley is marked by 3 separate cut-and-fill episodes, interpreted as higher-frequency Milankovitch-scale sequences (< 30,000 year frequency). The uppermost cut-and-fill sequence is in turn overlain by a widespread series of fluvial sandstones and floodplain mudstones and coals that constitute the upper part of sequence 1. These unconfined fluvial facies are the focus of this study. Unlike the underlying sequence 2, sequence 1 has no outcrops of linked, age-equivalent marine strata.

3.3 STUDY AREA, METHODOLOGY, AND DATA SET

The study area is in the Sweetwater Creek drainage, between the Henry Mountains and Utah Highway 24 (Fig. 19, 20). This location was chosen for its continuous, lightly weathered cliff exposures of channel-fill and floodplain deposits. The northern part of the study area exposes all of the youngest Ferron-Notom Sequence 1 from the base, where it truncates underlying marine strata (Parasequence 4 of Li et al. 2010 and Zhu et al. 2010) to the Blue Gate Shale that caps the succession (Fig. 20, 21A). The southern part exposes the upper part of the sequence (Fig. 20, 21B). The southern and northern parts of the study area cover a continuously exposed distance of about 1800m and 500m, respectively. The distance between the two study areas is about 2 kilometers with variable exposure in between these areas.

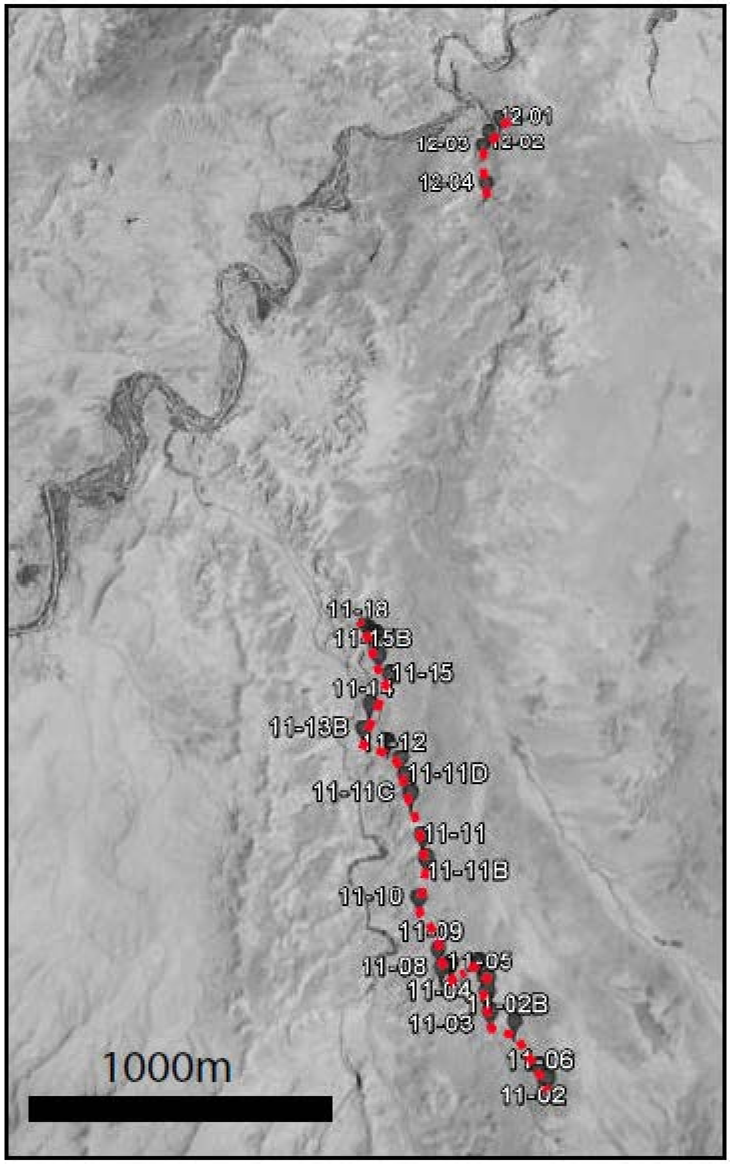

Figure 20.− Outline of cross sections in North and South Sweetwater Creek. This represents the area in the blue box in Figure 18 (Image from Google Earth).

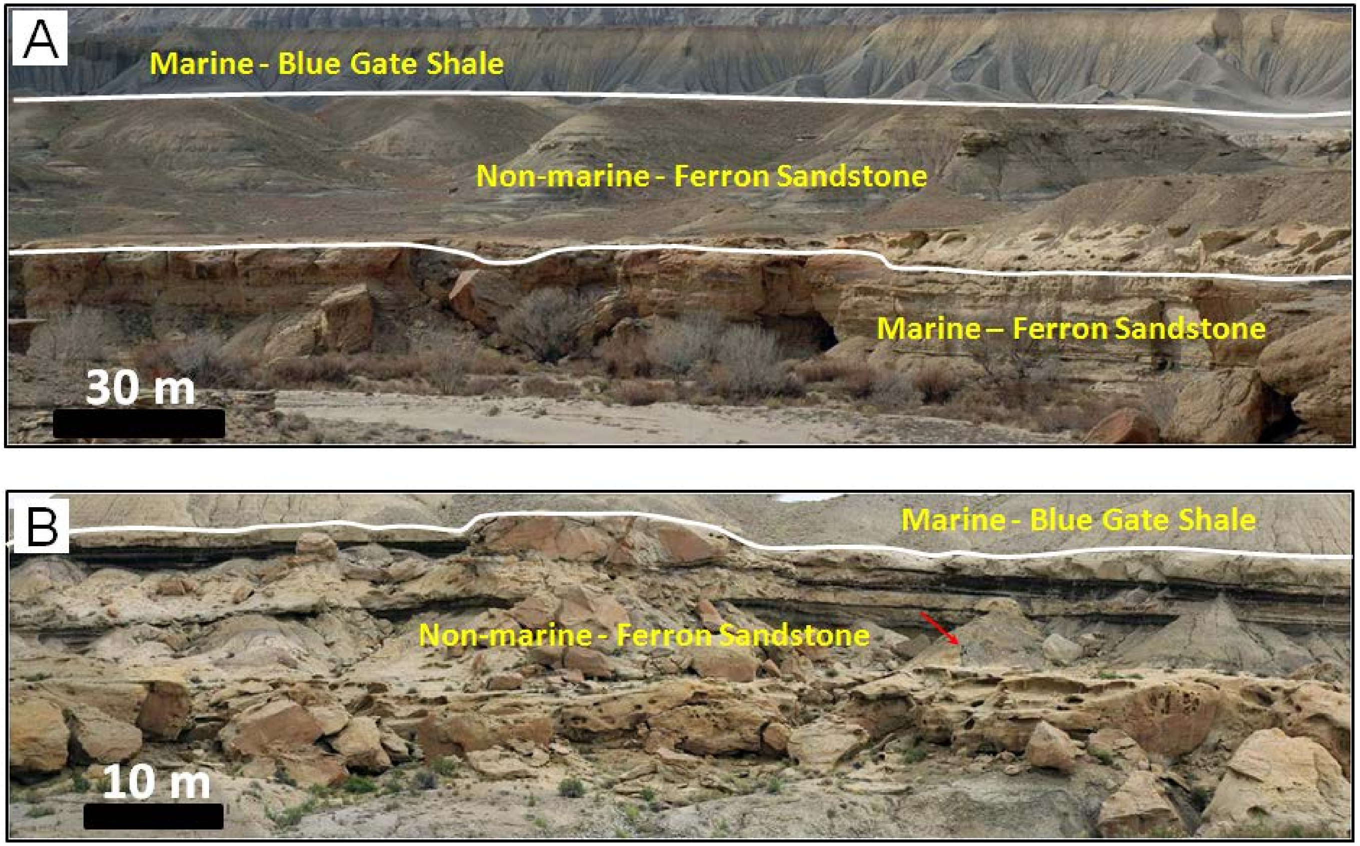

Figure 21.– The outcrop of Sequence 1 at Sweetwater Creek. **A)** The full sequence is exposed at North Sweetwater from the underlying marine parasequence to the top, and it is capped by the Blue Gate Shale. **B)** In South Sweetwater the underlying marine parasequence and the lower parts of the sequence are not exposed. Note the person (indicated by red arrow) for scale.

A total of 29 detailed stratigraphic sections were measured, 25 of which were measured in South Sweetwater and 4 were measured in North Sweetwater. Locations of measured sections were tracked by GPS, and were spaced according to distances indicated by GPS waypoints. All measured sections (e.g., Fig. 23) contain detailed outcrop descriptions, which include lithofacies, grain size, stratal thickness, sedimentary structures, paleoflow indicators, stratigraphic boundaries or discontinuities, trace fossils, and organic matter content.

Mudstones and paleosols were described for their color, structure, and other constituents (e.g., root traces, slickensides, glaebules, mottles, and organic-matter content). The intensity of rooting or rooting index (R.I.) of paleosols was also tracked and recorded. Determination of rooting index (R.I.) of a paleosol in the succession was based on visual comparison of strata without any root trace (R.I. = 0) to well-rooted paleosol horizons (R.I. = 5), and a rooting index of 2 or 3 for moderately rooted paleosol horizons.

A total of 356 paleocurrent measurements were obtained from cross-bed foresets, plan-view rib-and-furrow structures, and ripple-cross lamina in channel-fill sandstone facies. In terms of paleo-discharge calculations, estimation methods from Bridge and Tye (2000) and Bhattacharya and Tye (2004) were applied. Thicknesses of preserved channel-fill deposits and channel bar deposits were obtained to estimate bankfull-depth of paleochannels. The thickness of channel bar deposits is roughly 80%-90% of channel depth (Bridge and Mackey 1993; Bridge 2003).

Apparent widths of channel-fill sandstones were obtained from outcrop data and were adjusted to approximate true widths consistent with outcrop orientation and paleocurrent data. The approximate widths were compared with results from empirical width-estimation methods including:

Bridge and Mackey (1993);

$$w_c = 8.8\ (d_m)^{1.82} \qquad (1)$$

$$w_c = 59.86\ (d_m)^{1.8} \qquad (2)$$

and Fielding and Crane (1987);

$$w = 64.6\ (d_m)^{1.54} \qquad (3)$$

Where w_c and w = channel width, d_m = mean channel depth, and d = maximum channel depth. In cases where widths of channel-fill sandstones could not be obtained, due to out-crop orientation limitations, these numerical methods were applied to estimate the approximate channel widths. Channel cross-sectional area (A) was then calculated using:

$$A = 0.65\ (w*d) \qquad (4)$$

Multiplying cross sectional area by 0.65 accounts for the curvature of channels, as they are not fully rectangular (Bhattacharya and MacEachern 2009). Flow velocity (U) was estimated using the three-dimensional bedform phase diagram of Rubin and McCulloch (1980) based on grain size, bankfull channel depth, and dominant sedimentary structure in respective channel-fill sandstones. Bankfull paleo-discharge was then calculated using:

$$Q = A*\ U \qquad (5)$$

Correlation of measured sections was carried by out by physically walking and tracing bed-to bed contacts and lateral extents of individual bedding surfaces or channel belts in order to produce detailed stratigraphic cross sections of the two areas. The stratigraphic cross sections are both oriented slightly oblique to depositional strike of the Ferron Notom.

3.4 LITHOFACIES DESCRIPTION

A total of 11 lithofacies were identified (Table 3, Table 4) and are described under two headings: those that consist predominantly of sandstones, and those that contain predominantly mudstones and siltstones. These are discussed with slightly different focus on some of their characteristics. For example, color variations are more important in distinguishing mudstone and siltstone facies versus the sandstone facies, whereas geometry and architectural elements are more important in distinguishing sandstones versus mudstone and siltstone facies.

3.4.1 Sandstone Facies

3.4.1.1: Facies 1 (FA 1): Very fine- to fine-grained, bioturbated sandstone

Description – Facies 1 consists of 2 to 8 meter-thick sandstone bedsets. They extend laterally across the entire study area, where exposed. Bedsets consist of highly bioturbated, very fine-grained massive sandstones interbedded with slightly bioturbated, very fine- to fine-grained, hummocky cross-stratified, planar-stratified, and wave-ripple cross-laminated sandstones (Fig. 23). The associated trace fossil assemblage is diverse and includes *Ophiomorpha*, *Planolites*, *Paleophycus*, *Thalassinoides*, *Cylindrichnus*, and *Rosselia* suggesting a *Skolithos* ichnofacies.

Interpretation – Facies 1 is interpreted as shallow marine deposits of a middle to lower shoreface sandstone, and is similar in characteristics and depositional profile to classic shoreface models (Galloway and Hobday 1996; Clifton 2006; Plint 2010) and to those earlier described in the Ferron-Notom Delta (Fielding, 2010; Li et al. 2010; Zhu et al. 2012).

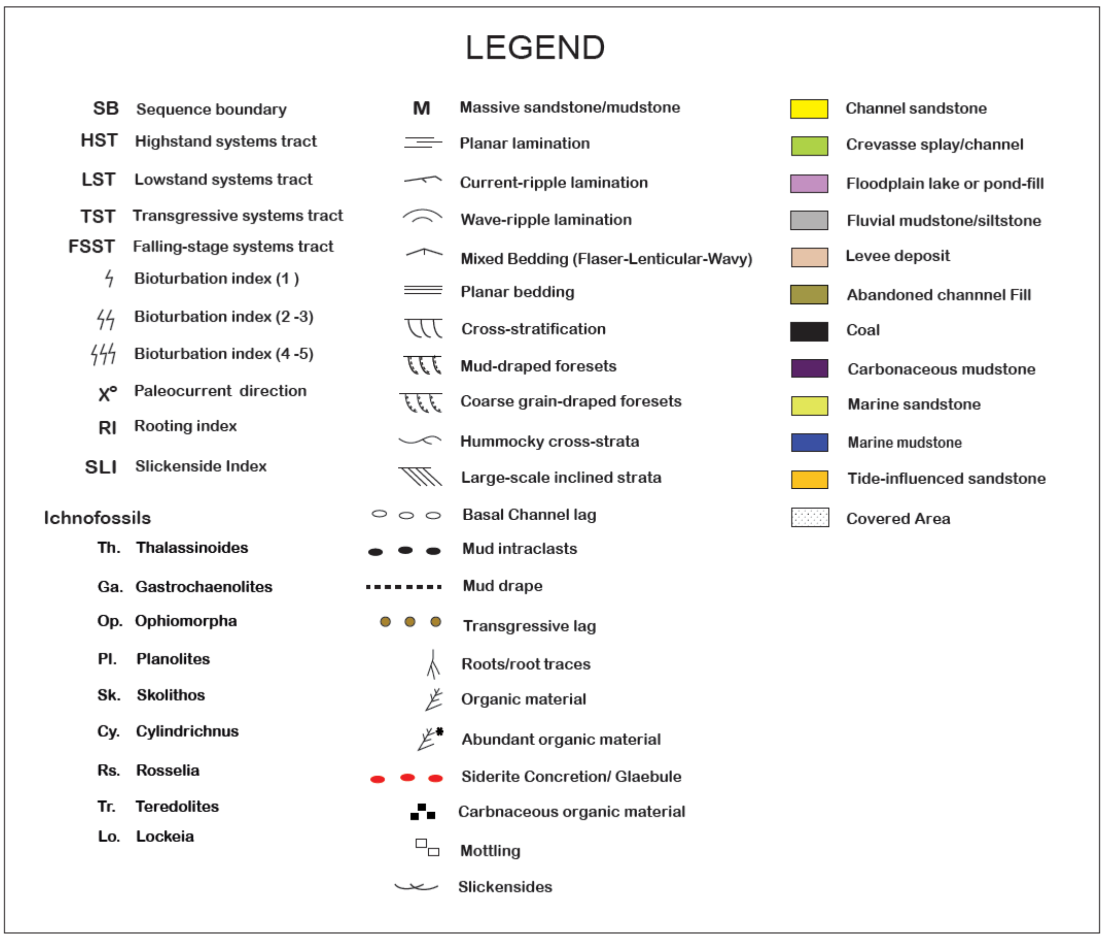

Figure 22.− Key to sections in Figures 23, 31, 32, 33, 37, and 38.

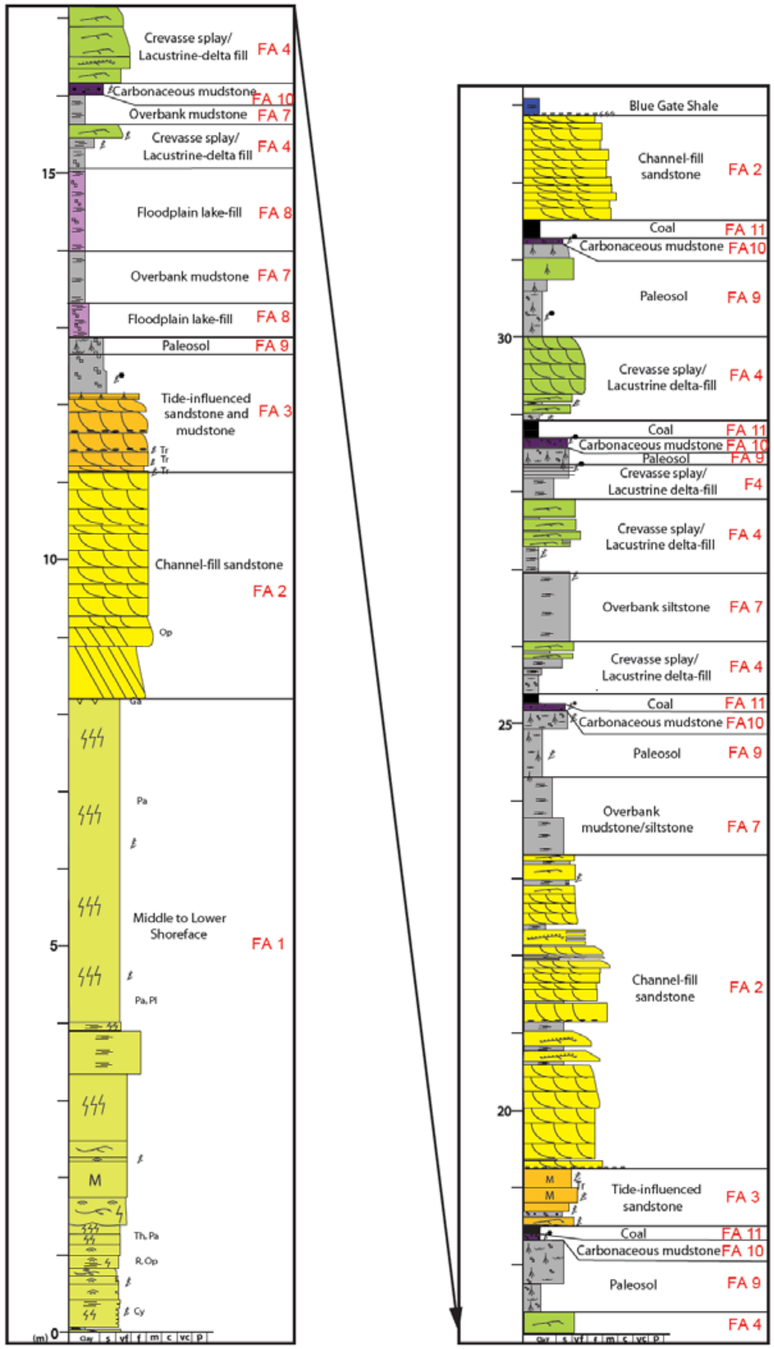

Figure 23.− Type measured section of representative fluvial facies successions in Sequence 1.The contact between the basal marine shoreface facies (FA 1) and the overlying channel-fill sandstone facies marks the base of Sequence 1. The top of the sequence is at the marine Blue Gate Shale contact. See legend in Figure 22.

3.4.1.2: Facies 2 (FA 2): Very fine- to very coarse-grained, scour-fill sandstone

Description – Facies 2 consists of 1 to 10 meter-thick very fine- to very coarse-grained sandstones that extend laterally for a few tens of meters to several kilometers across and in some cases beyond the study area (Fig. 24). Sedimentary structures include large-scale inclined-stratification (Fig 24A), small- to large-scale trough cross-bedding (Fig. 24 B), planar stratification, current-ripple cross-lamination, and convolute bedding (Fig. 24D). The bases of the sandstones are erosional and may be floored by very coarse-grained sandstone or pebble lags and basal intraformational mud clasts (Fig. 24C). A number of sandstones consist of dipping accretion sets of centimeter- to decimeter-thick cross-bedded or current-ripple cross-laminated sandstones that are draped by centimeter-thick mudstones (Fig. 25).

Sandstones show fining-upward profiles (Fig. 23) that may be erosionally truncated by successive fining-upward profiles. Well preserved fining-upward sandstones typically show an upward change in sedimentary structures from medium-scale trough cross-bedding to small-scale trough cross-bedding and eventually to current-ripple cross-lamination. Thickness of well-preserved fining-upward sandstone profiles vary from less than 1 meter up to about 7 meters, with a minimum of 1 and a maximum of 3 stacked fin-ing-upward sandstones. The very top of some sandstones are pedogenically modified. Sandstone bodies may have extensive sheet-like geometries or may appear as isolated lens-shaped bodies. Trace fossils, including *Gastrochaenolites*, *Ophiomorpha,* and *Skoli-thos* are stratigraphic ally controlled, as will be discussed in the stratigraphy section.

Interpretation – Facies 2 is interpreted as channel-fill sandstone. Medium-scale trough cross-bedding, large-scale inclined-stratification, planar-stratification, and current-ripple cross-lamination indicate unidirectional river flow. Medium-scale trough cross-bedding and ripple cross-lamination indicate active dune and ripple migration in a river (Miall 1996; Bridge and Lunt 2009).

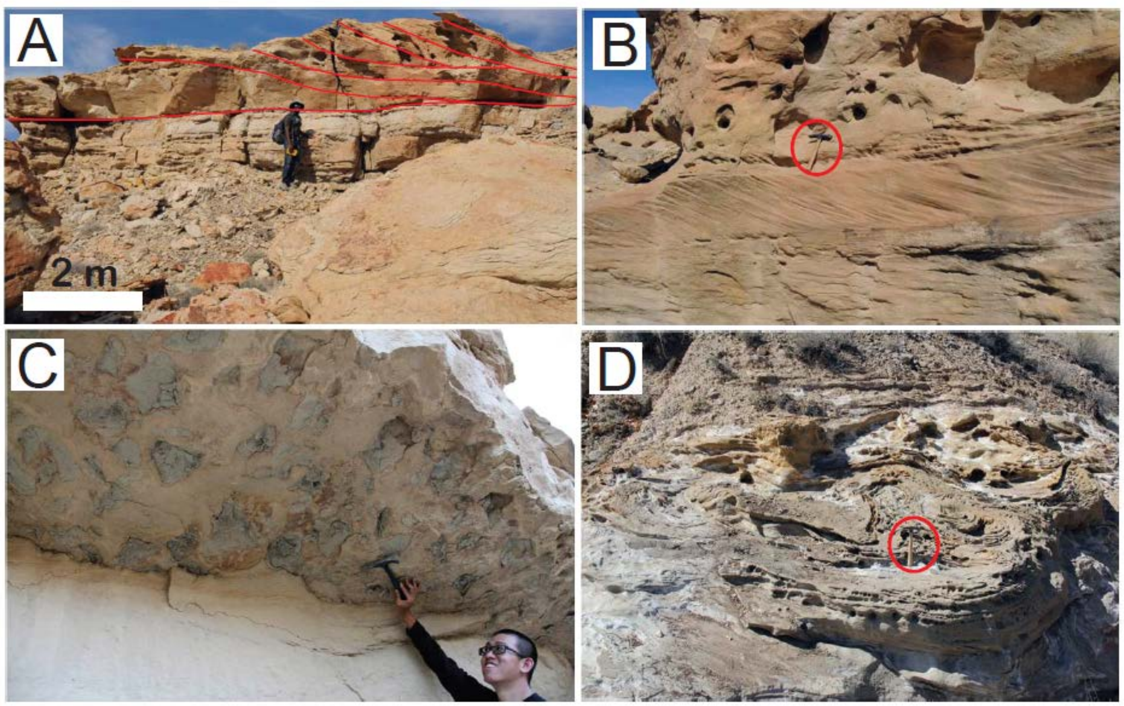

Figure 24.─ Sedimentary structures in channel-fill sandstones (FA 2). **A)** Large-inclined stratification in a channel unit bar. **B)** Medium-scale cross-bedded sandstone (rock hammer for scale). **C)** Basal intraformational mud clasts. **D)** Convolute bedding as an example of soft-sediment deformation in channel-fill sandstones.

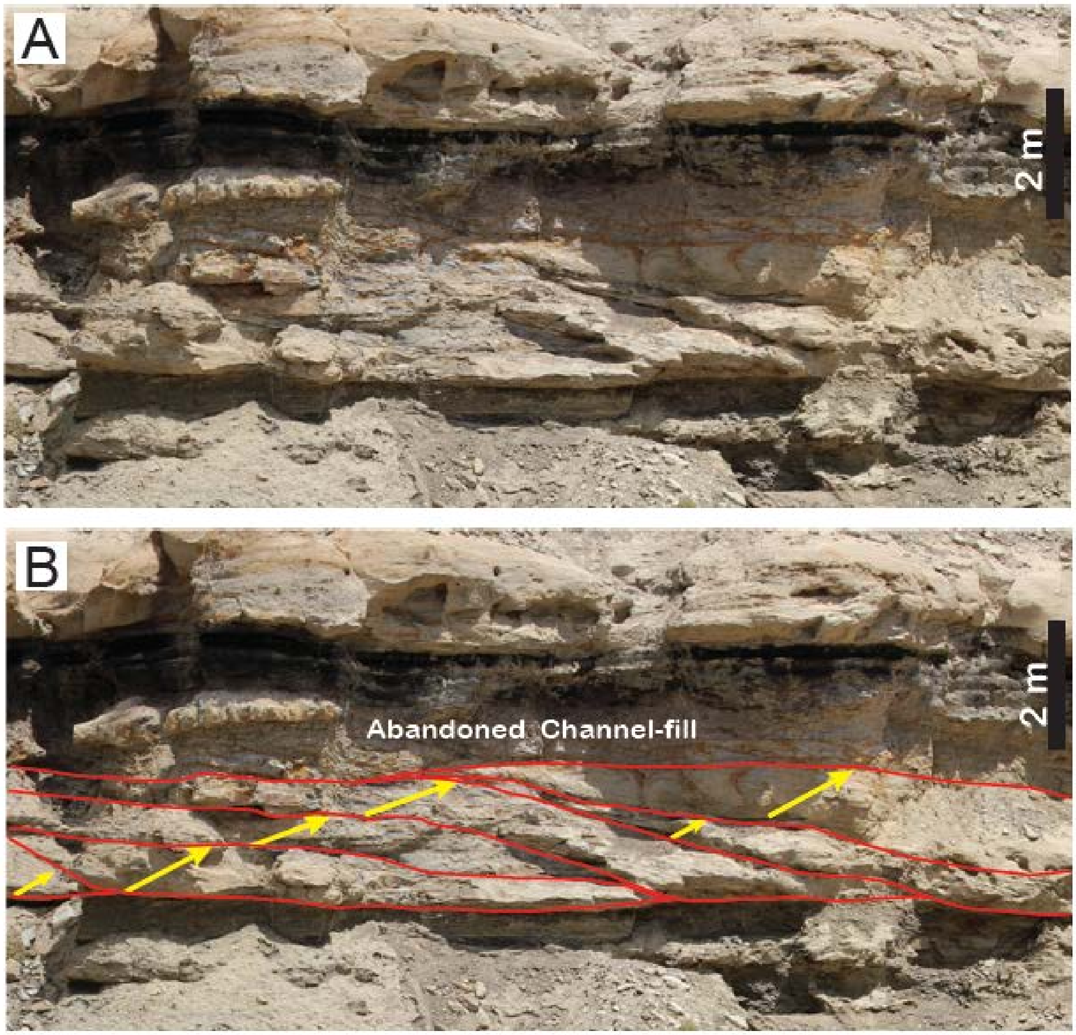

Figure 25.− Lateral-accretion sets in channel-fill sandstone draped by abandoned-channel fill.

Large-scale inclined-stratification indicates unit bar migration, either independently or as part of a compound bar in an actively depositing river (Bridge 2006; Bridge and Lunt 2009). Convolute bedding represents soft-sediment deformation structures, which may indicate rapid sediment deposition on an unstable substrate, or deformation due to seismic activity. An erosional base indicates active channelized flow and sediment transportation in a river. Dipping accretion sets of cross-bedded or current-ripple cross-laminated sandstone and the draping mudstones also represent the gradual growth or expansion of a compound river bar (Miall 1996, Bridge 2003).

The fining-upward sandstone profiles are channel storeys and each represents a phase of channel erosion and deposition. With continued aggradation, truncation by successive channel storeys results in amalgamated and multi-storey channel-fill sandstones (Bristow and Best 1993). Sheet sandstone geometries indicate active lateral channel migration, likely enhanced by erodible substrate, while isolated lenticular sandstones indicate limited lateral channel migration (Bristow and Best 1993; Aslan et al. 2005).

3.4.1.3: Facies 3 (FA 3): Very fine- to fine-grained sandstone with interbedded mudstone

Description – Facies 3 consists of 1 to 2 meter-thick, erosional-based, centimeter- to decimeter-thick accretion sandstone beds interbedded with mudstones and siltstones that extend for few hundred meters to several kilometers beyond the study area. Sandstones show an overall fining-upward profile (Fig. 23). Sedimentary structures include small- to medium-scale trough cross-bedding and current-ripple cross-lamination (Fig. 26B). Some sandstones show mud drapes on internal trough cross-beds, some of which are paired (Fig 26C). The interbedded mudstones and siltstones mostly show lenticular bedding, wavy bedding, and/or chaotic bedding, but some lack internal sedimentary structures (Fig. 26D, 26E). Bioturbation is low to moderate, with a restricted suite of trace fossils that include *Planolites*, *Thalassinoides*, *Lockeia*, and abundant *Teredolites* (Fig. 27). This facies contains a substantial amount of dispersed organic matter.

Interpretation – Facies 3 is interpreted as a tidally influenced channel-fill sandstone and mudstone. An erosional base indicates scouring in an active, channelized river, while small- to medium-scale cross-bedding and current-ripple cross-lamination suggests unidirectional flow. However, lenticular bedding, wavy bedding, and paired mud drapes suggests significant tidal influence. Lenticular and wavy bedding indicate intermittent phases of strong and weak tidal currents; resulting in deposition of alternating layers of mud and sand in different proportions (Reineck and Wunderlich 1968; Martin 2000). Paired mud drapes indicate deposition out of suspension during slack-water periods, after successive influxes of major and minor tidal currents within a fluvial channel (de Raaf and Boersma 1971; Terwindt 1971; Visser 1980). The *Teredolites* indicate marine-influenced woodground development (Bromley et al. 1984; Savrda 1991; Benton and Harper 1997; Gingras et al. 2004) and *Planolites*, *Thalassinoides*, and *Lockeia* (Fig. 27) also indicate marine influence (MacEachern and Pemberton 1992). This suggests an overall fluvio-estuarine setting on a marine influenced lower delta- or coastal plain.

3.4.1.4: Facies 4 (FA 4): Very fine- to medium-grained sheet sandstone

Description – Facies 4 consists of 0.2 to 2 meter-thick beds of laterally extensive, sheet sandstones, commonly proximal to the margins of channel-fill sandstones. The facies consists of centimeter- to decimeter-thick beds of very fine- to fine-grained sandstone that may be separated by centimeter-thick mudstones and siltstones with a higher proportion of sandstone to mudstone or siltstone (Fig. 23, 28A, 28B). Sedimentary structures in the sandstones include small- to medium-scale trough cross-bedding and current-ripple cross-lamination. Intervening mudstones may be planar laminated or massive. Facies 4 can be truncated by the erosional bases of overlying channel-fill sandstones. The basal contact of these sandstones with the underlying substrate may be gradational or abrupt (Fig. 23). When gradational, sheet sandstones show an initial coarsening-upward profile starting from underlying mudstones to siltstones or heterolithic strata and eventually to very fine- or fine-grained sandstones.

This coarsening-upward succession could progressively transition to a fining-upward succession, where fine-grained sandstones fine upwards to very fine-grained sandstones and to decimeter- thick planar laminated, massive or rooted organic-rich siltstones. When the bases are abrupt, they may or may not be erosional. If erosional, they are relatively more coarse-grained and show a characteristic fining-upward profile from base to a top that is commonly draped by rooted or massive siltstones (Fig. 28A). In addition, there are deposits that do not show upward- coarsening or upward-fining depositional profiles (Fig. 28 B).

Interpretation − Facies 4 is interpreted as crevasse-splay sandstone. Sandstone beds and their overlying mudstone beds are interpreted to be flood-generated sedimentation units (Bridge 1984) or rhythmites (Farrell 1987) that represent deposition during individual flood events (Bridge 1984; Kraus 1987; Miall 1992; Willis and Behrensmeyer 1994; Aslan and Autin 1999).

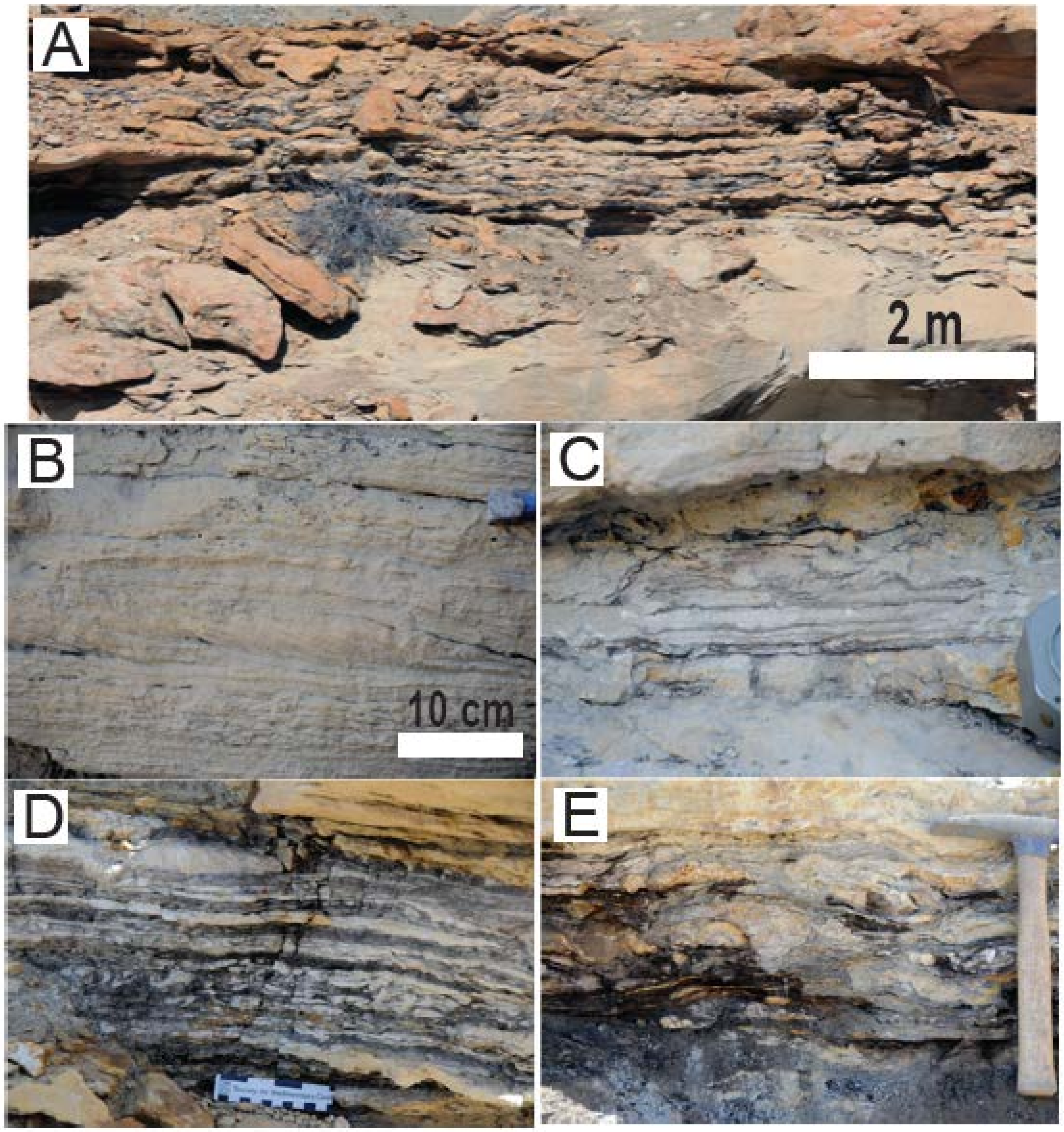

Figure 26.− Sedimentary structures in tidal facies (FA 3). **A)** Tide-influenced heterolithic facies (FA 3) overlying a channel-fill sandstone (FA 2). **B)** Ripple-cross laminated (lowermost strata) and small-scale sigmoidal cross-bedded sandstone (middle strata). **C)** Paired mud drapes. **D)** Lenticular bedding. **E)** Chaotic bedding.

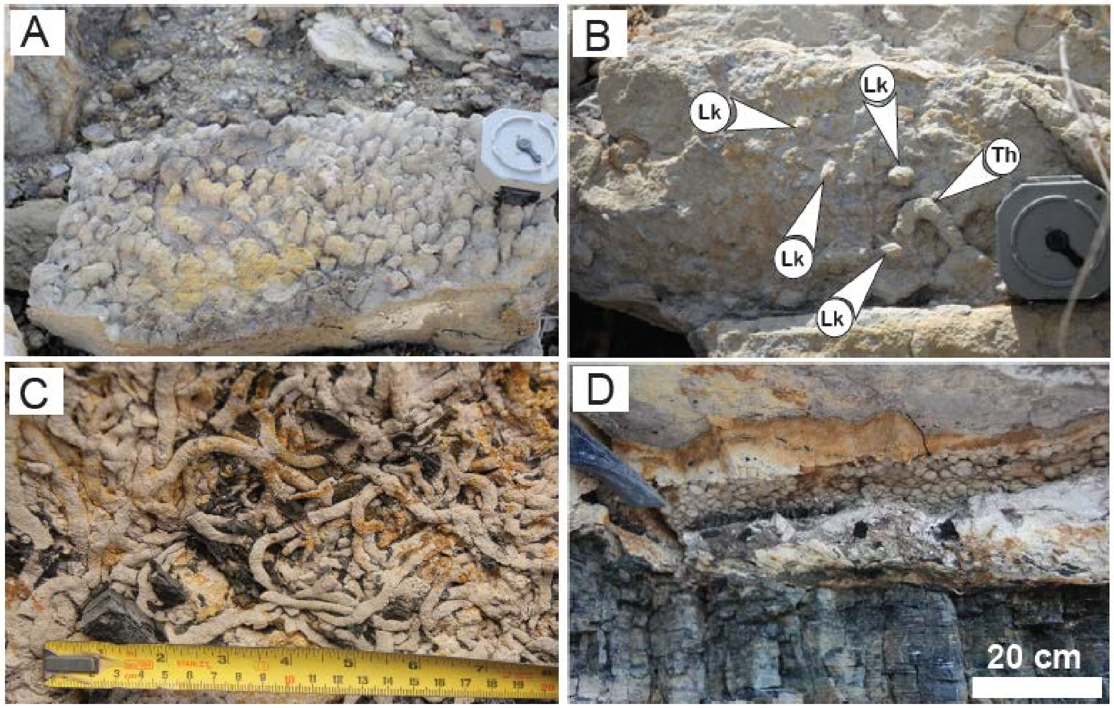

Figure 27.− Identified trace fossils. **A)** *Teredolites* at the base of tide-influenced channel-fill sandstone (FA 3). **B)** *Lockeia* (Lk) and *Thalassinoides* (Th) at the base of tide-influenced channel-fill sandstone (FA 3). **C)** *Thalassinoides* and **D)** *Teredolites* above coal bed indicate overlying marine transgression.

The gradual coarsening of successive sedimentation units record the progradation of a crevasse-splay onto the floodplain during waxing floods (Farrell 1987) and may prograde farther to partly or completely fill adjacent shallow floodplain lakes (Coleman 1966; Bridge 2003). These have been described as “floodplain distributary mouth bars” or “lacustrine–delta deposits” (Elliot 1974; Smith et al. 1989; Tye and Coleman 1989, Miall 1996; Aslan and Autin 1999; Bridge 2003). Gradual upward fining of the succession indicates a waning flood after active progradation. Overlying thick siltstones and colonization by plants roots indicate gradual abandonment (Bridge 1984; Farrell 1987).

Abrupt erosional contacts and associated fining-upward deposits indicate channelized flow. These crevasse channels act as conduits for water and sediments from the main river through the crevasse system, and into the adjacent floodplain (Allen 1965; Miall 1996; Bristow et al. 1999; Bridge 1984, 2003, 2006). Crevasse channels may erosionally truncate older and adjacent crevasse-splay deposits, and they typically consist of sediments relatively coarser than adjacent splay deposits. Shallowing and flow expansion in these channels result in sediment dispersion in unconfined sheet floods. Successive events of this type create a floodplain distributary system (Allen 1965; Miall 1996; Bridge 2003, 2006), which gives the crevasse splays their sheet-like cross-sectional or lobate plan-view geometry. Sheet floods may account for the abrupt but non-erosional basal contact of some crevasse-splay deposits and those crevasse-splay deposits that do not show any distinct grain-size profile.

3.4.1.5: Facies 5 (FA 5): Very fine- to fine-grained, wedge-shaped sandstone

Description – Facies 5 consists of 2 to 3 meter-thick very fine- to fine-grained sandstones that are proximal to channel margins and extend up to 50 meters in width (Fig. 28C, 28D). The predominant sedimentary structure in the sandstones is current-ripple cross-lamination. Sandstones consist of individual centimeter- to decimeter-thick sandstone beds that fine upwards into siltstones or mudstones. These individual fining-upward units are stacked to form a subtle coarsening-upward succession near the margins of channel-fill sandstones and their tops may be pedogenically modified. Some are truncated by crevasse channels near the margins of channel sandstones. They contain rare basal load casts and a trace fossil assemblage that includes *Cylindricum, Naktodemasis, Anorichnus,* and *Steinichnus* (Fig. 29).

Interpretation – Facies 5 is interpreted as levee deposit. The wedge-shaped geometry is a result of decrease in velocity away from the channel, which results in the deposition of coarser sediment near the channel margin and finer sediment away from the channel margin (Fisk 1944, 1947; Allen 1965; Kesel et al. 1975; Brierley et al. 1997; Aslan and Autin 1999; Bridge 2003). The levees here are mainly current-ripple cross-laminated due to this gradual decrease in flow velocity away from the main-channel axis (Allen 1965; Bridge 2003).

Centimeter- to decimeter-thick fining-upward units (or rhythmites) record successive overbank flood events (Farrell 1987; Miall 1996). The stacking of individual fining-upward units into a subtle coarsening-upward succession records the progradation of a levee onto the adjacent floodplain (Bridge 1984, 2003; Farrell 1987; Brierley 1997; Perez-Arlucea and Smith 1999). The coarsening-upward profile may be less pronounced farther away from the main channel, however, a transition from floodplain mudstone to very fine-grained levee deposits may still persist in the distal parts of the levee (cf. Fig 8 in Farrell 1987). Therefore, it may be difficult to distinguish levees from crevasse splays in distal parts of the floodplain, because both facies may show coarsening-upward profiles. The alluvial ridge, which consists of channel, levee, and splays, builds up over time.

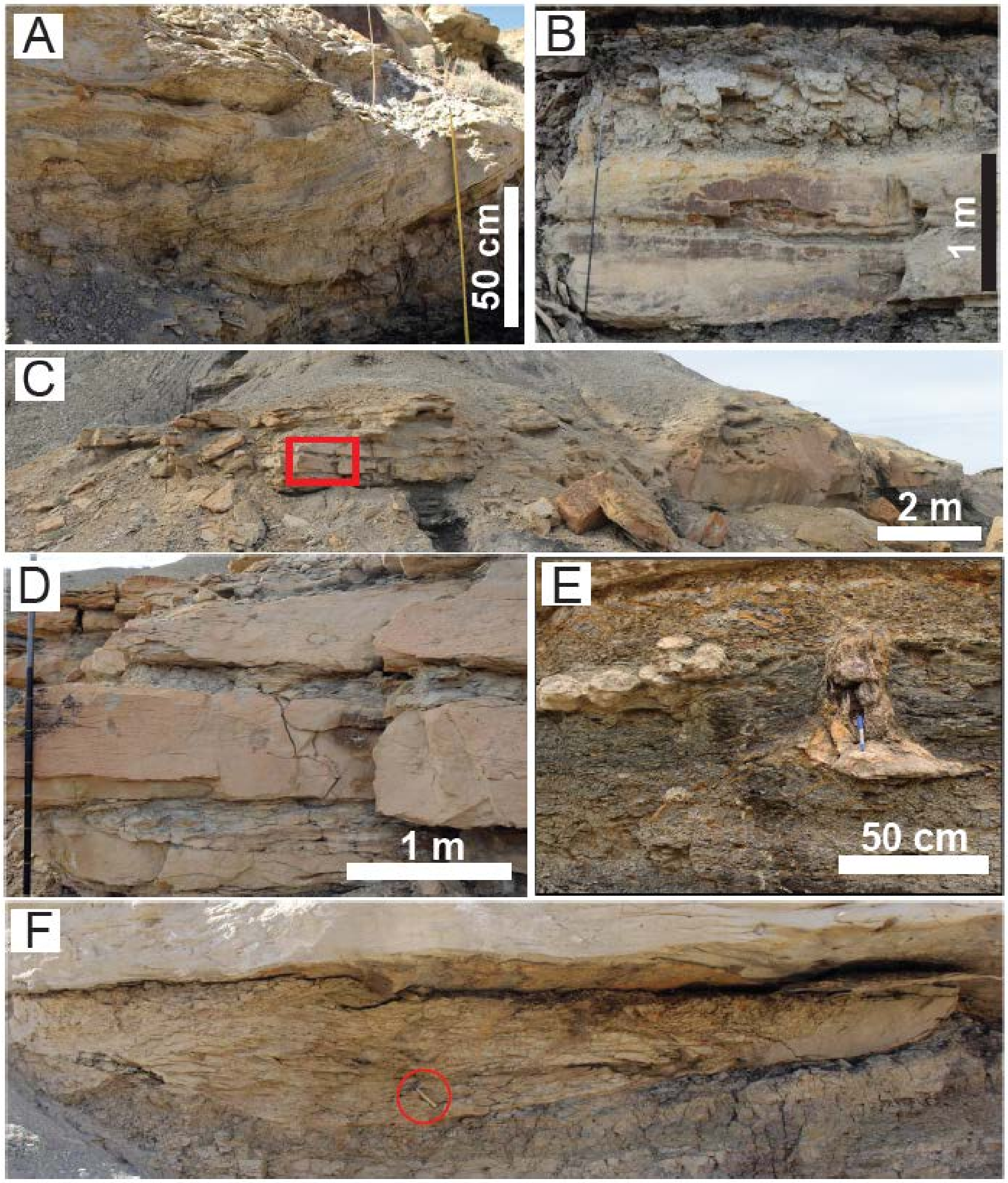

Figure 28.− Floodplain facies. **A)** Fining-upward crevasse-splay channel sandstone with an erosional base. **B)** Crevasse-splay facies showing two individual mudstone capped sandstones representing flood-generated sedimentation units (or rhythmites). **C)** Levee facies flanking channel-fill sandstone. **D)** An expanded view of the area marked by red square in Fig. 28C showing rhythmites **E)** Floodplain lake-fill facies with preserved tree stump and siderite concretions. **F)** Abandoned-channel fill preserved in channel thalweg (rock hammer for scale).

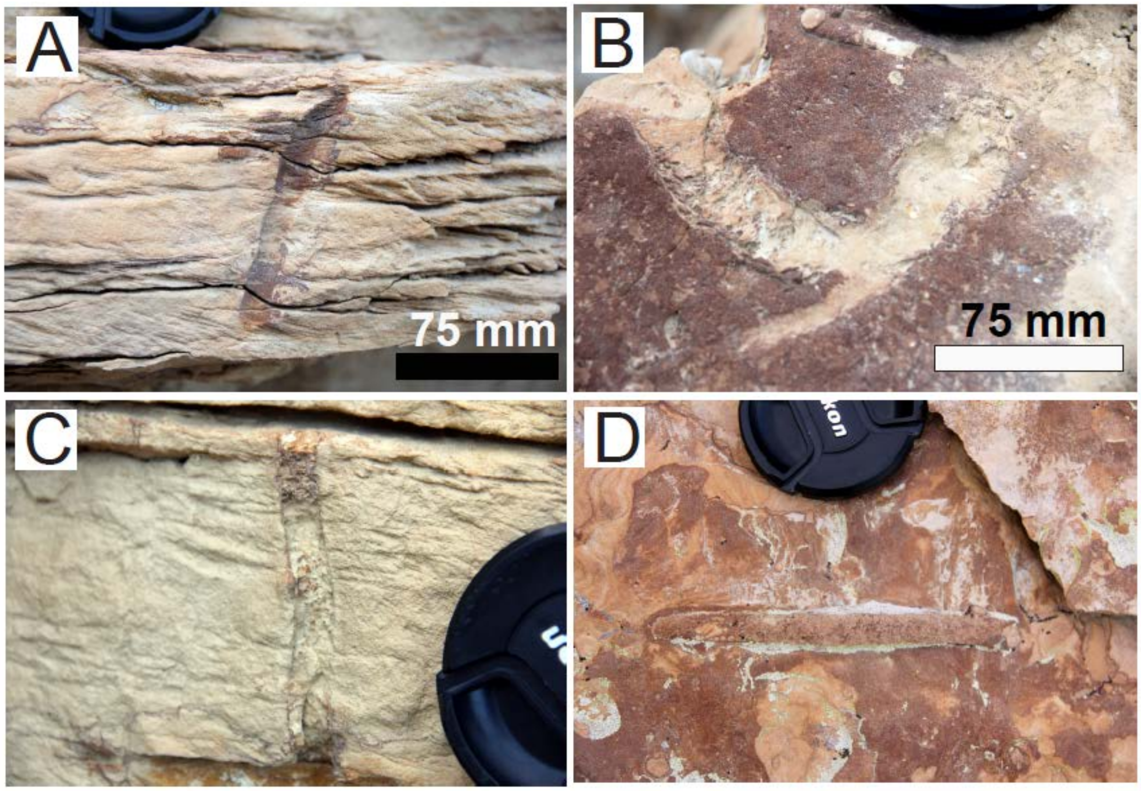

Figure 29.− Trace fossils in levee deposits (lens cover diameter is 75 mm) **A)** *Cylindrichum*. Note the sets of cross ripple lamination in the sandstone. **B)** *Naktodemasis*. **C)** *Anorichnus*. **D)** *Steinichnus*.

Splays and levees are intrinsically linked elements hence the difficulty in distinguishing them and similarity of facies and processes. *Cylindricum, Naktodemasis, Anorichnus,* and *Steinichnus* associated with levee deposits indicate high or fluctuating water table, typical of wet alluvial environments (Frey et al. 1984; Hasiotis and Bown 1992; Hasiotis 2002, 2004; Hasiotis and Bourke 2006; Hasiotis and Platt 2012).

3.4.2 Mudstone Facies

3.4.2.1: FA 6 (FA 6): Organic-rich very fine-grained sandstone, siltstone, and mudstone

Description – Facies 6 consists of less than 1 to about 3 meter-thick deposits of organic-rich, very fine-grained sandstones, siltstones, and mudstones (Figure 28F) that extend for 0.8 to 1.2 kilometers in the study area. Facies 6 caps channel sandstones and is thicker above channel thalweg deposits (Fig. 25). The facies often constitutes the upper muddy part of the upward-fining profile of channel-fill sandstones; however, the fining upward profile can be interrupted by stringers of relatively coarse sediments. The facies rarely shows visible sedimentary structures, but where present include current-ripple cross-lamination and soft-sediment deformation. The facies contains high amounts of organic material and shows pedogenic modification. Facies 6 is may be capped by coals and carbonaceous mudstones.

Interpretation – Facies 6 is interpreted as abandoned-channel fill. Abandonment results in sudden or gradual loss in flow velocity and little to no active sedimentation (Fisk 1944; Allen 1965; Bridge 2003, 2006). The lack of sedimentary structures indicates low flow velocity in the abandoned channel leading to stagnation and formation of shallow lakes or ponds, which become sites of slow deposition of suspended sediments and detrital organic matter. The interruption of the upward-fining profile by stringers of sandstone indicates short-lived episodes of higher flow velocity after partial abandonment. These sites may also receive suspended sediments from occasional overbank floods of nearby active rivers (Allen 1965). Later exposure and plant colonization resulted in significant pedogenic modification of the deposits. Overlying carbonaceous mudstone and coal indicate further isolation from active sediment influx. Similar deposits have been described in the Eocene Willwood Formation (Kraus and Davis-Vollum 2004).

3.4.2.2: FA 7: Extensive laminated or massive tabular mudstone and siltstone

Description - Facies 7 includes 0.5 to 1.5 meter-thick mudstones and siltstones that extend laterally for hundreds of meters to a few kilometers. Mudstones and siltstones exhibit a characteristic low-chroma, bluish-gray appearance with subtle variations in color from gray to light gray or olive gray. They also show variation in grain size over considerable distances. The predominant sedimentary structure is planar lamination (Fig. 23), but siltstones are often structureless. Sedimentary structures may also be obscured by burrowing activity of organisms or other pedogenic processes.

Interpretation – Facies 7 is interpreted as unconfined mudstones and siltstones that were deposited in a floodplain during periodic overbank flood events (Miall 1996), which may or may not be associated with crevassing and levee progradation. The characteristic low-chroma, bluish-gray appearance in mudstones and siltstones is a result of gleying. Gleying indicates a high degree of saturation and high soil moisture content in an oxygen-limited environment, typical of coastal-plain fluvial systems (Retallack 1997, 2001; McCarthy et al. 1999; Driese and Ober 2005). Color variations indicate periodic wetting and drying-out in the floodplain due to water table fluctuation. Planar lamination indicates clay or silt settling from suspension during overbank floods (Coleman 1966; Miall

1996). Variation in grain size (i.e., from siltstone to mudstone) reflect proximity to the active channel margin, where siltstones were deposited closer to the active channel margin and mudstones were deposited farther away in the floodplain. It also reflects variation in the magnitude of individual flood events.

3.4.2.3: FA 8: Confined laminated mudstone and siltstone

Description– This includes 0.5 to 1.5 meter-thick mudstones and siltstones that extend for 50 meters to 500 meters. They may show rare color variation from dark gray to light or olive gray and also show mottling. The predominant sedimentary structure is planar lamination (Fig. 28E), which is locally obscured due to burrowing activity of organisms or other pedogenic development. Remains of upright, *in situ* tree trunks (Fig. 28E) are well preserved in this facies and have associated siderite concretions. These deposits also contain varying amounts of organic material.

Interpretation– Facies 8 is interpreted as floodplain-lake fill. The thickness and extent of the deposits indicate that the lakes were a few meters or less deep and confined on the floodplain. Shallow floodplain lakes can develop as a result of local compaction of previously deposited floodplain sediments, which create depressions in which floodwaters accumulate (Coleman 1966). Planar lamination indicate slow settling of clay or silt from suspension under very quiet conditions (Coleman 1966; Miall 1996) or sediment-laden hyperpycnal flows and turbidity currents from prograding crevasse splays. High biological oxygen demand (anaerobic condition) and reduced rates of decay increase the preservation potential of organic matter in floodplain lakes. In addition, preservation of upright tree trunks suggests a high water table typical of wetlands (Demko and Gastaldo 1996). Color variations indicate rapid lake-level changes because it is in the dark gray mudstones (wetter mudstones) that tree trunks preservation is mostly observed. Siderite concretions are early diagenetic features, associated (Coleman 1966) with the decay of plant matter.

3.4.2.4: FA 9: Rooted and gleyed mudstone, siltstone and sandstone

Description**–** Facies 9 consists of 0.2 to 2 meter-thick mudstones and siltstones. Facies occurrences extend the whole length of the study area and several kilometers beyond (Fig. 23). They show poor to moderate development of multiple horizons characterized by distinctive low chroma gray colors (Fig. 30A). They are characterized by light-gray, pale-orange, or pale brownish-yellow mottles.

Root traces often appear as vertical or sub-vertical penetrations that show basal branching. They are either preserved as carbonized impressions of the original plant material or as clay-filled or unfilled (open) branching voids (Fig. 30B). Facies contain a moderate to high amount of organic materials. Facies occurrences also show poor to good development of angular blocky subangular blocky aggregates, or wedge-shaped aggregates. Aggregates are separated from each other on all sides by voids, and their surfaces consist of clay coatings often called cutans. The clay smeared surfaces of aggregates often have a waxy (or greasy) luster and may consist of striations and grooves (Fig 30C).

Interpretation– Facies 9 is interpreted as floodplain paleosol. Floodplain deposition was followed by plant and animal colonization, which disrupted original sedimentary structures (Retallack, 2001). Low chroma gray colors of paleosol indicate gleying, which is a product of iron or manganese reduction by anaerobic bacteria under poorly drained, oxygen-limited conditions (Retallack 1997, 2001; McCarthy et al. 1999; Driese and Ober 2005). Carbonaceous root traces also indicate non-decay of organic material under reducing conditions, whereas clay-filled branching voids suggest the removal carbonized remains, leaving a void that is either filled with clay or left unfilled.

Poorly to well-expressed angular blocky to subangular blocky soil aggregates are referred to as peds. Clay smeared surfaces are referred to as stress cutans or pressure faces. They represent the pressing of peds against one another under pressure due to repeated shrinking and swelling caused by alternating wet (poor drainage) and dry (better drainage) phases during paleosol development (Brewer 1964; Retallack 2001; Driese and Ober 2005), due to fluctuating water level (McCarthy et al. 1999; Driese and Ober 2005). Striations and grooves associated with peds cutans are called slickensides (Leckie et al. 1989; Retallack 1997, 2001). Slickensides are well-expressed in mudstone paleosols, where are associated with wedge -shaped peds.

Floodplain paleosols in this study vary from weakly developed to well-developed based on stages of paleosol development suggested by Retallack (1988, 2001). This variation in development is indicated by weakly- to well-developed ped structures, low to high intensity of rooting, and weak to better horizon development. Floodplain paleosols in this study are equivalent to modern-day Entisols, Inceptisols, Vertisols, and Alfisols

(U.S. Soil Survey Staff 1999). Entisols develop in a few tens to a few hundreds of years, while Inceptisols and Vertisols develop in a about a thousand to less than five thousand years, and Alfisols develop in about five thousand to less than fifteen thousand years (McCarthy and Plint 1998; Birkeland 1999).

3.4.2.5: Facies 10 (FA 10): Carbonaceous mudstone or siltstone

Description– Facies 10 consists of 2 to 60 centimeter-thick highly organic-rich or carbonaceous dark gray mudstones or siltstones, which extend for about 100 meters to several kilometers beyond the study area. Facies 10 typically overlies rooted mudstone or siltstone paleosols (Fig. 23), but may overlie other pedogenically modified floodplain deposits (e.g., crevasse splay sandstones). The facies usually underlies floodplain coal beds (Fig. 30A) but may overlie them as well. Carbonaceous mudstones (not siltstones) commonly contain relatively abundant slickensides compared to underlying facies.

Interpretation– Facies 10 is interpreted as peat swamp mudstone. The association of organic-rich peat-swamp mudstones with coal beds suggests peat accumulation with some amount of sediment influx. Peat forms by the accumulation of partially decayed organic material in mires or 'protected' planar/low-relief areas of the floodplain; away from sediment influx, where reducing conditions exist to prevent aerobic decay of organic matter or where the rate of organic matter accumulation is greater than the rate of aerobic decay (Retallack 2001).

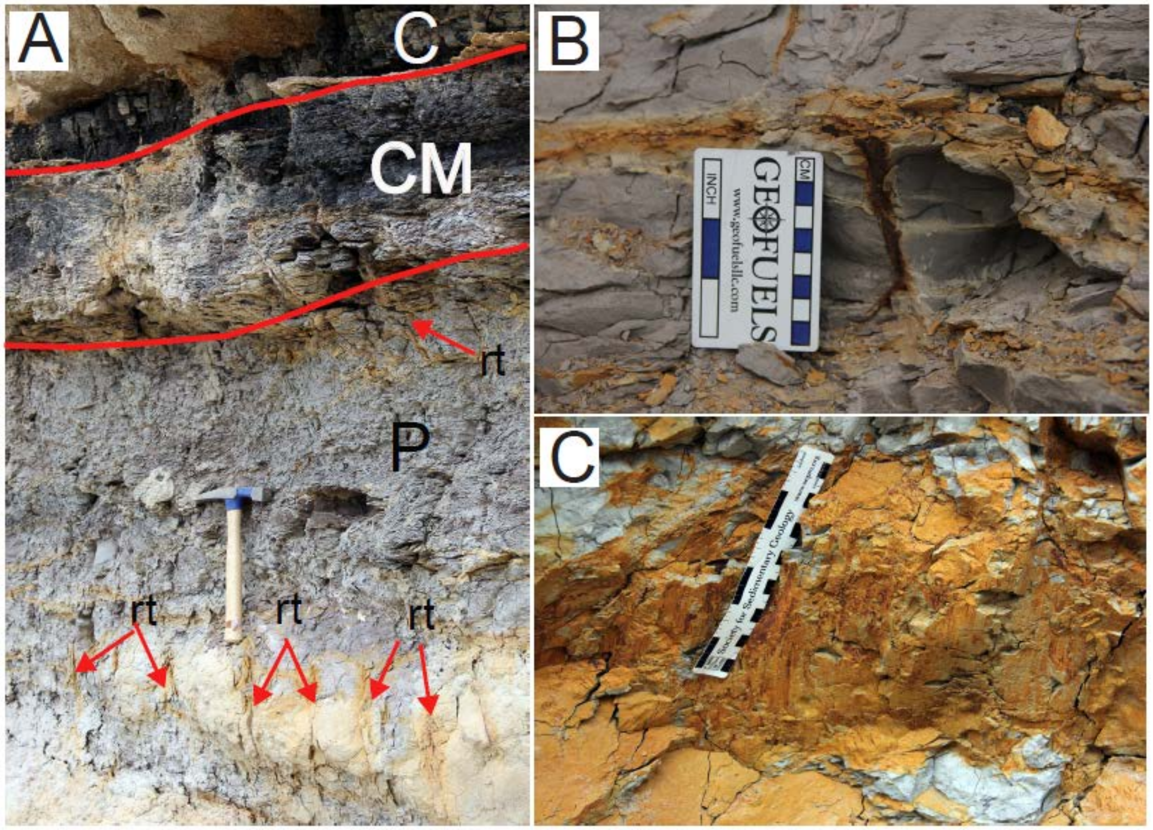

Figure 30.− Paleosols features. A) Paleosol consisting of abundant root traces (rt) is overlain by carbonaceous mudstone (CM) and a coal bed (C). Coal and carbonaceous stratum comprise a coal zone. B) Downward branching carbonized root trace in a mudstone paleosol with yellowish brown coating on it margins. C) Slickensides in a mudstone paleosol. Yellowish brown color reflects oxidation due to modern day weathering and exposure.

Intense water logging or poor drainage conditions (paludification) due to locally or externally-influenced water-level rise are required for this type of accumulation (Diesel 1992; Retallack 2001; Driese and Ober 2005). However, with a considerable amount of sediment influx, pure peat will not form, and the result will be a mix of peat and mudstones or siltstones. Therefore, the carbonaceous mudstones and siltstones can be thought of as more or less impure coals (McCabe 1984; Miall 1996).

3.4.2.6: Facies 11 (FA 11): Coal

Description– Facies 11 comprises 5 to 40 centimeter-thick black coal beds that extend for 100 meters to several kilometers beyond the study area. The laterally extensive coal beds are underlain or overlain by carbonaceous mudstones or siltstones (Fig. 23, 30A) and both overlie floodplain paleosols. Coal beds can also be segmented or split by intervening carbonaceous mudstones and siltstones or rare, very fine-grained sandstone beds. The trace fossils *Teredolites* and *Thalassinoides* were found in abundance above and below some coal beds (Fig. 27C, 27D).

Interpretation− Peat accumulation and preservation occurs in coastal peat swamps and when the rate of organic production exceeds the rate of decay, under poor drainage conditions (paludification) caused by persistent water table rise (Diesel 1992). The compaction of peat after burial and diagenesis leads to formation of coal with a significant reduction in thickness ((Flores and Hanley 1984; Diesel 1992; Retallack 2001). Alternating periods of sediment influx and organic matter accumulation can result in layered or split coal beds, resulting in interfingering carbonaceous strata. The trace fossil *Teredolites* above and below coal beds suggests the formation of a marine-influenced woodground (Bromley et al. 1984; Savrda 1991; Gingras et al. 2004) during marine transgression, and *Thalassinoides* suggests continued marine influence (MacEachern and Pemberton 1992; Benton and Harper 1997; Bohacs and Suter 1997). Coals and associated carbonaceous mudstones or siltstones, referred to as coal zones in this study, are classified as Histosols (U.S. Soil Survey Staff 1999). Histosols develop in a few thousand to a few tens of thousands of years (Birkeland 1999; Retallack 2001). Estimated period of accumulation of peat and organic matter in coal zones will be discussed in the next section.

3.5 CYCLIC HIERARCHY AND SEQUENCE STRATIGRAPHY

In this study, small- to large-scale genetically related fluvial stratigraphic successions bounded by hiatal pedogenic or erosional surfaces have been identified. Similar types of fluvial stratigraphic cycles have been previously described by Bridge (1984), Kraus (1987), Willis and Behrensmeyer (1994), and Aslan and Autin (1999; their Fig. 8). Atchley et al. (2004, 2013), Prochnow et al. (2006), and Cleveland et al. (2007), in hierarchical order, described these as: fluvial aggradational cycles (FACs), fluvial aggradational cycle sets (FAC-sets), and fluvial sequences. These terminologies will be adopted in this discussion. The identification criteria, characteristics, and interpretation of these hierarchical units are discussed below.

3.5.1 Fluvial Aggradation Cycles

Fluvial aggradation cycles (henceforth FACs) observed in the Ferron Notom are mappable decimeter to meter-scale units that are bounded by pedogenically modified surfaces of rooting and burrowing or surfaces representing erosional truncation.

Table 3. — Summary of predominantly sandstone facies recognized in the study interval.

Facies	Lithology	Sedimentary Structures and depositional profile	Biota	Geometry and Architectural Element	Depositional feature
1	Very fine- to fine-grained bioturbated sandstone	Hummocky cross stratification, wave ripple-lamination, and planar stratification. Moderate to high bioturbation	*Ophiomorpha*, *Paleophycus*, *Thalassinoides*, *Planolites*, *Roselia* and *Cylindrichnus*.	Mainly tabular and extensive sandstones. Erosionally truncated top	Middle to Lower Shoreface
2	Very fine- to very coarse-grained scour-fill sandstones	Large-scale inclined stratification, small- to large-scale trough cross-bedding, planar stratification, and current-ripple cross-lamination. Convolute bedding. Single or multiple (often truncated) upward-fining profiles. Basal coarse-grained or pebble lags and intraformational mud clasts.	*Gastrochaenolites* at the erosional base. *Ophiomorpa* and *Skolithos* near the base. Root traces at the upper most portion.	Erosionally based, extensive, amalgamated sheet sandstones with dipping unit and compound bars. Isolated lenticular sandstones. Some show dipping cm- to dm- thick accretion sets	Channel Sandstone
3	Very fine- to fine-grained sandstone and interbedded mudstone (heterolithics)	Small- to medium-scale trough cross-bedding, current-ripple cross-lamination, lenticular, wavy, and chaotic bedding, mud drapes (with some paired). Low to moderate bioturbation. Upward-fining profile	*Teredolites*, *Skolithos*, *Thalassinoides*, *Planolites* and *Lockeia*	Erosionally-based gently to steeply dipping accretion sets that consists of cm- to dm-thick sandstones and interbedded mudstones	Tide-influenced channel sandstone

Table 3. ─ Continued.

Facies	Lithology	Sedimentary Structures and depositional profile	Biota	Geometry and Architectural Element	Depositional feature
4	Very fine to medium-grained sheet or sandstone	Small- to medium-scale cross-bedding, current-ripple cross-lamination. A Mostly upward- coarsening , some upward- fining and few indefinite profiles	Root traces at the uppermost portion or may penetrate the entire thickness	Gradational to abrupt base. Sheet or lobate sandstones that consist of cm- to dm-thick sandstones and cm-thick mudstones (rhythmites)	Crevasse-splay/channel and lacustrine-delta fill
5	Very fine- to fine-grained wedge-shaped sandstone	Predominantly current-ripple cross-lamination. Rare basal load casts	*Cylindricum, Naktodemasis, Anorichnus,* and *Steinichnus*.	Wedge-shaped sandstones that consist of cm- to dm-thick sandstones and interbedded mudstones	Levee
6	Organic-rich very fine-grained sandstone and siltstone	Massive, rare current-ripple cross-lamination and soft-sediment deformation features	Root traces at the uppermost portion or may penetrate the entire thickness. Abundant organic matter content.	Thicker in channel thalwegs and thinner away. Some internal lens-shaped sandstone units	Abandoned Channel-fill

Table 4. Summary of predominantly mudstone facies recognized in the study interval.

Major facies	Lithology	Color	Sedimentary Structures	Biota	Depositional feature
7	Extensive laminated or massive mudstone and siltstone	Gray, Light gray or olive gray	Planar lamination, low bioturbation	None	Overbank flood deposit
8	Confined laminated mudstone and siltstone	Dark gray, gray, light or olive gray. Gleyed	Planar lamination, Low bioturbation	Rare preserved in situ tree trunks. Animal burrow	Floodplain lacustrine- fill
9	Rooted, and gleyed and mottled mudstone	Dark gray, light gray, olive gray. Gleyed	Horizonation. Angular to sub-angular blocky ped structures. Slickensides. Mottling	Root traces and drab-haloed root traces	Floodplain paleosol
10	Carbonaceous mudstone and siltstone	Dark gray to black. Gleyed	Massive.	Fecal Pellets	Peat swamp or backswamp deposit
11	Coal	Black	Fractures. Sulphur Residue	*Teredolites*	Peat swamp or and backswamp deposit

A single FAC is represented by paleosol-capped or erosionally top-truncated decimeter- to meter-thick single-storied channel-fill sandstone, or a decimeter- to meter-thick simple flood-plain bedset. An example is shown in figure 31A, where a paleosol-capped coarsening-upward floodplain bedset, consists of a basal shallow floodplain-lake fill (FA 8). Crevasse –splay pro-gradation resulted in floodplain lake-infilling by coarsening-upward lacustrine mouth-bar (FA 4) deposits. The rooted siltstone paleosol (FA 9) unit above the lacustrine mouth bar indicates cre-vasse-splay abandonment followed by subaerial exposure and soil development.

A total of 33 FACs were recorded in the studied interval. A comparison of the cross sections (Fig. 32, 33) from the northern and southern part of the study area shows that the total numbers of FACs recognized in both locations vary. In any one section, the number of vertically stacked FAC's ranges from about 20-23, particularly where sequence 1 is completely exposed such as in northern part of the study area (Fig. 32). The southern part of the study area exposes the upper part of sequence 1 and shows between about 10-14 FAC's (Fig. 33). The FAC's can be correlated for distances of hundreds of meters to a few kilometers, after which they thin out laterally or are erosionally truncated.

3.5.2 FAC Interpretation

Fluvial aggradation cycles record episodes of rapid floodplain and channel deposition that are followed by abandonment, which can be related to periodic channel avulsions (Bridge 1984; Kraus 1987; Atchley et al. 2004). Abandonment is followed by a short hiatus (10 to < 500 years), marked by a paleosol, which is represents a period of subaerial exposure and pedogenic devel-opment. However, soils that form during this period are immature, due to short-lived or incipient pedogenic development. This relatively short period of pedogenesis is attributed to a short inter-avulsion period, resulting in frequent deposition, which terminates pedogenesis.

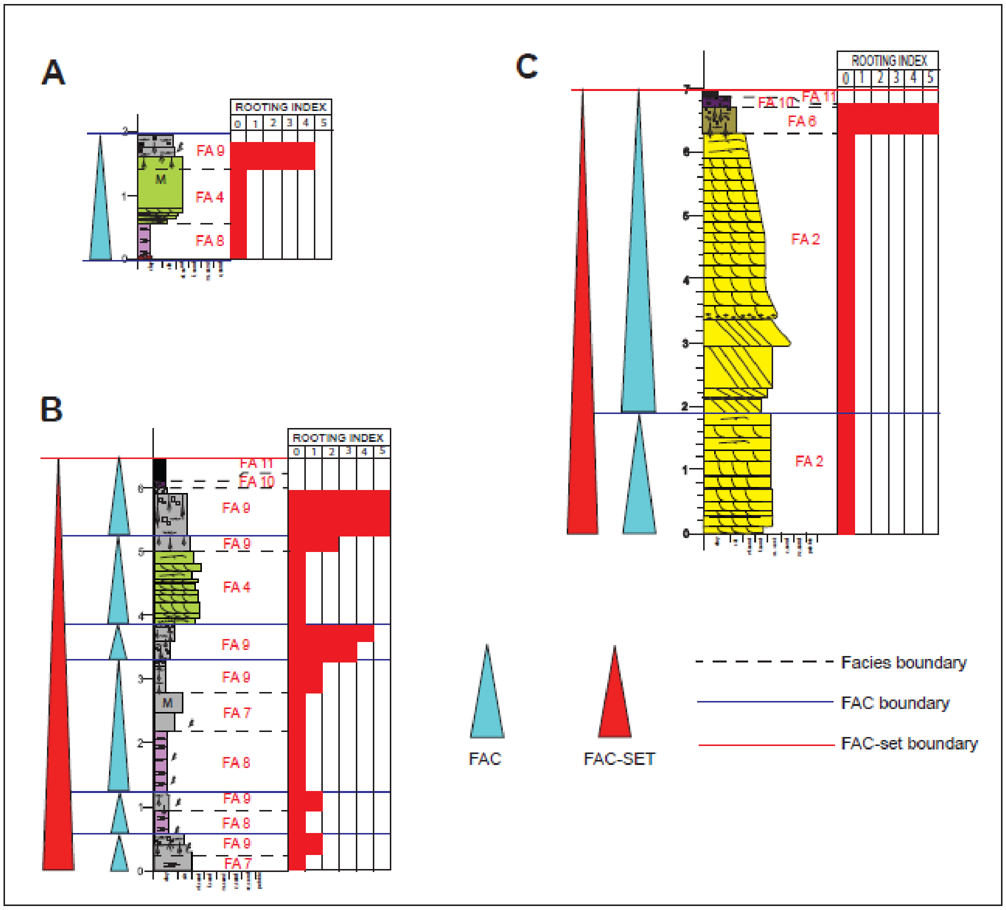

Figure 31.— Fluvial aggradation cycles and fluvial aggradation cycle sets. **A)** Paleosol-capped fluvial aggradation cycle (FAC) consisting of floodplain deposits. **B)** Fluvial aggradation cycle set (FAC-set) consisting of successive fluvial aggradation cycles. The uppermost FAC is capped by a mature paleosol and coal facies. **C)** Alternate paleosol- and coal-capped fluvial aggradation cycle set (FAC-sets) consisting of fining-upward channel stories. The lower FAC is truncated by the upper FAC. The upper FAC is capped by abandoned channel siltstone, which has been pedogenically modified. It is capped by carbonaceous siltstone and coal. The intensity of rooting increases upward in both fluvial aggradation cycle sets. See legend in Figure 22.

Variation in the distribution of FACs in the studied interval suggests that the factors that control their distribution are internal to the fluvial system which also explains their limited extent (Willis and Behrensmeyer, 1994). Prochnow et al. (2006) and Cleveland et al. (2007) made a similar observation within the Triassic Chinle Group, where FACs in different study locations could not be correlated.

In order to estimate the approximate time development for FACs, sediment accumulation rates in modern rivers that drain adjacent mountain belts, analogous to the Ferron Notom were considered (e.g., Po River (Italy), Ebro River (Spain), and Rhone River (France)). Bhattacharya and Tye (2004) have earlier suggested that these rivers might be appropriate modern analogs for the Ferron in terms of location, size of catchment area, and mean annual discharge. Sediment accumulation rates in these rivers vary from 4 to 30 mm yr^{-1} (Frignani and Langone 1991; Ibanez et al 1997; Hensel et al. 1999).

Therefore, based on this range of sedimentation rates, and thickness of FACs (0.1m to 6.5m) in the studied interval, the estimated time for channel or floodplain deposition (interavulsion periods) likely varies from as short as 5 up to 1,500 years. However, inter-avulsion period of ~500 years or less might be appropriate, similar to those in modern analogs of the Ferron (Bridge 2003; Vella et al. 2005; Correggiari et al. 2005). An inter-avulsion period of 1500 years is closer to that of modern continental-scale rivers like the Mississippi (Autin et al. 1991), which is not a suitable analog for the Ferron **(**Bhattacharya and Tye 2004).

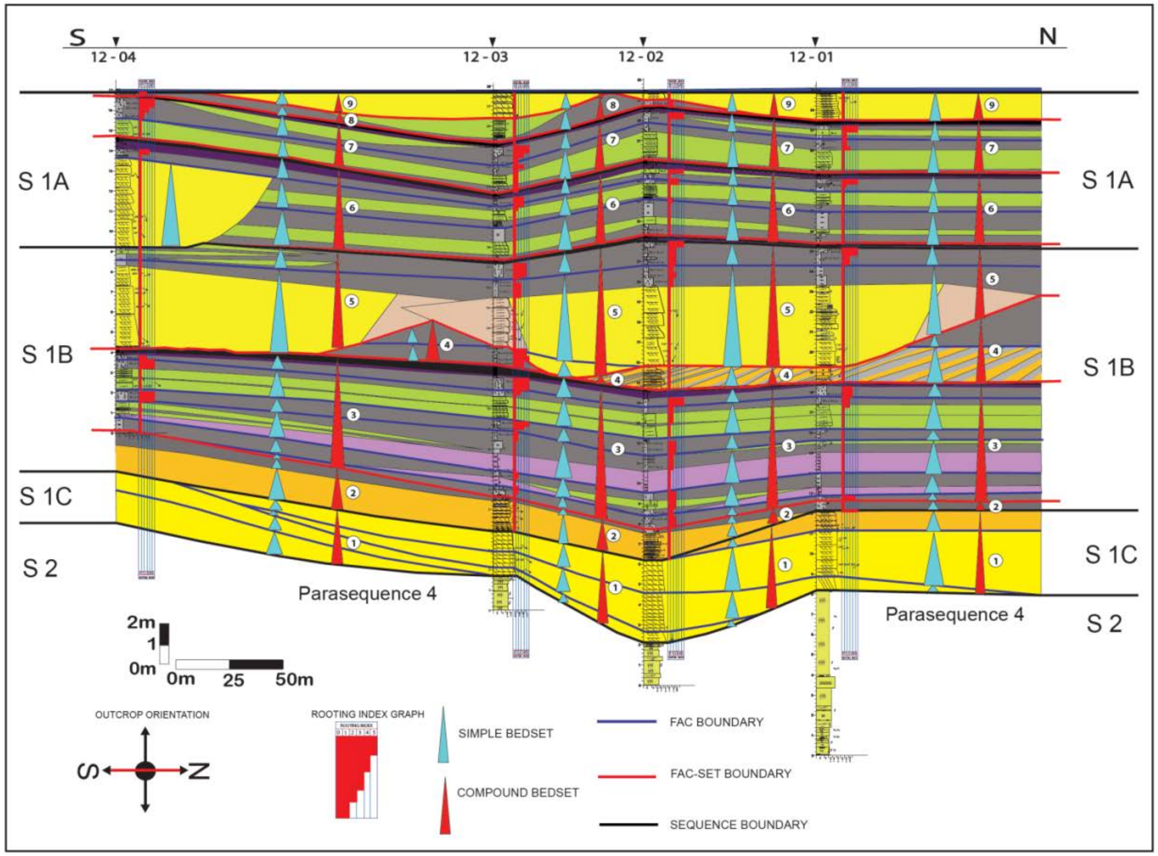

Figure 32.− Two-dimensional stratigraphic cross-section of the Ferron Notom in North Sweetwater showing the stacking of fluvial aggradation cycles and fluvial aggradation cycle sets in to three fluvial sequences (sequence 1C, 1B, and 1A). See cross section outline in Figure 20 and see legend in Figure 22.

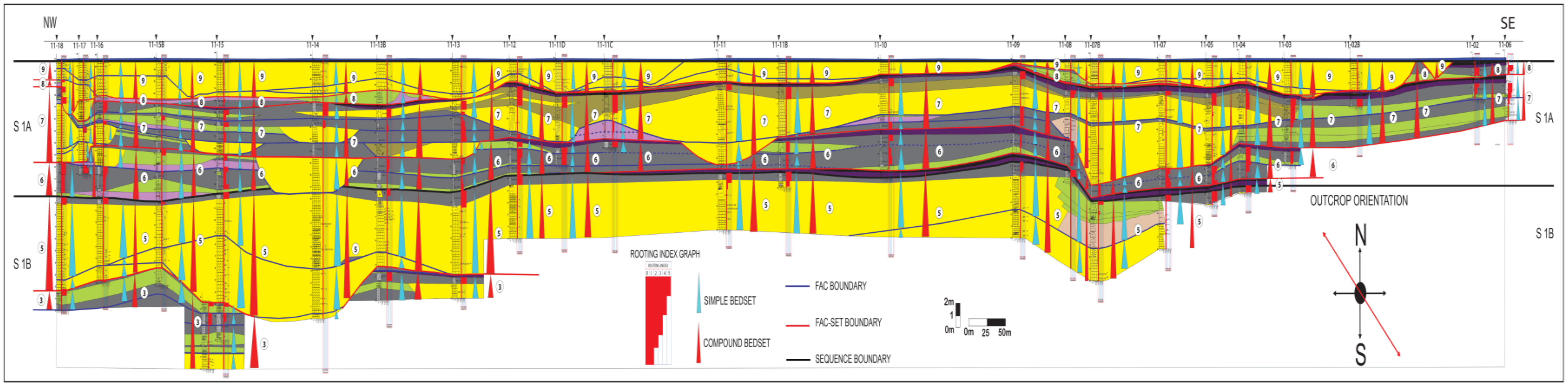

Figure 33.─ Two-dimensional stratigraphic cross-section of the Ferron Notom in South Sweetwater showing the stacking of fluvial aggradation cycles and fluvial aggradation cycle sets in to 2 fluvial sequences (Sequence 1B and 1A). Sequence 1C is not exposed in south Sweetwater. See cross section outline in Figure 20 and legend in figure 22.

A short hiatus, based on time of incipient pedogenic development required to produce an immature soil (or Entisol), as we observe in the Ferron, would last from 10 to less than 500 years (Birkeland 1999; Retallack 2001). Therefore, based on these estimates, and comparison with interavulsion periods in a number of modern river-deltas, FACs in this interval likely represent no more than 1,500 years of development and may be more likely in the range of <1000 years.

This estimation is at best conservative and may be further revised downward if accurate sediment accumulation rates of sedimentation of individual sequences within the Ferron Notom are known. Previous average sedimentation estimates of 0.2mm/yr (Zhu et al. 2012) are probably too low for a river system that drained an adjacent mountain belt in a humid sub-tropical to tropical climate with probably high amount of precipitation and high storm influence (Milliman and Syvitsky 1992; Bhattacharya and MacEachern 2009).

3.5.3 Fluvial Aggradation Cycle Sets

Nine fluvial aggradation cycle sets (henceforth FAC-sets) were identified in this study. They are mappable meter- to decameter-thick aggregates of FACs. They are bounded by pedogenically modified surfaces of rooting and burrowing, or are erosionally top-truncated**.** The subaerially exposed surfaces are commonly capped by coals and carbonaceous mudstones or siltstones. FAC-sets are marked by an upward increase in the degree of rooting and disruption of original sedimentary structures. They are either represented by compound floodplain bedsets or multi-storey channel-fill sandstones that are both capped by relatively mature paleosols.

Figure 31 shows two examples of a FAC-set. The first example (Fig. 31B) consists of 6 vertically stacked, paleosol-capped floodplain bedsets (or FACs). The uppermost paleosol is relatively well- rooted with a thicker zone of disruption compared to other paleosols in the set. The upper paleosol is also capped by carbonaceous mudstone and coal (i.e., a coal zone). In the second example (Fig. 31C), 2 multi-storey channel-fill sandstones are capped by a well-rooted paleosol that is overlain by carbonaceous siltstone and coal.

FAC-sets are laterally extensive and, barring local erosion by overlying channel belts, can be correlated across each section, for a minimum of several kilometers (Fig. 32, 33). The coal zones that cap the bounding surface of FAC-sets also aid in their correlation. Given that there are no pinchouts of the FAC-sets (excepting local top-truncation), it is very likely that FAC-sets extend for distances that greatly exceed the study area, likely tens of kilometers and possibly greater. Similar studies have shown that FAC-sets can be correlated over areas of several tens of kilometers, but few studies have attempted correlation across larger distances (Cleveland et al. 2007). The 9 preserved FAC-sets are named in ascending numerical order from bottom to top and are discussed in detail below.

3.5.3.1: FAC-set 1

A major erosional surface separates FAC-set 1 from the underlying marine shoreface (FA 1) deposits (Fig. 23, 32A). FAC-set 1 varies from 2 to 4 meters in thickness, and consists of amalgamated, multi-storey channel-fill sandstones (FA 2), overlain by tide-influenced channel-fill sandstones (FA 3). The juxtaposition of these fluvial sandstones of FAC-set 1 and underlying marine shoreface deposits (Facies 1), across an intervening erosional surface, represents a basinward shift in facies (Walker and Plint 1992; Posamentier et al. 1992; Posamentier and Allen 1999). This basinward shift in facies accompanied valley incision that led to truncation of underlying marine facies. The erosional surface represents a sequence boundary (Posamentier and Vail 1988; Van Wagoner et al. 1990; Posamentier and Allen 1999) and the base of Sequence 1 (Li et al. 2010; Zhu et al. 2012; Fig. 32A, 34). FAC-set 1 represents the fluvial sandstones that immediately followed the valley incision phase.

The trace fossil *Gastrochaenolites*, identified at the sequence boundary, and *Ophiomorpha* and *Skolithos* identified in the lower portions of the valley-fill sandstones in FAC-set 1 (Fig. 35A, 35B), indicate firmground development and colonization by marine organisms after the erosion of an unconsolidated or semi-consolidated marine substrate (MacEachern et al. 1992; Benton and Harper 1997). The trace fossil suite also suggests the existence of short-lived marine or marginal-marine conditions before increased fluvial deposition (MacEachern et al. 1992; Bromley 1996). The existence of marine or marginal-marine conditions indicate proximity of this part of the incised valley to the shoreline (MacEachern et al. 1997), thus presenting an example of a coastal-plain incised valley.

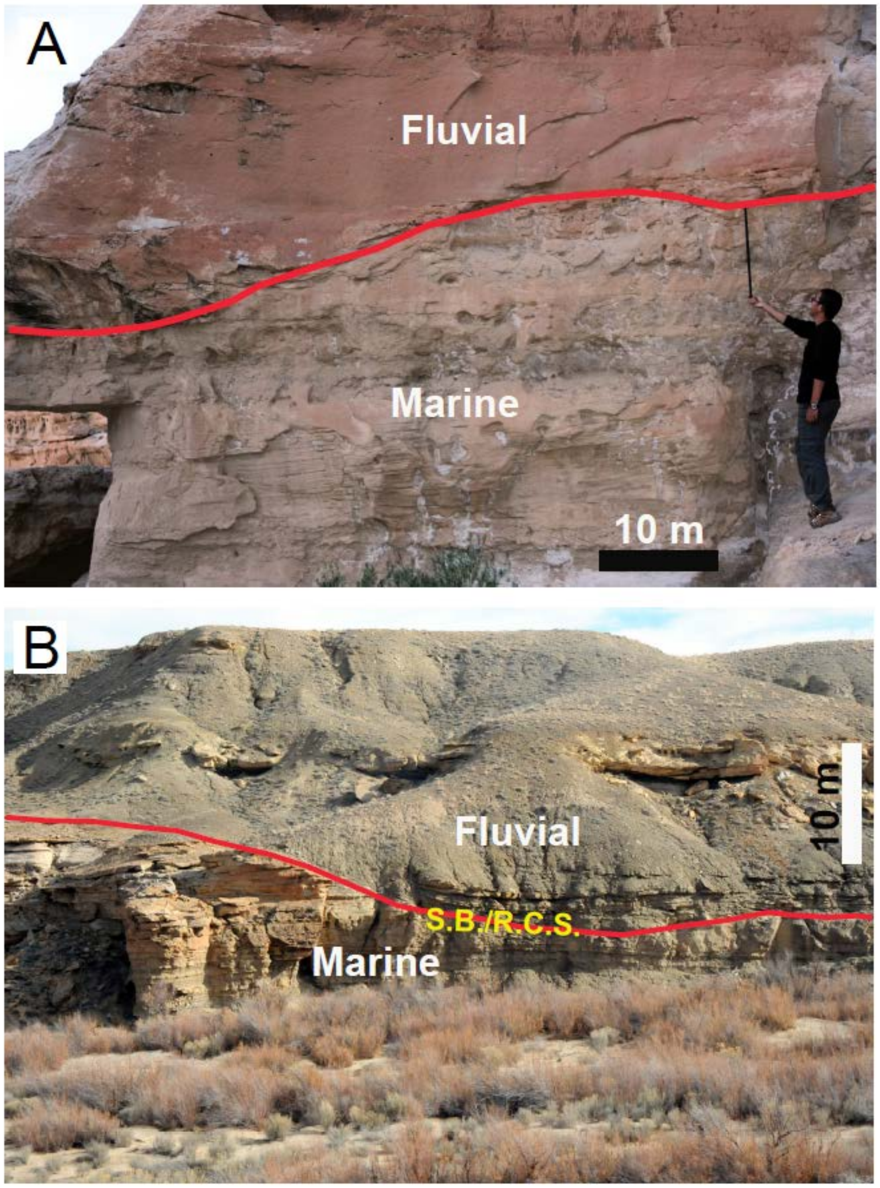

Figure 34.− Sequence boundary. **A)** Truncation of underlying hummocky cross-stratified and bioturbated marine shoreface sandstone by the overlying fluvial sandstone (FAC-set 1) with an intervening erosional surface represents a sequence boundary. **B)** Second phase of erosion truncated FAC-set 1 and underlying marine shoreface facies. This formed a compound erosional sequence boundary or regional composite scour surface (RCS). The resulting valley is filled with tide-influenced heterolithics comprising sandstones and interbedded mudstones (FAC-set 2).

Paleocurrent data (Fig. 36) indicate a north to northwest paleo-flow direction for all valley-fill sandstones in FAC-set 1. Based on the thickness of large-scale inclined strata (2.8 - 3.2 meters), which are interpreted to represent unit bars in the formative channel, paleo-flow depths of 3.6 to 4 meters were estimated (Bridge 2003). Estimated width (using numerical methods), based on bankfull depth vary from 500 to 650 meters, and flow velocity based on medium-grained sandstones and abundance of dune-scale cross bedding varied from 0.6 to 1.5 m / sec. Based on these parameters, the estimated bankfull paleo-discharge (Q) for the rivers in the paleo-incised valley is estimated to have varied from 750 to 2500 m^3 / sec. (Table 5).

3.5.3.2: FAC-set 2

A major erosional surface separates FAC-set 1 from the overlying FAC-set 2, which is about 1 to 2 meters thick (Fig. 32, 34B). This erosional surface truncates both FAC-set 1 and locally erodes into the underlying marine shoreface deposits. This suggests another erosional event associated with valley incision. FAC-1 therefore represents a preserved terrace. The resulting second incision was filled with tide-influenced heterolithic strata capped by an organic-rich and burrowed siltstone (FA 3) and comprises FAC-set 2. Figure 34B shows this younger incised valley truncating underlying marine shoreface deposits and cutting out the deposits of FAC-set 1. Root traces (Fig. 35C) in truncated sandstones of underlying FAC-set 1, indicate plant colonization and vegetative growth due to subaerial exposure. Paleocurrent data obtained from the heterolithic strata indicate a bimodal paleo-flow trend (Fig. 36) suggesting landward tidal flow and shoreward river flow.

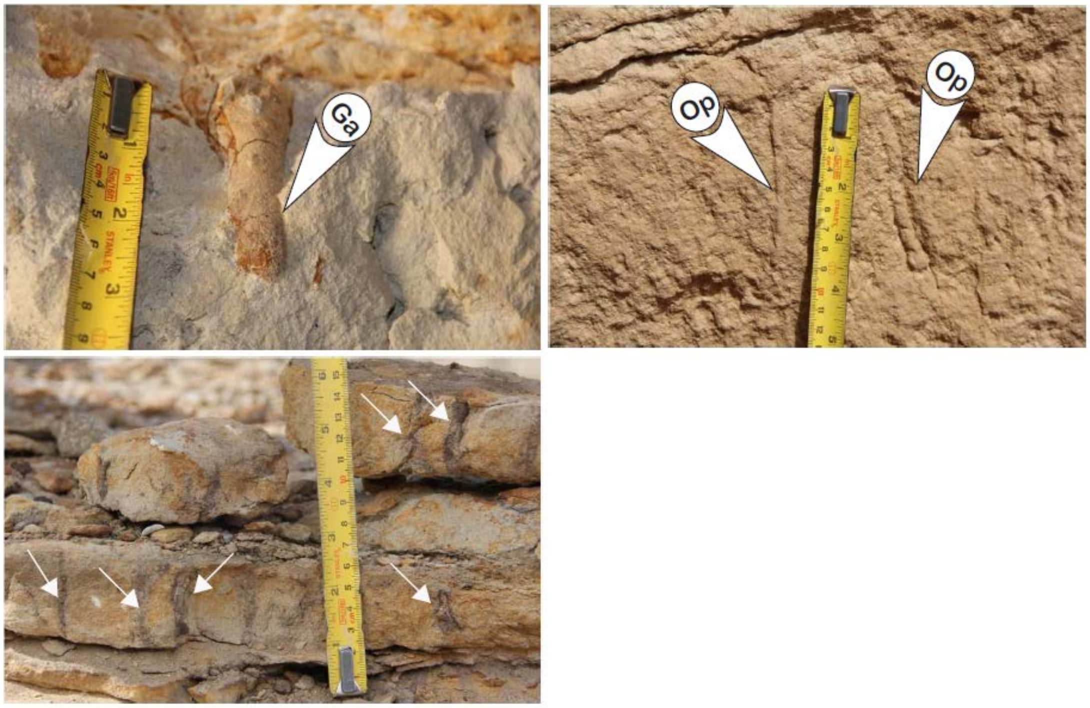

Figure 35.─ Incised-valley trace fossils and valley terrace relic. **A)** *Gastrochaenolites* (Ga) at the erosional contact between marine shoreface sandstone and fluvial incised-valley fill (i.e., FAC set-1) suggests firmground development and colonization by marine organisms after the erosion of unconsolidated or semi-consolidated marine substrate. **B)** *Ophiomorpha* (Op) in the lower portion of the incised-valley fill (FAC-set 1) suggests short-lived marine or marginal-marine conditions before increased fluvial deposition. **C)** Root traces (identified with arrows) in truncated sandstones of FAC-set 1 suggest terrace development and plant colonization.

Paleo-flow depth of 1.6 to 1.8 meters in the associated channel was estimated based on thicknesses of preserved channel storeys. Estimated width (using numerical methods), based on paleo-flow depth vary from 150 m to 170 meters. Flow velocity, based on very fine- to fine-grained sandstones and abundance of dune-scale cross bedding, varied from 0.7 to 1.2 m / sec. Based on these parameters, the estimated bankfull paleo-discharge (Q) for the river likely varied from 120 to 200 m^3 / sec. (Table 5).

3.5.3.3: FAC-set 3

FAC-set 2 is capped by FAC-set 3, which is a 4 to 9 meter-thick mudstone-prone unit (Fig. 32, 33). It consists of partially exposed isolated channel-fill sandstones (FA 2) encased in floodplain deposits (FA 4, 7 - 11). FAC-set 3 is capped by Coal-zone 1 (CLZ 1), which is an extensive coal zone that has been identified and mapped in other parts of the Ferron Notom Delta (Zhu et al. 2012; Fig 19) and is thus regional in nature. Limited exposure of channel-fill sandstones prevented the collection of paleocurrent data and consequent estimation of channel-fill dimensions in this FAC-set.

3.5.3.4: FAC-set 4

Overlying FAC-set 3 is FAC-set 4, which is about 2 to 3 meters thick. It is mostly erosionally truncated by the overlying FAC-set 5 and is only exposed in the North study area (Fig. 32). It consists of a tide-influenced, heterolithic channel-fill (FA 3) encased in floodplain mudstones (FA 7, 9, and 10). The heterolithic channel-fill consists of south-dipping accretion sets. Paleocurrent data indicate east to northeast paleo-flow, thus laterally accreting channels.

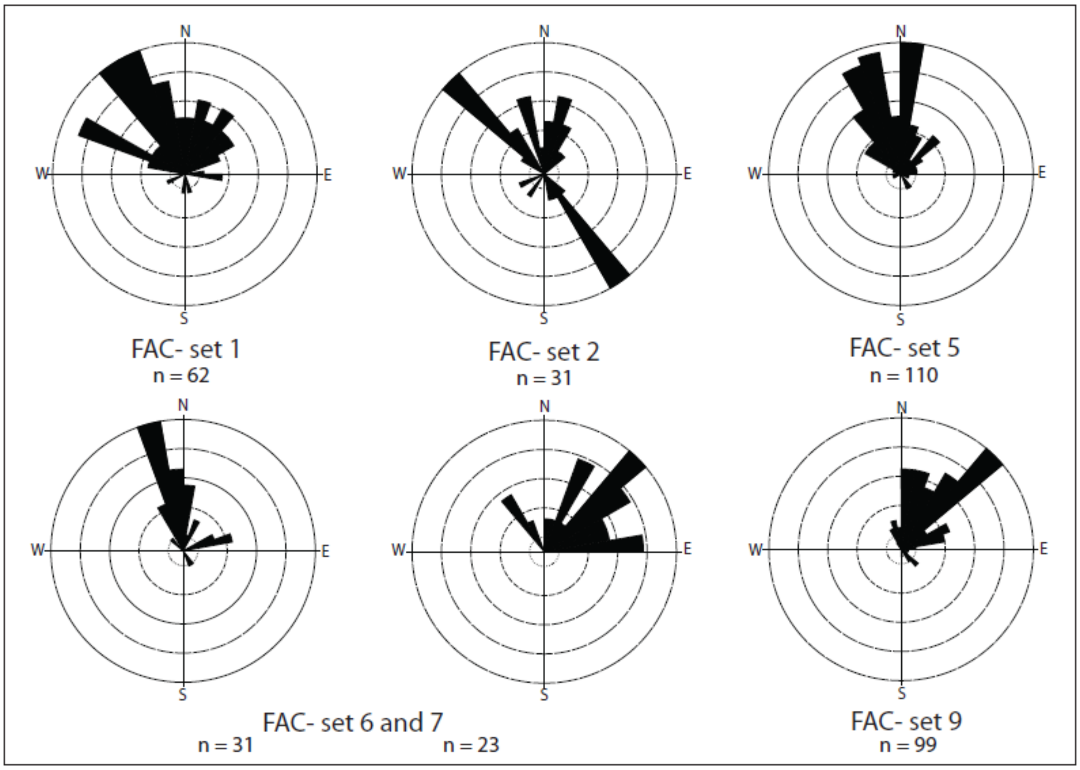

Figure 36.− Rose diagrams showing paleocurrent directions for channel-fills in the respective FAC-sets. Data for FAC-set 4 and FAC-set 8 are unavailable due to limited exposure.

Paleo-flow depth of 2.1 meters was estimated based on thicknesses of the preserved channel storey. Estimated width (using numerical methods), based on paleo-flow depth vary from 200 to 230 meters. Flow velocity, based on very fine- to fine-grained sandstones and abundance of dune-scale cross bedding, varied from 0.8 to 1.2 m / sec. Based on these parameters, the estimated bankfull paleo-discharge (Q) for the depositing river may have varied from 220 m^3 / sec to 400 m^3 / sec. (Table 5).

3.5.3.5: FAC-set 5

FAC-set 5 is 4 to 10 meters thick (Fig. 32, 33), and it consists of laterally extensive, amalgamated and locally multi-storey channel-fill sandstones (FA 2) with attached crevasse splay (FA 4) and levee (FA 5) deposits overlain by floodplain deposits (FA 7, 9 - 12). The paleosols that cap this unit represent the most developed paleosols observed in this study (i.e., equivalent to modern well-developed Inceptisols and Vertisols, or Alfisols). These paleosols are capped by Coal-zone 2 (CLZ 5). The thickness of fully preserved channel storeys varies from 3 to 6.5 meters. Paleocurrent data (Fig. 36) indicate a predominant north to northwest paleo-flow direction for the depositing river.

Estimated paleo-flow depth is based on the thicknesses of these preserved storeys (3 – 6.5 meters). Channel widths were estimated using numerical methods based on paleo-flow depth, and preserved channel width from outcrop data. These width estimates vary from 200 to 1200 meters. Flow velocity, based on medium- to coarse-grained sandstones and abundance of dune-scale cross bedding, varied from 0.6 to 1.5 m / sec. Based on these parameters, the estimated bankfull paleo-discharge (Q) for the depositing river may have varied from 350 m^3 / sec to 4200 m^3 / sec. (Table 5).

3.5.3.6: FAC-set 6 and 7

FAC-set 6 and FAC-set 7 are successive mudstone-prone units. The thicknesses of these FAC-sets vary from more than 1 to 5 meters (Fig. 32, 33). They consist of a series of well-exposed lens-shaped, isolated channel-fill sandstones (FA 2) that are encased in floodplain deposits (FA 4-11). FAC-set 6 and 7 are capped by Coal-zones 3 and 4, respectively. Isolated channel-fill sandstones are mostly single-storey, and full storey thicknesses vary from less than 1 to up to a maximum of 5 meters. Paleocurrent data (Fig. 36) show that paleo-flow direction varies for individual channel-fill sandstones; however, they may indicate northeast, north, or northwest paleo-flow directions. Centimeter- to decimeter-thick, dipping accretion sets are observed in some isolated channel-fill sandstones (Fig. 25) and their dip is often perpendicular to paleo-flow direction, thus indicating lateral accretion.

Paleo-flow depth of 1 to 5 meters was estimated based on thicknesses of preserved channel storeys. Channel widths were estimated using numerical methods based on paleo-flow depth, preserved channel widths, and preserved lateral accretion sets. These width estimates vary from 25 to 270 meters. Flow velocity, based on very fine- to medium-grained sandstones and abundance of dune-scale cross bedding, varied from 0.5 to 1.4 m / sec. Based on these parameters, the estimated bankfull paleo-discharge (Q) for the depositing river may have varied from 25 m^3 / sec to 800 m^3 / sec. (Table 5).

3.5.3.7: FAC-set 8

FAC-set 8 is mostly erosionally top-truncated (Fig. 32, 33) by the overlying FAC-set 9, leaving less than 1 meter to 2 meters of preserved strata, which consist predominantly of floodplain deposits (FA 4, 7-11). FAC-set 8 is capped by Coal-zone 5 (CLZ 5).

Table 5.— Estimated channel-belt dimensions and corresponding paleodischarge estimates

FAC-set	Paleo-channel Depth (m)	Estimated width (m) from empirical methods	Estimated width (m) from Outcrop Data	Flow Velocity (m/sec)	Discharge (Q) (m^3 / sec)
1	3.6 – 4.0	500 - 650	-	0.60 - 1.50	750 - 2500
2	1.6 – 1.8	150 - 170	-	0.75 - 1.20	120 - 200
4	2.1*****	200 - 230	-	0.80 - 1.20	220 - 400
5	3.0 – 6.5	200 - 1200	200 -	0.60 - 1.50	350 - 4200
6 & 7	1.4 – 5.0	25 - 270	25 - 230	0.50 - 1.40	25 - 800
9	2.0 – 4.0	300 - 360	360 -	0.65 - 1.65	350 - 1000

***** Only one channel belt was estimated in FAC-set 4 due to exposure limitations.

3.5.3.8: FAC-set 9

FAC-set 9 consists of laterally extensive, amalgamated and multi-storey channel-fill sandstones (FA 2). The thickness of fully preserved channel storeys varies from 2 to 4 meters (Fig. 32, 33). FAC-set 9 is capped by the fissile, dark-gray, parallel-laminated strata of the Blue Gate Shale with an intervening unconformity marked by a coarse-grained lag. Fossil fish scales and shark teeth are preserved at this contact (Li et al. 2010). Paleocurrent data from channel-fill sandstones indicates paleo-flow in a predominantly northeast direction (Fig. 36).

Paleo-flow depth was estimated based on thicknesses of preserved channel storeys (i.e., 2 - 4m). Channel widths were estimated using numerical methods based on paleo-flow depth and preserved channel widths. These width estimates vary from 300 to 600 meters. Flow velocity, based on medium- to coarse-grained sandstones and abundance of dune-scale cross bedding, varied from 0.65 to 1.65 m / sec. Based on these parameters, the estimated bankfull paleo-discharge (Q) for the depositing river may have varied from 350 m^3 / sec to 1000 m^3 / sec. (Table 5).

3.5.4: FAC-set Interpretation

FAC-sets are interpreted to record successive phases of FAC development that eventually culminate in relatively long periods of stability (1,000 to < 5,000 years), characterized by abandonment, exposure, and significant pedogenic development, indicating major channel avulsions and a corresponding shift in locus of sedimentation (Bridge 1984; Kraus 1987; Atchley et al. 2004; Cleveland et al. 2007). Upward increase in the intensity of rooting in FAC-sets also provides additional evidence of extensive vegetative growth (Retallack 1988) and soil development in the abandoned areas. High root abundance percentages observed by Nordt et al. (2012) in Upper Cretaceous to Lower Tertiary strata of the Western Interior Seaway, also corresponded with bounding surfaces of FAC-sets.

Capping carbonaceous mudstones or siltstones and coals, such as are common in this study, suggest significant reduction in siliciclastic sediment input and increased organic matter preservation in the abandoned area. Marine trace fossils (*Teredolites* and *Thalassinoides*) above coals suggest marine transgression either as a result of compactional subsidence of the abandoned area (Ryer 1981) or eustatic sea-level rise (Bohacs and Suter 1997; Ryer and Anderson 2004).

In attempt to estimate the time of deposition of coal beds that cap bounding surfaces of FAC-sets, an average peat compaction ratio of 7:1 was used, based on the compilation of Ryer and Langer (1980). Using an average peat accumulation rate of 2.5 mm/yr, which is common for modern tropical deltas (Emery and Myers 1996; Page et al. 2010), a 30 cm coal bed (Fig. 31A) would decompact to yield 2.1 meters of peat, which could represent 800 to 1000 years of peat accumulation (Table 6). A 60 cm coal zone could represent 1500 to 2000 years of peat accumulation.

Table 6.— Estimated duration of peat accumulation for coal bed and coal zones that cap FAC-sets.

Coal Zone	**Associated FAC-SET**	**Coal Bed – Coal Zone Thickness (mm)**	**Decompacted Thickness (x 7 mm)**	**Accumulation Period (years) (2.5 mm/yr)**
1	3	300 - 600	2100 - 4200	850 - 1700
2	5	200 - 600	1400 - 4200	560 - 1700
3	6	300 -700	2100 - 4900	850 - 2000
4	7	250 - 700	1750 - 4900	300 - 2000
5	8	200 - 450	1400 - 3150	560 - 1300

Based on the estimated ages of constituent FACs (< 1500 years), the time of pedogenic development (1,000 to < 5,000 years) on bounding surfaces of FAC-sets (Birkeland 1999; Retallack 2001), and the estimated period of peat accumulation on the bounding surfaces (300 to 2,000 years), FAC-sets in this study likely represent intervals of an order of no more than 10^4 years. The paleosols that bound FAC-set 5 likely represents a relatively longer time of pedogenic development (i.e., 5,000 to 15,000 years), compared to other FAC-sets, and suggests a significant stratigraphic surface of non-deposition different from that caused by avulsion.

3.5.5: Fluvial Sequences

In the studied interval, fluvial sequences are mappable decameter-scale units that consist of multiple vertically-stacked FAC-sets that are bound by major disconformities (erosional or non-depositional). Similar to marine sequences, fluvial sequences consist of systems tracts, which include: falling-stage, lowstand, transgressive, and highstand (Van Wagoner et al. 1988; Shanley and McCabe 1993, 1994; Miall 1991; Wright and Marriot 1993; Posamentier and Allen 1999). FAC-sets are not equivalent to systems tracts; a single FAC-set may represent parts of two systems tracts. Likewise, a single FAC-set or multiple FAC-sets may represent a single systems tract (cf. Atchley et al. 2004). The characteristics of each FAC-set and its relationship to underlying and overlying strata determine its systems-tract designation.

The depositional history of the units in this study are illustrated in cross-sections to show the different hierarchies of strata (Fig. 32, 33) and on Wheeler diagrams (Fig. 37A, 37B) to show stratigraphic relationships in time and space. The equivalent marine strata to this fluvial succession are not preserved due to modern erosion; hence direct comparisons could not be made. However, the lower Ferron contains a well-studied marine component that we can compare to. The designation of FAC-sets to systems tracts and sequences are based on; (i) interpreted changes in process and environments in between successive FACs and FAC-sets, (ii) fluvial sequence-stratigraphic models (Miall 1991, 1996; Wright and Marriot 1993), and (iii) similar field observations from other studies (Olsen et al. 1995; Yoshida et al. 1996; Plint et al. 2001; Fanti and Catuneanu 2010).

We interpret valley incision and the erosion of underlying marine shoreface deposits to be a result of base-level fall, forming the equivalent to a falling-stage systems tract. Valley filling was marked by moderate stream discharge and deposition of amalgamated multi-storey channel-fill sandstones and tide-influenced channel-fill sandstones of FAC-set 1. These are interpreted as lowstand to early transgressive systems tract.

Another phase of erosion and valley incision and terrace development, as a result of base-level fall, resulted in truncation of the underlying incised-valley fill (FAC-set 1) and marine shoreface deposits. This represents another falling stage systems tract. Subsequent base-level rise led to deposition of tide-influenced heterolithic strata (FAC-set 2), that is interpreted as representing the lowstand to early transgressive systems tract. Zhu et al. (2012) interpreted the organic-rich and burrowed capping surface of FAC-set 2 as a marine flooding surface. Alternatively, this may be interpreted entirely as an early transgressive systems tract (Dalrymple et al, 1994). In that case, the amalgamated channel-fill deposits that would typically represent the lowstand systems tract were probably not deposited at this location. Deposition of FAC-set 2 concludes the incised-valley deposition phase.

FAC-set 1 and FAC-set 2 represent separate incised-valley deposits in a compound incised-valley system, where FAC-set 1 represents the first cut-and-fill phase, and FAC-set 2 represents the second phase of truncation and filling. Multiple cut-and-fill episodes produced a diachronous erosional surface or a regional composite scour surface (RCS) (Holbrook and Bhattacharya 2012).

Continued base-level rise was accompanied by deposition above and outside the compound incised valley. This was marked by increased floodplain deposition and preservation, and deposition of channel-fill sandstones with limited lateral continuity (FAC-set 3). FAC-set 3 is interpreted as a late transgressive systems tract. Abundant marine trace fossils found in Coal Zone 1, which caps FAC-set 3, indicate marine transgression due to continued rise in base level, and may represent a maximum flooding surface. Zhu et al. (2012), based on more regional correlations to the north, also interpreted this surface as a marine flooding surface.

The signature of this marine transgression is evident in the overlying FAC-set 4, where evidence of marine influence is also observed in the laterally accreting heterolithic channel-fill (Fig. 32A). FAC-set 4 is interpreted as an early highstand systems tract and marks the beginning of the ‘turn-around’ or decrease in the rate of base-level rise. Decrease in base-level rise continued through the deposition of FAC-set 5, which eroded most of the early highstand deposits of FAC-set 4 and was characterized by deposition of laterally extensive, amalgamated channel-fill sandstones. This reduced floodplain preservation due to continued reworking and removal of floodplain sediments by laterally migrating channels. This is interpreted as the late highstand systems tract.

The subsequent falling stage, lowstand, and possibly early transgressive systems tracts are not represented in the succession. Erosion and deposition that accompanied these missing systems tracts probably occurred in distal parts of the delta, down depositional dip away from the study area. However, the most developed paleosol in the interval caps FAC-set 5, suggesting a sequence boundary, or a correlative conformity landward of a sequence boundary (Van Wagoner et al. 1990). Coal-zone 2 that caps the paleosols suggests initial marine transgression. FAC-set 5 is directly overlain by FAC-set 6 and 7, which are characterized by increased preservation of floodplain deposits, and deposition of isolated channel-fill sandstones. This interval is interpreted as another transgressive systems tract. Abundant marine trace fossils found in the extensive Coal-zone 4 that cap FAC-set 7 indicate marine transgression, and it is interpreted as the fluvial equivalent of a maximum flooding surface.

FAC-set 8 is interpreted as an early highstand systems tract and marks the beginning of decrease in base-level rise. Most of FAC-set 8 was eroded during the subsequent late highstand systems tract, which was characterized by continued decrease in base-level rise which led to deposition of laterally extensive amalgamated channel-fill sandstones and reduced floodplain preservation (FAC-set 9).The contact between deposits of this late highstand systems tract (FAC-set 9) and the overlying Blue Gate Shale is both a regional unconformity, which is likely tectonic in origin, and a regional transgressive surface of erosion, as indicated by the coarse-grained sandstone lag at the contact (Fig. 32B; Li et al. 2010; Zhu et al. 2012).

The above interpretation reveals three separate depositional sequences (Fig. 32, 33, 37A, 37B) in what was formerly interpreted as a single depositional sequence (i.e. Sequence 1), these are: Sequence 1C (oldest), Sequence 1B, and Sequence 1A (youngest). The first and oldest sequence (Sequence 1C) comprises falling stage, lowstand, and transgressive systems tracts. The second sequence (Sequence 1B) comprised falling stage, lowstand, transgressive, and highstand systems tracts. The third and youngest sequence 1A comprises a transgressive and highstand systems tract. Both Sequences 1C and 1B may be classified as simple sequences that comprise a sequence set, whereas Sequence 1A represents a 'stand-alone' simple sequence. More broadly, the originally defined Sequence 1, of Zhu et al. (2012) is not a simple sequence, but comprises a possible sequence set and a simple sequence. Analysis of parasequences in the marine parts of the Ferron Notom Delta complex (Sequence 3) record sequence sets that are analogous in duration and scale (Zhu et al. 2012).

The basal boundaries of the first two sequences (i.e. Sequences 1C and 1B) have the characteristics of a classic sequence boundary (i.e. erosional vacuity and basinward shift in facies). The basal boundary of the third and youngest sequence (Sequence 1A) is subtle compared to the sequence boundaries of older underlying sequences, and it is embedded in fluvial strata. The only diagnostic feature of this boundary is the relatively mature paleosol at its top (Fig. 32, 33). This emphasizes that sequence boundaries in fluvial strata may be cryptic and are not always easily identified (Yoshida et al. 1996).

The compound incised-valley system represented by Sequence 1C (FAC-set 1) and Sequence 1B (FAC-set 2) has been documented earlier by Li et al. (2010) and more recently by Li and Bhattacharya (2013), where three phases of valley incision and subsequent filling (V3, V2, and V1, respectively) were recognized. The lower incised-valley fill that constitutes FAC-set 1 in this study is likely equivalent to V3 in their study, while the upper incised-valley fill that constitute FAC-set 2 in this study is likely equivalent to V2 or V1 in their study. However, V2 and V1 in their study have basal amalgamated channel-fill sandstones that are overlain by tide-influenced heterolithic strata. These basal amalgamated channel-fill sandstones are not present in FAC-set 2, and the incised valley is only filled with tide-influenced heterolithic strata.

A comparison of the thickness (~ 6 m) of the basal compound incised valley that comprises Sequence 1C and parts of Sequence 1B, to the thicknesses of the same compound incised valley (up to 30 m) recorded by Li et al. (2010) and Li and Bhattacharya 2013), suggests that it either represents a shallow lateral extension of the compound incised valley or a tributary to a deeper trunk valley farther north.

The models and field-based studies on which the above interpretations are based contrasts with models of Shanley and McCabe (1993, 1994) and Posamentier and Vail (1988), both of which assigned increased floodplain deposition and limited lateral continuity of channel-fill sandstones to the highstand systems tract, amalgamation of channel-fill sandstones in incised valleys to the lowstand systems tract, and tide-influenced strata above amalgamated channel-fill sandstones to the transgressive systems tract. Their models did not predict amalgamation of channel-fill sandstones outside incised valleys, which is the case in FAC-set 5 and FAC-set 9.

3.6 CONTROLS ON CYCLICITY AND RELATIONSHIP TO MARINE SEQUENCES

Zhu et al. (2012) attributed individual sequences in the Ferron Notom to relatively high-frequency Milankovitch-scale sequences (~100,000 years), and simple sequences within a forced regressive sequence set to the shortest higher frequency Milankovitch-scale cycles (< 30,000 years). Li and Bhattacharya (2013) attributed repeated incision and erosion in the basal compound incised valley of Sequence 1 to stepped falls in relative sea level (i.e. stepped, forced regressions) followed by sea-level rises. Each ‘fall and rise’ phase was also correlated with higher frequency Milankovitch-scale cycles of less than 30,000 years. Therefore, interpreted sequences in the studied interval (Sequence 1C, 1B, and 1A) likely correlate to the shortest, higher frequency Milankovitch-scale cycles (~20,000; 40,000) similar to that of Li and Bhattacharya (2013). Observations from this study suggest that sequence boundary development in this sequence spans 5,000 to 15,000 years (Birkeland 1999, Retallack 2001). Fielding (2011) recognized the tectonic effects in the deposition history of the Ferron Notom. However, the uppermost part of the Ferron Notom in this study that is equivalent to the ‘upper member’ in the Fielding (2011) study, appears to have been unaffected by tectonic movements.

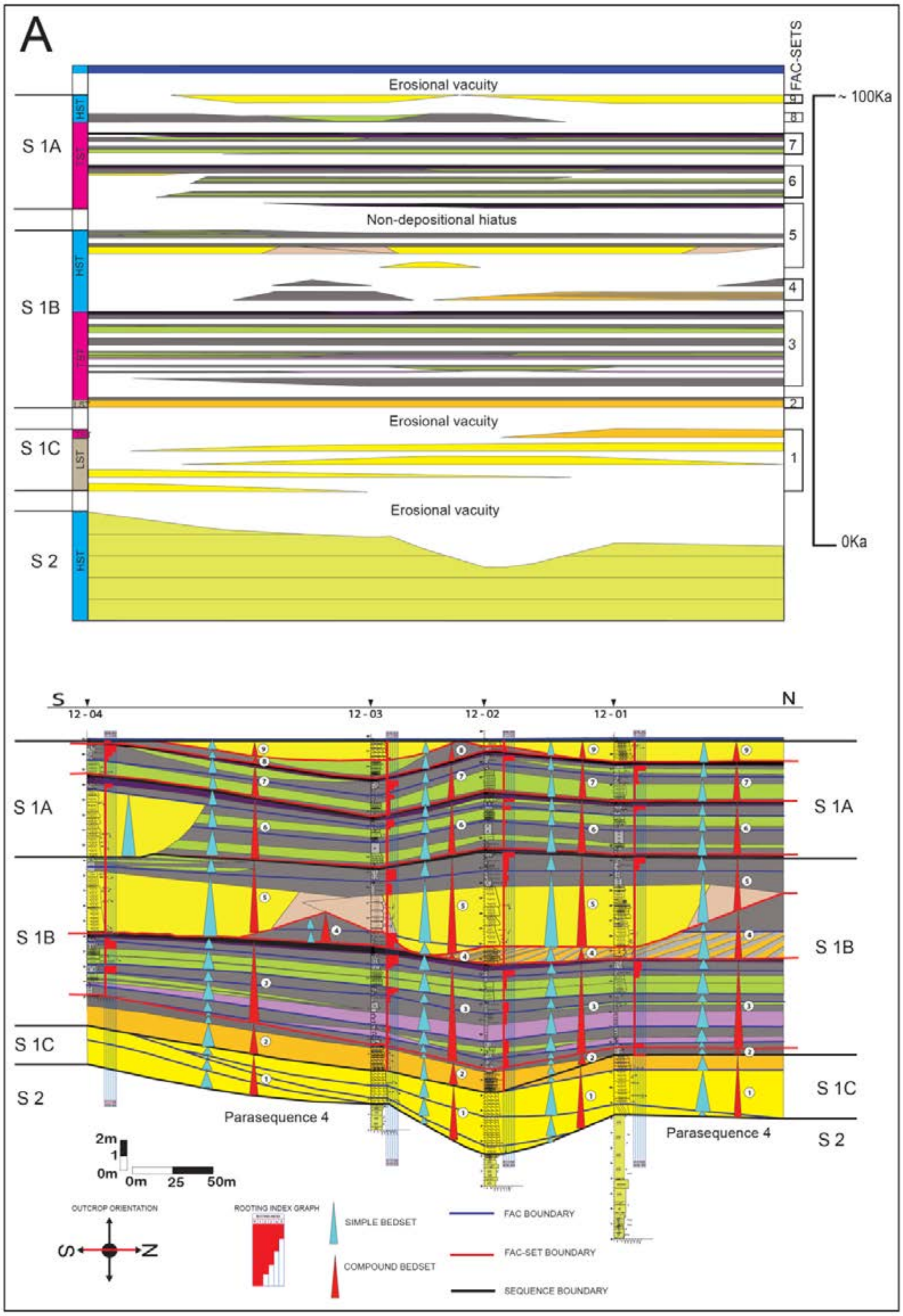

Figure 37A.− Caption on next page.

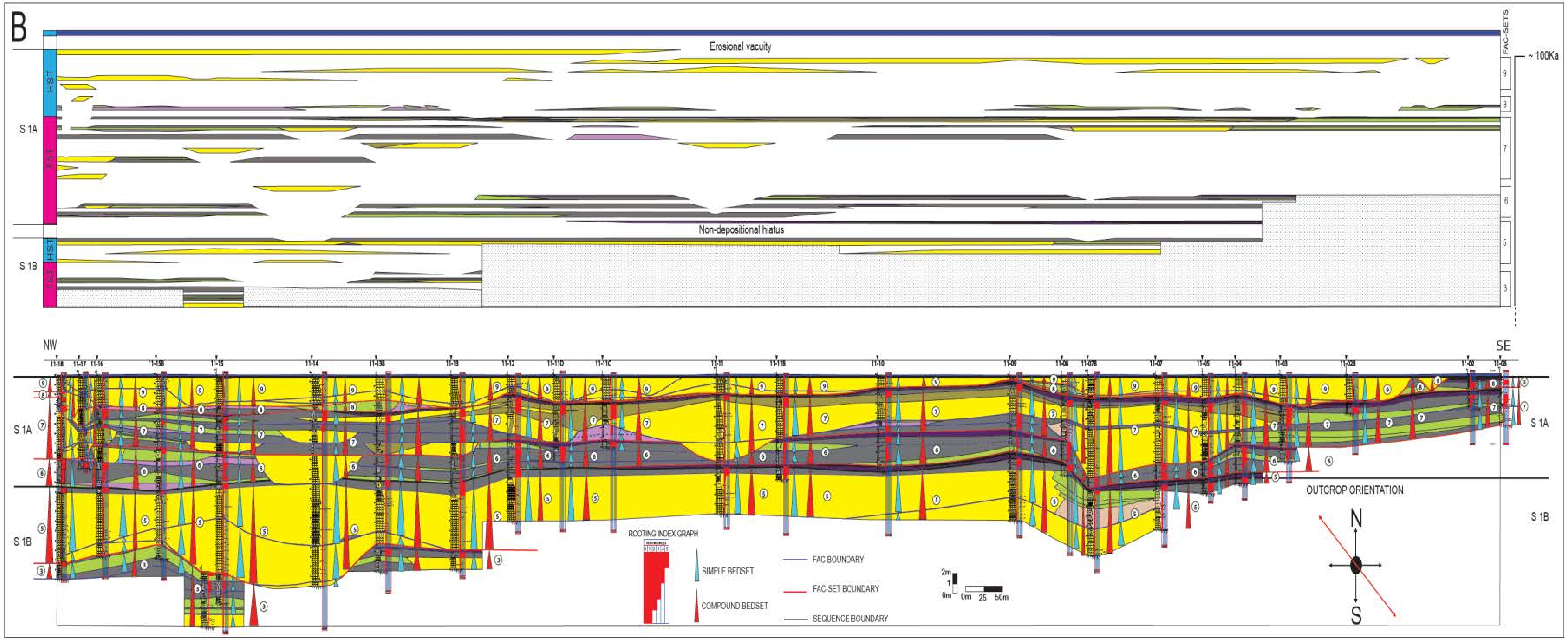

Figure 37.− Wheeler diagrams illustrating the depositional history of the succession in north **(A)** and south Sweetwater **(B)**. FAC-sets are identified by the numbers on the right. The first two sequence boundaries (S1C and S1B) are represented by valley incision during relative sea-level fall and valley filling during subsequent rise. The basal boundary of Sequence 1A is represented by a period of non-deposition marked by extensive pedogenic development. The contact between the Ferron Notom and the Blue Gate Shale is a regional unconformity that is likely tectonic.

The cyclicity in FACs is attributed to episodic channel avulsion and stability (Atchley et al. 2004). The period of deposition of FACs before avulsion and stability represents an interavulsion period (Tornqvist 1994), which is most likely < 500 years in the studied interval (similar to the Po and the Rhone fluvio-deltaic systems). Cyclicity in FAC-sets is attributed to longer term avulsive trends within fluvial systems (Atchley et al. 2004). This scale of cyclicity is comparable to those estimated for marine parasequences in the Ferron Notom delta (10,000 to 15,000 years), which suggests a possible link between FAC-set development in the coastal plain and down-dip marine parasequence development. Constituent FACs may be linked to bedset-scale features that constitute parasequences and perhaps the coal zones that cap FAC-sets are coastal-plain extensions of parasequence boundaries.

3.7 CONCLUSIONS

A detailed outcrop characterization of what was originally interpreted as a single 100Ka, 4^{th} or 5^{th} order depositional sequence, consisting of three broadly defined parasequences reveals 11 depositional facies. These facies, in turn, combine to build at least 33 distinct fluvial aggradation cycles (FACs), 9 fluvial aggradation cycle sets (FAC-sets), and 3 fluvial sequences.

Fluvial aggradation cycles (FACs) in the studied interval are represented by floodplain bedsets or individual channel storeys that are capped by relatively immature paleosols or erosional surfaces. They extend for hundreds of meters up to a few kilometers. FACs represent rapid floodplain or channel depositional events that span 5 to 1500 years due to periodic avulsions, and are followed by short periods (10 to 500 years) of stability characterized by abandonment, subaerial exposure, and incipient pedogenesis. Inter-avulsion periods for FACs in this study, are likely not more than 500 years, which is comparable to those in modern analogs of the deltaic system.

Fluvial aggradation cycle sets (FAC-sets) are aggregates of FACs that are capped by relatively mature paleosols or erosional surfaces. They are represented by compound floodplain bedsets or multistory channel fills that are bound by relatively mature pale-osols, which are capped by coals and carbonaceous strata. They extend for a few kilome-ters to tens of kilometers. FAC-sets record successive phases of FAC development that eventually culminate in relatively long periods of stability (1,000 to < 5,000 years) char-acterized by abandonment, exposure, and significant pedogenic development, indicating a major avulsion and shift in locus of sedimentation. Overlying coals and carbonaceous mudstones were deposited as a result of marine transgression either due to compactional subsidence of the abandoned and exposed area, or due to sea-level rise. FAC-sets in the studied interval represent an estimated development time of not more than 10,000 years. This scale of cyclicity is also comparable to those estimated for marine parasequences in the entire Ferron Notom delta (10,000 to 15,000 years), which suggests a possible link between non-marine and marine cyclicity.

Detailed facies description, correlation of FACs and FAC-sets, and time-stratigraphic analysis reveal 3 high frequency Milankovitch-scale (~20,000; 40,000 years) fluvial depositional sequences that consist of complete or incomplete suites of depositional systems tracts. The oldest Sequence 1C truncates underlying marine shoreface sandstones and consists of falling stage, lowstand, and transgressive systems tract. Sequence 1B truncates underlying sequence 1C and underlying marine shoreface sandstones forming a compound erosional surface. Sequence 1B consists of falling stage, lowstand, transgressive, and highstand systems tract. The youngest Sequence 1A consist of transgressive and highstand systems tract. This study shows that detailed integration of channel and floodplain deposits in the characterization of fluvial strata results in high-resolution sequence-stratigraphic interpretations.

CHAPTER 4

SUMMARY AND CONCLUSIONS

This study documents the characteristics of hydromorphic floodplain paleosols, other floodplain facies, and channel-fill facies in the youngest non-marine (100Ka) sequence in the Cretaceous Ferron Notom Deltaic Complex. It integrates vertical organization observed in floodplain facies with channel-fill facies to produce a high-resolution, sequence stratigraphic interpretation of the sequence, and compares cyclicity observed in the non-marine strata to associated marine strata.

Hydromorphic floodplain paleosols in this study vary from very weakly developed to well-developed. They consist of distinct pedogenic features that indicate fluctuating drainage conditions, thus suggesting alternating wet and dry and conditions, where wet periods were more prevalent than dry periods. These observed characteristics do not fit the conventional description of hydromorphic paleosols as everwet and weakly developed. It also highlights the potential of hydromorphic paleosols as useful paleoenvironmental, paleohydrological, and paleoclimatic indicators.

The integration of floodplain facies and channel-fill facies in the sequence led to the recognition of 33 fluvial aggradation cycles, 9 fluvial aggradation cycle set, and 3 high-frequency sequences (~20Ka; 40Ka) in what was initially interpreted as a single sequence. The scale of cyclicity observed in the fluvial aggradation cycle sets and sequences is comparable the scale observed in associated marine parasequences and sequences, respectively. This study represents the first detailed description of paleosols in the Cretaceous Ferron Notom and other Ferron deltas. It also shows that detailed facies analysis and integration of floodplain and channel-fill strata can produce a high resolution sequence stratigraphic interpretation of fluvial strata.

REFERENCES

ALLEN, J.R.L., 1965, A review of the origin and characteristics of recent alluvial sediments: Sedimentology, v. 5, p. 89–191.

ARNDORFF, L., 1993, Lateral relations of deltaic palaeosols from the Lower Jurassic Rønne Formation on the island of Bornholm, Denmark: Palaeogeography, Palaeclimatology, Palaeoecology, v. 100, p. 235-250.

ASHLEY, G.M., DEOCAMPO, D.M., AND KAHMAN-ROBINSON, J., 2013, Groundwater-fed wetland sediments and paleosols: It's all about water table, *in* Driese, S.G., Nordt, L.C., and McCarthy, P.J., eds., New Frontiers in Paleopedology and Terrestrial Climatology: Paleosols and soil surface analog systems: SEPM Special Publications 104, p. 47 -61.

ASLAN, A., AND AUTIN, W.J., 1999, Evolution of the Holocene Mississippi River floodplain, Ferriday, Louisiana: Insights on the origin of fine-grained floodplains: Journal of Sedimentary Research, v.69, p. 800 -815.

ASLAN, A., AUTIN, W. J., AND BLUM, M.D., 2005., Causes of river avulsion: insights from the late Holocene avulsion history of the Mississippi river, U.S.A.: Journal of Sedimentary Research, v. 75, p. 648-662.

ATCHLEY, S.C., NORDT, L.C., AND DWORKIN, S.I., 2004, Eustatic control on alluvial sequence stratigraphy: a possible example from the Cretaceous–Tertiary transition of the Tornillo Basin, Big Bend National Park, West Texas: Journal of Sedimentary Research, v. 74, p. 391–404.

ATCHLEY, S.C., NORDT, L.C., DWORKIN, S.I., CLEVELAND, D.M., MINTZ, J.S., HARLOW, R.H., 2013, Alluvial Stacking Pattern Analysis and Sequence Stratigraphy: Concepts and Case Studies, *in* Driese, S.G., Nordt, L.C., and McCarthy, P.J., eds., New Frontiers in Paleopedology and Terrestrial Climatology: Paleosols and soil surface analog systems: SEPM Special Publications 104, p. 109 -129.

AUTIN, W. J., AND ASLAN, A., 2001, Alluvial pedogenesis in Pleistocene and Holocene Mississippi River deposits: Effects of relative sea-level change: Geological Society of America Bulletin, v. 113, p. 1456-1466.

AUTIN, W. J., BURNS, S. F., MILLER, B. J., SAUCIER, R. T., AND SNEAD, J. I., 1991, Quaternary geology of the Lower Mississippi Valley, *in* Morrison, R. B., ed., Quaternary nonglacial geology: Conterminous U.S.: Boulder, Colorado, Geological Society of America, Geology of North America, v. K-2, p. 547-582.

BENTON, M.J., AND HARPER, D.A.T., 1997, Basic Paleontology: Longman, Harlow, Essex, London, U.K., 342 p.

BESLY, B. M., AND FIELDING, C. R., 1989, Palaeosols in the Westphalian coal-bearing and red-bed sequences, Central and Northern England: Palaeogeography, Palaeclimatology, Palaeoecology, v. 70, p. 303-330.

BHATTACHARYA, J.P., AND TYE, R.S., 2004, Searching for modern Ferron analogs and applications to subsurface interpretation, *in* Chidsey, T.C., Adams, R.D., and Morris, T.H., eds., Regional to Wellbore Analog for Fluvial–Deltaic Reservoir Modeling: The Ferron Sandstone of Utah: American Association of Petroleum Geologists, Studies in Geology, v. 50, p. 39-57.

BIRKELAND, P. W., 1999, Soils and Geomorphology: Oxford University Press, New York, 448 p.

BOHACS, K. M., AND J. SUTER, 1997, Sequence stratigraphic distribution of coaly rocks: fundamental controls and examples: American Association of Petroleum Geologists Bulletin, v. 81, p. 1612– 1639.

BOWN, T.M., AND KRAUS, M.J., 1987, Integration of channel and floodplain suites I. Developmental sequence and lateral relations of alluvial paleosols: Journal of Sedimentary Petrology, v. 57, p. 587-601.

BREWER, R., 1964, Fabric and Mineral Analysis of Soils: John Wiley and Sons Inc., New York, 470 p.

BRIDGE, J.S., 1984, Large-scale facies sequences in alluvial overbank environments: Journal of Sedimentary Petrology, v. 54, p. 583–588.

BRIDGE, J.S., 1995, Architecture of Miocene overbank deposits in Northern Pakistan-Discussion: Journal of Sedimentary Petrology, v. B65, p. 401 – 407.

BRIDGE, J.S., 2003, Rivers and Floodplains: Oxford, U.K., Blackwell Science, 491 p.

BRIDGE, J. S., 2006, Fluvial facies models: recent development, *in* Posamentier H.W. and Walker R.G., eds., Facies Models Revisited, SEPM Special Publication 84, p. 85–170.

BRIDGE, J. S., AND LUNT, I.A., 2009, Depositional models of braided rivers, *in* Sambrook Smith, G.H.., Best, J.L., Bristow, C.S. and Petts, G.E., eds., Braided Rivers Process, Deposits, Ecology, and Management: International Association of Sedimentologists, Special Publication 36, p. 11-50.

BRIDGE, J.S., AND MACKEY, S.D., 1993a, A revised alluvial stratigraphy model, *in* Marzo, M., and Puidefabregas C., eds., Alluvial Sedimentation: International Association of Sedimentologists, Special Publication 17, p. 319–337.

BRIDGE, J.S., AND TYE, R.S., 2000, Interpreting the dimensions of ancient fluvial channel bars, channels, and channel belts from wireline-logs and cores: American Association of Petroleum Geologists Bulletin, v. 84, p. 1205–1228.

BRIERLEY, G.J., FERGUSON, R.J., AND WOOLFE, K.J., 1997, What is a fluvial levee?: Sedimentary Geology, v. 114, p. 1–9.

BRISTOW, C.S., AND BEST, J.L., 1993, Braided rivers: perspectives and problems, *in* Best, J.L., and Bristow, C.S., eds., Braided Rivers: Geological Society of London, Special Publication 75, p. 1–11.

BRISTOW, C.S., SKELLY, R.L., AND ETHRIDGE, F.G., 1999, Crevasse splays from the rapidly aggrading, sand-bed, braided Niobrara River, Nebraska: effect of base-level rise: Sedimentology, v. 46, p. 1029–1047.

BROMLEY, R. G., 1996, Trace Fossils: Biology, Taphonomy and Applications, Second Edition: London, U.K. Chapman and Hall, 361 p.

BROMLEY, R.G., PEMBERTON, S.G., AND RAHMANI, R.A., 1984, A Cretaceous woodground: the *Teredolites* ichnofacies: Journal of Paleontology, v. 58, p. 488-498.

BULLOCK, P., FEDOROFF, N., JONGERIUS, A., STOOPS, G., TURSINA, T., AND BABEL, U., 1985, Handbook for soil thin section description: Waine Research Publications, Wolverhampton, England, 152 p.

BUOL, S.W., HOLE, F.D., AND MCCRACKEN, R.J., 1973, Soil Genesis and Classification: Iowa University Press, Ames, 360 p.

CECIL, C. B., 2003, The concept of autocyclic and allocyclic controls on sedimentation and stratigraphy, emphasizing the climatic variable, *in* Cecil, C.B., and Edgar, N.T., eds., Climate Controls on Stratigraphy: Society of Economic Paleontologists and Mineralogists Special Publications 77, p. 13–20.

CECIL, C.B., AND DULONG, F.T., 2003, Precipitation models for sediment supply in warm climates, *in* Cecil, C.B., and Edgar, N.T., eds., Climate Controls on Stratigraphy: Society of Economic Paleontologists and Mineralogists Special Publication 77, p. 21–27.

CHIDSEY T.C., JR., ADAMS, R.D., AND MORRIS, T.H., 2004, eds., Regional to Wellbore Analog for Fluvial-Deltaic Reservoir Modeling: The Ferron Sandstone of Utah: AAPG Studies in Geology No. 50, AAPG, Tulsa, 568 p.

CLEVELAND, D.M., ATCHLEY, S.C., AND NORDT, L.C., 2007, Continental sequences stratigraphy of the Upper Triassic (Nortian-Rhaetian) Chinle strata, northern New Mexico, U.S.A.: allocyclic and autocyclic origins of paleosol-bearing alluvial successions: Journal of Sedimentary Research, v. 77, p. 909-924.

CLIFTON, H.E., 2006, A reexamination of facies models for clastic shoreline, *in* Walker, R.G., and Posamentier, H., eds., Facies Model Revisited: SEPM Special Publication 84, p. 293–337.

COBBAN, W.A., WALASZCZYK, I., OBRADOVICH, J.D., and MCKINNEY, K.C., 2006, A USGS zonal table for the Upper Cretaceous middle Cenomanian-Maastrichtian of the Western Interior of the United States based on ammonites, inoceramids, and radiometric ages: Open-File Report – U.S. Geological Survey, OF 2006 -1250, 46 p.

COLLINSON, J. D., 1978, Vertical sequence and sand body shape in alluvial sequences, *in* A. D. Miall, ed., Fluvial Sedimentology: Canadian Society of Petroleum Geologists Memoir 5, p. 577-586.

CORREGGIARI, A., CATTANEO, A., TRINCARDI, F., 2005, The modern Po Delta system: Lobe switching and asymmetric prodelta growth: Marine Geology, v. 222-223, p. 49-74.

COTTER, E., 1976, The role of deltas in the evolution of the Ferron Sandstone and its coals, Castle Valley, Utah: Brigham Young University Geological Studies, v. 22, p. 15-42.

DALRYMPLE, R.W., BOYD, R., AND ZAITLIN, B.A., 1994, History of research, types and internal organization of incised-valley systems: introduction to the volume, *in* Dalrymple, R.W., Boyd, R., and Zaitlin, B.A., eds., Incised-Valley Systems: Origin and Sedimentary Sequences: SEPM Special Publication 51, p. 3–10.

DECELLES, P.G., AND GILES, K.A., 1996, Foreland basin systems: Basin Research, v. 8, p. 105-123.

DECELLES, P.G., LAWTON, T.F., MITRA, G., 1995, Thrust timing, growth of structural culminations, and synorogenic sedimentation in the type Sevier Orogenic Belt, western United States: Geology, v. 23, p. 699 – 702.

DEMKO, T.M., AND GASTALDO, R.A., 1992, Paludal environments of the Mary Lee coal zone, Pottsville Formation, Alabama: stacked clastic swamps and peat mires: International Journal of Coal Geology, v. 20, p. 23-47.

DEMKO, T.M., AND GASTALDO, R.A., 1996, Eustatic and autocyclic influences on deposition of the lower Pennsylvanian Mary Lee coal zone, Warrior Basin, Alabama: International Journal of Coal Geology, v. 31, p. 3-19.

DE RAAF, J.F.M., AND BOERSMA, J.R., 1971, Tidal deposits and their sedimentary structures: Geologie en Mijnbouw, v. 50, p. 479-504.

DIESSEL, C.F.K., 1992, Coal-Bearing Depositional Systems: Springer-Verlag, Berlin, 721 p.

DRIESE, S.G., AND FOREMAN, J.L., 1992, Paleopedology and paleoclimatic implications of Late Ordovician vertic paleosols, southern Appalachians: Journal of Sedimentary Petrology, v. 62, p. 71-83.

DRIESE, S.G., AND OBER, E.G., 2005, Paleopedologic and Paleohydrology of Precipitation seasonality from early Pennsylvanian “underclay” paleosols, U.S.A., Journal of Sedimentary Research, v.75, p.997-1010.

DRIESE, S.G., LI, Z.H., AND MCKAY, L.D., 2008, Evidence for multiple, episodic, mid-Holocene Hypsithermal recorded in two soil profiles along an alluvial floodplain catena, southeastern Tennessee, USA: Quaternary Research, v. 69, p. 276-291.

DRIESE, S.G., LUDVIGSON, G.A., ROBERTS, J.A., FOWLE, D.A., GONZÁLEZ, L.A., SMITH, J.J., VULAVA, V.M., AND MCKAY, L.D., 2010, Micromorphology and stable-isotope geochemistry of historical pedogenic siderite formed in PAH-contaminated alluvial clay soils, Tennessee, USA: Journal of Sedimentary Research, v. 80, p. 943-954.

DUCHAUFOUR, P., 1982, Pedology: Allen and Unwin, London, 448 p.

ELLIOTT, T., 1974, Interdistributary bay sequences and their genesis: Sedimentology, v. 21, p. 611–622.

ELLIS, S., AND MELLOR, A., 1995, Soils and Environment: Routledge, New York, 392 p.

EMERY, D., AND MYERS, K.J., 1996, Sequence Stratigraphy, London, Uxbridge: 297 p.

ETHRIDGE, F. G., WOOD, L. J., AND SCHUMM, S. A., 1998, Cyclic variables controlling fluvial sequence development: Problems and Perspectives, *in* Shanley, K. W. and McCabe, P. J., eds., Relative Role of Eustasy, Climate and Tectonism in Continental Rocks: Society of Economic Paleontologists and Mineralogists Special Publication 59, p.17-29.

FANTI, F., AND CATUNEANU, O., 2010, Fluvial sequence stratigraphy: the Wapiti Formation, West-Central Alberta, Canada: Journal of Sedimentary Research, v. 80, p. 320-338.

FARRELL, K.M., 1987, Sedimentology and facies architecture of overbank deposits of the Mississippi River, False River region, Louisiana, *in* Ethridge, F.G., Flores, R.M., and Harvey, M.D., eds., Recent Developments in Fluvial Sedimentology: SEPM Special Publication 39, p.111–120.

FASTOVSKY, D.E., AND MCSWEENEY, K., 1987, Paleosols spanning the Cretaceous-Paleogene transition, eastern Montana and western North Dakota: Geological Society of America Bulletin, v.99, p. 66-77.

FIELDING, C.R., 2010, Planform and facies variability in asymmetric deltas: facies analysis and depositional architecture of the Turonian Ferron Sandstone in the western Henry Mountains, South-Central Utah, U.S.A.: Journal of Sedimentary Research, v. 80, p. 455–479.

FIELDING, C.R., 2011, Foreland basin structural growth recorded in the Turonian Ferron Sandstone of the Western Interior Seaway Basin, U.S.A.: Geology, v. 39, p.1107–1110.

FIELDING, C.R., AND CRANE, R.C., 1987, An application of statistical modeling to the prediction of hydrocarbon recovery factors in fluvial reservoir sequences, *in* Ethridge, F. G., Flores, R. M., and Harvey M. D., eds., Recent developments in fluvial sedimentology: SEPM Special Publication 39, p. 321–327.

FISK, H.N., 1944, Geological Investigations of the Alluvial Valley of the Lower Mississippi River: U.S. Army Corps of Engineers, Waterways Experimentation Station, Mississippi River Commission, Vicksburg, MS. 78 pp.

FISK H. N., 1947, Fine-grained Alluvial Deposits and Their Effects on Mississippi River Activity: U.S. Army Corps of Engineers, Mississippi River Commission Report, Vicksburg, Mississippi, 82 p.

FLAIG, P.P., MCCARTHY, P.J., AND FIORILLO, A.R., 2013, Anatomy, evolution, and paleoenviromental interpretation of an ancient arctic coastal plain: Integrated paleopedology and palynology from the upper Cretaceous (Maastrichtian) Prince Creek

Formation, North Slope, Alaska, USA, *in* Driese, S.G., Nordt, L.C., and McCarthy, P.J., eds., New Frontiers in Paleopedology and Terrestrial Climatology: Paleosols and soil surface analog systems: SEPM Special Publications 104, p. 179 -230.

FLORES, R.M. and HANLEY, J.H., 1984, Anastomosed and associated coal-bearing fluvial deposits: Upper Tongue River Member, Paleocene Fort Union Formation, northern Powder River Basin, Wyoming USA, *in* Rahmani, R.A., and Flores, R.M., eds., Sedimentology of Coal and Coal-bearing Sequences: International Association of Sedimentologists, Special Publication 7, p. 85-103.

FRAZIER, D. E., 1967, Recent deltaic deposits of the Mississippi River: Their development and chronology: Gulf Coast Association of Geological Societies, Transactions, v. 17, p. 287-311.

FREY, R.W., PEMBERTON, S.G., AND FAGERSTROM, J. A., 1984, Morphological, ethological, and environmental significance of the Ichnogenera *Scoyenia* and *Ancorichnus*, Journal of Paleontology, v. 58, p. 511-528.

FRIGNANI, M., AND LANGONE, L., 1991, Accumulation rates and 137Cs distribution in sediments off the Po River delta and the Emilia-Romagna coast (northwestern Adriatic Sea, Italy): Continental Shelf Research, v. 11. p. 525-542.

GALLOWAY, W.E., AND HOBDAY, D.K., 1996, Terrigenous Clastic Depositional Systems: Applications to Fossil Fuel and Groundwater Resources, Second Edition: New York, Springer, 489 p.

GARDNER, M.H., 1995, Tectonic and eustatic controls on the stratal architecture of mid-Cretaceous stratigraphic sequences, central western interior foreland basin of North America, *in* Dorobek, S.L., and Ross, G.M., eds., Stratigraphic Evolution of Foreland Basins: SEPM Special Publication 52, p. 243–281.

GARDNER, T.W., WILLIAMS, E.G., AND HOLBROOK, P.W., 1988, pedogenesis of some Pennsylvanian underclays; Ground-water, topographic, and tectonic controls: Geological Society of America, Special Paper 216, p. 81-101.

GINGRAS, M.K., MACEACHERN, J.A., AND PICKERILL, R.K., 2004, Modern perspectives on the *Teredolites* ichnofacies from the Willapa Bay, Washington: Palaios, v. 19, p. 79-88.

GRAY, M.B., AND NICKELSEN R.P., 1989, Pedogenic slickensides, indicators of strain and deformation processes in redbed sequences of the Appalachian foreland: Geology, v. 17, p. 72-75

HASIOTIS, S.T., 2002, Continental Trace Fossils: SEPM Short Course Notes, no. 51, 132 p.

HASIOTIS, S.T., 2004, Reconnaissance of Upper Jurassic Morrison Formation ichnofossils, Rocky Mountain Region, USA: paleoenviromental, stratigraphic, and paleoclimatic significance of terrestrial and freshwater ichnocoenoses: Sedimentary Geology, v. 167, p. 177-268.

HASIOTIS, S.T., AND BOURKE, M.C., 2006, Continental trace fossils and museum exhibits: Displaying burrows as organism behavior frozen in time. The Geological Curator, v. 8, p. 211-226.

HASIOTIS, S.T., AND PLATT, B.F., 2012, Exploring the sedimentary, pedogenic, and hydrologic factors that control the occurrence and role of bioturbation in soil formation and horizonation in continental deposits: an integrative approach: The Sedimentary Record, v. 10, p. 4-9.

HENSEL, P. E., DAY JR., J.W., AND PONT, D., 1999, Wetland vertical accretion and soil elevation change in the Rhône River Delta, France: The importance of riverine flooding: Journal of Coastal Research, v. 15, p. 668-681

HILL, R.B., 1982, Depositional environments of the Upper Cretaceous Ferron Sandstone south of Notom, Wayne County, Utah: Brigham Young University Geology Studies, v. 29, p. 59-83.

HOLBROOK, J.M., AND BHATTACHARYA, J.P., 2012, Reappraisal of the sequence boundary in time and space: case and considerations for an SU (subaerial unconformity) that is not sediment bypass surface, a time barrier, or an unconformity: Earth-Science Reviews, v.113, p. 271-302.

HURT, G. W., AND CARLISLE, V. W., 2002, Delineating hydric soils, *in* Richardson, J. L. and Vepraskas, M. J., eds., Wetland soils: genesis, hydrology, landscapes, and classification, CRC Press, p. 183-206.

HURT, G. W., WHITED, P.M., AND PRINGLE, R.M., 1998, Field Indicators of Hydric Soil in the United States, Version 4.0: US Department of Agriculture, Natural Resources Conservation Service, Ft. Worth, Texas. 30 p.

IBÀÑEZ, C., CANICIO, A., DAY, J.W., AND CURCÓ A., 1997, Morphologic development, relative sea-level rise and sustainable management of water and sediment in the Ebre Delta, Spain: Journal of Coastal Conservation, v. 3, p. 191-202

KEMP, R.A., 1985, Soil Micromorphology and the Quaternary: Quaternary Research Association Technical Guide, No. 2, Cambridge, 80 p.

KOVDA, I., AND MERMUT, A.R., 2010, Vertic Features, *in* Stoops, G., Marcelino, V., and Mees, F., eds., Interpretation of micromorphological features of soils and regoliths: Elsevier. p. 109-127.

KRAUS, M.J., 1987, Integration of channel and floodplain suites; II, Vertical relations of alluvial paleosols: Journal of Sedimentary Petrology, v. 57, p. 602-612.

KRAUS, M.J., 1999, Paleosols in clastic sedimentary rocks: their geologic applications: Earth Science Reviews, v. 47, p. 41-70.

KRAUS, M.J., AND BROWN, T.M., 1988, Pedofacies Analysis; A new approach to reconstructing ancient fluvial sequences: Geological Society of America, Special Paper 216, p. 143-152.

KRAUS, M.J., AND DAVIS-VOLLUM, S., 2004, Mud rock-dominated fills formed in avulsion splay channels: examples from the Willwood Formation, Wyoming: Sedimentology, v. 51, p. 1127 -1144.

LECKIE, D., FOX, C., TARNOCAI, C., 1989, Multiple paleosols of the late Albian Boulder Creek Formation, British Columbia, Canada: Sedimentology, v. 36, p. 307-323.

LI, W., BHATTACHARYA, J.P., AND CAMPBELL, C., 2010, Temporal evolution of fluvial style within a compound incised valley, the Ferron Notom Delta, Henry Mountains region, Utah: Journal of Sedimentary Research, v. 80. P. 529-549.

LI, Y., AND BHATTACHARYA, J.P., 2013, Facies-architecture study of a stepped, forced regressive compound incised valley in the Ferron Notom Delta, Southern Central Utah, U.S.A.: Journal of Sedimentary Research, v. 83, p. 206-225.

LINDBO, D.L., AND RICHARDSON J.L., 2000, Hydric soils and wetlands in riverine systems, *in* Richardson, J. L. and Vepraskas, M. J., eds., Wetland Soils: Genesis, Hydrology, Landscapes, and Classification, p. 183-206.

LUDVIGSON, G.A., GONZÁLEZ, L.A., FOWLE, D.A., ROBERTS, J.A., DRIESE, S.G., VILLARREAL, M.A., SMITH, J.J., AND SUAREZ, M.B., 2013, Paleoclimatic implications and modern process studies of pedogenic siderite, *in* Driese, S.G., Nordt, L.C., and McCarthy, P.J., eds., New Frontiers in Paleopedology and Terrestrial Climatology: Paleosols and soil surface analog systems: SEPM Special Publications 104, p. 79 -87.

MACEACHERN, J.A., RAYCHAUDRI, I., AND PEMBERTON, S.G., 1992, Stratigraphic applications of the *Glossifungites* ichnofacies: delineating discontinuities in the rock record, *in* Pemberton, S.G., ed., Application of Ichnology to Petroleum Exploration: SEPM Core Workshop 17, p. 169-198.

MACK, G.H., 1992, Palaeosols as indicators of climatic change at the Early-Late Cretaceous boundary, southwestern New Mexico: Journal of Sedimentary Petrology, v.62, p. 483-494.

MACK, G.H., JAMES, W.C., AND MONGER, H.C., 1993, Classification of paleosols: Geological Society of America Bulletin, v. 105, p. 129-136.

MARTIN, A.J., 2000, Flaser and wavy bedding in ephemeral streams: a modern and an ancient example: Sedimentary Geology, v. 136, p. 1-5.

MCCABE, P.J., 1984, , Depositional environments of coal and coal-bearing strata, *in* Rahmani, R.A., and Flores, R.M., eds., Sedimentology of Coal and Coal-bearing Sequences: International Association of Sedimentologists, Special Publication 7, p.13-42.

MCCARTHY, P. J., FACCINI, U.F., AND PLINT, A.G., 1999, Evolution of an ancient coastal plain: palaeosols, interfluves and alluvial architecture in a sequence stratigraphic framework, Cenomanian Dunvegan Formation, NE British Columbia, Canada: Sedimentology, v. 46, p. 861-891.

MCCARTHY, P.J., AND PLINT, A.G., 1998, Recognition of interfluve sequence boundaries: integrating paleopedology and sequence stratigraphy: Geology, v. 26, p. 387–390.

MCCARTHY, P.J., AND PLINT, A.G., 1999, Floodplain paleosols of the Cenomanian Dunvegan Formation, Alberta and British Columbia, Canada: Micromorphology, pedogenic processes and palaeoenvironmental implications, Geological Society, London, Special Publications 163, p. 289-310

MCCARTHY, P.J., AND PLINT, A.G., 2003, Spatial variability of palaeosols across Cretaceous interfluves in the Dunvegan Formation, NE British Columbia, Canada: paleohydrological, paleogeomorphological and stratigraphic implications: Sedimentology, v. 50, p. 1187–1220

MCCARTHY, P.J., AND PLINT, A.G., 2013, A pedostratigraphic approach to nonmarine sequence stratigraphy: A three-dimensional paleosol-landscape model from the Cretaceous (Cenomanian) Dunvegan formation, Alberta and British Columbia, Canada, *in* Driese, S.G., Nordt, L.C., and McCarthy, P.J., eds., New Frontiers in Paleopedology and Terrestrial Climatology: Paleosols and soil surface analog systems: SEPM Special Publications 104, p. 159 -177.

MCSWEENEY, K., AND FASTOVSKY, D.E., 1987, Micromorphological and SEM analysis of Cretaceous-Paleogene petrosols from eastern Montana and western North Dakota: Geoderma, v. 40, p. 49-63.

MIALL, A.D., 1991, Stratigraphic sequences and their chronostratigraphic correlation: Journal of Sedimentary Petrology, v. 61, p. 497-505.

MIALL, A.D., 1992, Alluvial deposits, *in* Walker, R. G. and James, N.P., eds., Facies Models: Response to Sea-level Change: St. Johns, Newfoundland, Geological Association of Canada, p. 119-142.

MIALL, A.D., 1996, The Geology of Fluvial Deposits: Sedimentary Facies, Basin Analysis and Petroleum Geology: Heidelberg, Springer-Verlag, 582 p.

MILLIMAN, J.D., AND SYVITSKY, J.P.M., 1992, Geomorphic/tectonic control of sediment discharge to the ocean: The importance of small mountainous rivers: The Journal of Geology, v. 100, p. 525 to 544.

MUNSELL SOIL-COLOR CHARTS, 2009, The Munsell Color Company, Baltimore.

NORDT, L.C. DWORKIN, S.I., AND ATCHLEY S.C., 2011, Ecosystem response to soil biogeochemical behavior during the Late Cretaceous and early Paleocene within the western interior of North America: Geological Society of America Bulletin, v. 123, p. 1745 -1762.

NUMMEDAL, G., HASAN, S.F., AND POSAMENTIER, H., 2003, A framework for deltas in Southeast Asia, *in* Hasan, S.F., and Allen, G. P., eds., Tropical deltas of Southeast Asia: sedimentology, stratigraphy and petroleum geology: SEPM Special Publications 76, p. 159 -177.

OLSEN, T., STEEL, R., HOGSETH, K., SKAR, T., AND ROE, S.L., 1995, Sequential architecture in a fluvial succession: sequence stratigraphy in the Upper Cretaceous Mesaverde Group, Price Canyon, Utah: Journal of Sedimentary Research, v. B65, p. 265-280.

PAGE, S.E., WÜST, R., AND BANKS, C., 2010, Past and present carbon accumulation and loss in Southeast Asian peatlands: PAGES News, v. 18, p. 25-26.

PEMBERTON, S.G., VAN WAGONER, J.C., AND WACH, G.D., 1992, Ichnofacies of a wave-dominated shoreline, *in* Pemberton, S.G., ed., Applications of Ichnology to Petroleum Exploration: SEPM Core Workshop 17, p. 339–382.

PEREZ-ARLUCEA, M., AND SMITH, N.D., 1999, Depositional patterns following the 1870s avulsion of the Saskatchewan River (Cumberland Marshes, Saskatchewan): Journal of Sedimentary Research, v. 69, p.62–73.

PETERSON, F., AND RYDER, R.T., 1975, Cretaceous rocks in the Henry Mountains region, Utah and their relation to neighboring regions, *in* Fassett, J.E., and Wengerd, S.A., eds., Canyonlands Country: Four Corners Geological Society Guidebook, 8th Field Conference, p. 167-189.

PLINT, G., 2010, Wave- and storm-dominated shoreline and shallow-marine systems, *in* James, N.P., and Dalrymple, R.W., eds., Facies Model Revisited: SEPM Special Publication 90, p. 167–199.

PLINT, A.G., MCCARTHY, P.J. AND FACCINI, U.F., 2001, Non-marine sequence stratigraphy: Updip expression of sequence boundaries and systems tracts in a high-resolution framework, Cenomanian Dunvegan Formation, Alberta foreland basin, Canada: American Association of Petroleum Geologists, Bulletin, v. 85, p. 1967–2001.

POSAMENTIER, H.W., AND ALLEN, G.P., 1999, Siliciclastic Sequence Stratigraphy: Concepts and Applications: Tulsa, SEPM Concepts in Sedimentology and Paleontology, v. 7, 210 p.

POSAMENTIER, H.W., ALLEN, G.P., JAMES, D.P., AND TESSON, M., 1992, Forced regressions in a sequence stratigraphic framework: concepts, examples, and exploration significance: American Association of Petroleum Geologists, Bulletin, v.76, p. 1687-1709.

POSAMENTIER, H.W., AND VAIL, P.R., 1988, Eustatic controls on clastic deposition II sequence and systems tract models, *in* Wilgus, C.K., Hastings, B.S., Kendall, C.G.St.C., Posamentier, H.W., Ross, C.A., and Van Wagoner, J.C., eds., Sea-level Changes: An Integrated Approach: SEPM Special Publication 42, p. 125–154.

PROCHNOW, S.J., ATCHLEY, S.C., BOUCHER, T., NORDT, L.C., AND HUDEC, M.R., 2006, The influence of salt withdrawal subsidence on paleosol maturity, sedimentation rates, and cyclic fluvial deposition in the Triassic Chinle Formation: The Big Bend minibasin near Castle Valley, Utah: Sedimentology, v. 53, p. 1319–1345.

REINECK, H.E., AND WUNDERLICH, F., 1968, Classification and origin of flaser and lenticular bedding: Sedimentology, v.11, p. 99-104.

RETALLACK, G.J., 1988, Field recognition of paleosols: Geological Society of America, Special Paper 216, p. 1-20.

RETALLACK, G.J., 1997, A Colour Guide to Paleosols: Wiley, Chichester, 175p.

RETALLACK, G.J., 2001, Soils of the Past, Second Edition: Oxford, U.K. Blackwell Science, 404 p.

RICHARDS, B.H., 2014, Fluvial to marine facies transition in a flood-topped Compound Incised Valley In the Ferron Notom Delta, Utah. [Unpublished Masters Thesis]: University of Houston, Houston, Texas, 50p.

RYER, T.A., 1981, Deltaic coals of Ferron Sandstone Member of Mancos Shale: Predictive model for Cretaceous coal-bearing strata of Western Interior: American Association of Petroleum Geologists, Bulletin, v. 65, p. 2323-2340.

RYER, T.A., AND ANDERSON, P.B., 2004, Facies of the Ferron Sandstone, East-Central Utah, in Chidsey, T.C., Adams, R.D., and Morris, T.H., eds., Regional to Wellbore Analog for Fluvial–Deltaic Reservoir Modeling: The Ferron Sandstone of Utah: American Association of Petroleum Geologists, Studies in Geology 50, p. 59–78.

RYER, T. A., AND LANGER, A.W., 1980, Thickness change involved in the peat-to-coal transformation for a bituminous coal of Cretaceous age in central Utah: Journal of Sedimentary Petrology, v. 50, p. 987–992.

SAVRDA, C.E., 1991, Teredolites, wood substrates, and sea-level dynamics: Geology, v. 19, p. 905-908.

SHANLEY, K.W. AND MCCABE, P.J., 1993, Alluvial architecture in a sequence stratigraphic framework: a case history from the Upper Cretaceous of southern Utah, USA, *in* Flint, S.S., and Bryant, I.D., eds., Quantitative Modeling of Clastic Hydrocarbon Reservoirs and Outcrop Analogues: International Association of Sedimentologists, Special Publication 15, p. 21–55.

SHANLEY, K.W. AND MCCABE, P.J. 1994, Perspectives on the sequence stratigraphy of continental strata: American Association of Petroleum Geologists, Bulletin, v.78, p. 544–568.

SHELDON, N.D., RETALLACK, G.J., AND TANAKA, S., 2002, Geochemical climofunctions from North American soils and application to paleosols across the Eocene–Oligocene boundary in Oregon: Journal of Geology, v. 110, p. 687–696.

SHELDON, N.D., AND TABOR, N.J., 2009, Quantitative paleoenviromental and paleoclimatic reconstruction using paleosols: Earth-Science Reviews, v. 95, p. 1-52.

SMITH, N.D., CROSS, T.A., DUFFICY, J.P., AND CLOUGH, S.R., 1989, Anatomy of an avulsion: Sedimentology, v. 36, p. 1–23.

SOIL SURVEY STAFF, 1975, Soil Taxonomy: 436, Soil Conservation Service, U.S. Department of Agriculture 436, Washington, D.C., 754 p.

SOIL SURVEY STAFF, 1993, Soil Survey Manual: Soil Conservation Service, U.S. Department of Agriculture Handbook 18, Washington, D.C., 437 p.

SOIL SURVEY STAFF, 1999, Soil Taxonomy: A Basic System for Soil Classification for Making and Interpreting Soil Surveys: U.S. Department of Agriculture, Washington, D.C. 869 p.

SOUTHARD, R.J., DRIESE, S.G., AND NORDT, L.C., 2011, Vertisols, *in* Huang, P.M., Li, Y, and Sumner, M.E., eds., Handbook of Soil Science, 2nd Edition, CRC Press, Boca Raton, Florida, p. 33-82 to 33-97

.

STAUB, J.R., AND GASTALDO, R.A., 2003, Late Quaternary Sedimentation and peat Development in Rajang River Delta, Sarawak, East Malaysia, *in* Hasan, S.F., and Allen, G. P., eds., Tropical deltas of Southeast Asia: sedimentology, stratigraphy and petroleum geology: SEPM Special Publications 76, p. 159 -177.

TERWIWNDT, J.H.J., 1971, Lithofacies of inshore estuarine and tidal inlet deposits: Geologie en Mijnbouw, v. 50, p. 515-526.

TÖRNQVIST, T.E., 1994, Middle and late Holocene avulsion history of the River Rhine (Rhine-Meuse delta, Netherlands: Geology, v. 22, p. 711-714.

TYE, R.S., AND COLEMAN, J.M., 1989, Evolution of Atchafalaya lacustrine deltas, south-central Louisiana: Sedimentary Geology, v. 65, 95-112.

UFNAR, D.F., 2006, Pedofeatures from a modern soil chronosequence, a technique for estimating the relative age of ancient pedogenic features: Gulf Coast Association of Geological Societies Transactions, v. 56, p. 827-843.

UFNAR, D.F., 2007, Clay coatings from a modern soil chronosequence: A tool for estimating the relative age of well-drained paleosols: Geoderma, v. 141, p. 181-200.

UFNAR, D.F., GONZALEZ, L.A., LUDVIGSON, G.A., BRENNER, R.L., WITZKE, B.J., AND LECKIE, D., 2005, Reconstructing a mid-Cretaceous landscape from paleosols in Western Canada: Journal of Sedimentary Research, v. 75, p. 984–996.

URESK, J., 1978, Sedimentary environment of the Cretaceous Ferron Sandstone near Caineville, Utah: Brigham Young University Geology Studies, v. 26, p. 81-100.

VAN WAGONER, J.C., MITCHUM, R.M., CAMPION, K.M., AND RAHMANIAN, V.D., 1990, Siliciclastic Sequence Stratigraphy in Well Logs, Cores, and Outcrops: American Association of Petroleum Geologists, Methods in Exploration Series 7, 55 p.

VISSER, M.J., 1980, Neap-spring cycles reflected in Holocene subtidal large-scale bedform deposits: A preliminary note: Geology, v. 8, p. 543-546.

WALKER, R.G., AND PLINT, A.G., 1992, Wave- and storm-dominated shallow marine systems, in Walker, R.G., and James, N. P., eds., Facies Models: Response to Sea-level Change: Geological Association of Canada, p. 219 -238

WILLIAMS, G.D., AND STELCK, C.R., 1975, Speculations on the Cretaceous paleogeography of North America, *in* Caldwell, W.G.E., ed., The Cretaceous System in the Western Interior of North America: The Geological Association of Canada, Special Paper 13, p. 1–20.

WILLIS, B.J., AND BEHRENSMEYER, A.K., 1994, Architecture of Miocene overbank deposits in Northern Pakistan: Journal of Sedimentary Research, v. B64, p. 60–67.

WRIGHT, V.P., 1989, Paleosols in deltaic sequences, *in* Allen, J.R.L., and Wright, V.P., eds., Paleosols in siliciclastic sequences: P.R.I.S. Short Course Notes, 001, University of Reading, p. 70-79.

WRIGHT, V.P., 1992, Paleosol recognition: a guide to early diagenesis in terrestrial setting, *in* Wolf, K.H., and Chilingarian, G.V., eds., Diagenesis, III, p. 591-619.

WRIGHT, V.P., AND MARRIOTT, S.B., 1993, The sequence stratigraphy of fluvial depositional systems: the role of floodplain storage. Sedimentary Geology, v. 86, p. 203–210.

WRIGHT, V.P., TAYLOR, K.G., AND BECK, V.H., 2000, The paleohydrology of Lower Cretaceous seasonal wetlands, Isle of Wight, Southern England: Journal of Sedimentary Research, v.70, p. 619 -632.

VELLA, C., FLEURY, T-J., RACCASI, G., PROVANSAL, M., SABATIER, F., BOURCIER, M., 2005, Evolution of the Rhone delta plain in the Holocene: Marine Geology, v.222-223, p. 235-265.

YOSHIDA, S., WILLIS A., AND MIALL, A. D., 1996, Tectonic control of nested sequence architecture in the Castlegate Sandstone (Upper Cretaceous), Book Cliffs, Utah: Journal of Sedimentary Research, v. 66, p. 737–748.

ZHU, Y., BHATTACHARYA, J.P., LI, W., LAPEN, T.J., JICHA, B.R., AND SINGER, B.S., 2012, Milankovitch-scale sequence stratigraphy and stepped forced regressions of the Turonian Ferron Notom deltaic complex, south-central Utah, U.S.A.: Journal of Sedimentary Research, v. 82, p.723 -746.